Nonlinear stability analyses of problems in patterned ground formation and penetrative convection

by

Geoffrey McKay

A thesis submitted to the Faculty of Science, University of Glasgow, for the degree of Doctor of Philosophy

Department of Mathematics,
University of Glasgow
August, 1992

To Mum, Dad,

Kirsty and Fiona

Contents

Page

Preface iv

Summary v

Chapter 1 Introduction

1.1 Penetrative convection 1

Chapter 2 Continuous dependence on the heat supply for the Boussinesq equations with a cubic density law

2.1 Introduction 7

2.2 Continuous dependence on the heat supply forward in time 9

2.3 Continuous dependence on the heat supply backward in time 13

Chapter 3 Continuous dependence on a boundary heat flux for the Boussinesq equations

3.1 Introduction 25

3.2 Continuous dependence on the boundary data forward in time 26

3.3 Continuous dependence on the boundary data backward in time 30

Chapter 4 Nonlinear energy stability and convection near the density maximum

4.1 Introduction 37

4.2 Conditional energy stability for the cubic density relation 40

4.3 Unconditional (weighted energy) stability for the cubic density 47

4.4 Conditional energy stability for the fifth order relation 50

4.5 Unconditional energy stability for the quintic density relation 53

4.6 Numerical results and conclusions 55

4.6.1 Numerical results 55

Page

4.6.2 Discussion 64

4.6.3 Conclusion 66

Chapter 5 Convection with internal heat generation near the density maximum

5.1 Introduction 67

5.2 Convection in a horizontal layer 69

(i) Cases I, II, III Non-zero heat supply 70

(ii) Case IV No internal heat generation 81

Chapter 6 The influence of a cubic density law on patterned ground formation

6.1 Introduction to patterned ground formation 85

6.2 Convection in a porous medium with a cubic density law 91

6.2.1 Linear instability 94

6.2.2 Nonlinear stability 95

6.3 Numerical results and conclusions 100

6.3.1 Tables and results 100

6.3.2 Discussion 105

6.3.3 Conclusion 106

Chapter 7 Patterned ground formation and solar radiation ground heating

7.1 Introduction: Time–periodic heating 108

7.2 The time–periodic model 110

7.3 Linear instability 113

7.4 Nonlinear energy analysis 117

7.4.1 Global stability 117

7.4.2 A heuristic approach to unconditional stability 121

7.5 Numerical results and discussion 123

7.5.1 Tables and figures 123

Page

7.5.2 Discussion 129

7.5.3 Conclusion 131

Chapter 8 Patterned ground formation under water

8.1 Introduction 132

8.2 A model for patterned ground formation under water 134

8.3 Numerical results and conclusions 144

8.3.1 Tables and figures 144

8.3.2 Discussion 152

Chapter 9 The stabilizing influence of rotation on a plane layer subject to internal heating

9.1 Introduction 157

9.2 Model for a rotating fluid layer 159

9.3 Monotonic stability 166

9.4 Conditional stability condition 171

References 176

Preface

This thesis is submitted to the University of Glasgow in accordance with the requirements for the degree of Doctor of Philosophy.

I would like to express my gratitude to my supervisor Professor B. Straughan for his guidance, assistance and encouragement throughout the period of my research.

My sincere thanks also go to Professor R. W. Ogden for the help and advice he has given me during my time in the Department of Mathematics.

I also thank the Science and Engineering Council of Great Britain for financing this research through a three year earmarked award.

Finally, I am very grateful to my family for their patience and tolerance during all my days at University.

Summary

In this thesis we present nonlinear energy stability analyses of a number of problems associated with the phenomenon of penetrative convection. In particular, we consider penetrative convection models which incorporate nonlinear buoyancy terms or internal heat generation (either together or separately).

To begin we give a brief account of penetrative convection and situations in which it naturally occurs in geophysics. We also discuss the energy methods which we shall employ in later chapters. Our analysis begins by proving continuous dependence of the solution to the Boussinesq equations, both forward and backward in time, on a heat source and on the heat flux on the lower boundary. Linear theory and the energy method are then employed to study the effect of nonlinear density relations or a non uniform heat source on the onset of penetrative convection.

We next introduce and describe patterned ground, a geological phenomenon whose formation is believed to involve penetrative convection in a saturated porous medium. We discuss the influence of a cubic density law and time–periodic solar radiation on the stability of the porous layer and on the size of the stone polygons. We then perform a linear analysis of a two layer problem which models the formation of patterned ground under water. Our predictions for patterned ground are compared with observations made by field workers and results from previous mathematical analyses.

To conclude, we use a generalized energy to prove the stabilizing influence of rotation on a fluid layer, even when the layer is subject to internal heating.

Chapter 1

Introduction

1.1 Penetrative convection

In recent years there have been many articles dealing with the phenomenon of *penetrative convection* in fluid motions. The topics and models discussed in these papers encompass a wide range of approaches to penetrative convection, including numerical simulations, experimental work, as well as theoretical analyses of the linear and nonlinear systems. Moreover, many of the studies are concerned with the application of penetrative convection to several areas of geophysical fluid dynamics. Such an application is found in the model for the Earth's atmosphere. As the ground or ocean that forms the atmosphere's lower bounding surface is heated by solar radiation, the air near the surface becomes warmer than the upper air. Since the resulting system is gravitationally unstable, when convection occurs the warmer air rises and penetrates into stably stratified regions. The application of penetrative convection to other fields in geophysics and convection in stars is described in Veronis (1963).

The analysis of Veronis (1963) is based on an experiment for a layer of water. Since water has a maximum density at approximately 4°C, Veronis (1963) adopts for the density law in the body force

$$\rho(T) = \rho_4(1 - \alpha(T-4)^2), \tag{1.1}$$

where $\rho(T)$ is the density, T is temperature, ρ_4 is the density at 4°C and $\alpha \simeq 7.68 \times 10^{-6}(^\circ\mathrm{C}^{-2})$. Equation (1.1) is almost exact near 4°C and involves a 10% error at 14°C. The model Veronis (1963) describes involves a layer of water with

temperature 0°C at the lower boundary and temperature greater than 4°C at the upper surface. Due to the density maximum of water, the fluid below the 4°C plane is gravitationally unstable while that above is stable. When convective motions occur in the lower region fluid will penetrate into the upper layer, thus producing penetrative convection. Veronis (1963) considers the linearized system and employs a weakly nonlinear finite amplitude analysis for two stress free boundaries. The analysis determines critical Rayleigh numbers for the onset of convection and suggests the existence of possible subcritical instabilities (where convection occurs for a Rayleigh number below the critical value of linear theory).

Veronis' (1963) work based on the quadratic relation (1.1) has inspired many subsequent papers. Moore & Weiss (1973) construct a two-dimensional simulation of penetrative convection using the Veronis (1963) model and discuss the resulting convection cell structure. Similar numerical studies are carried out by Watson (1972) and Robillard & Vasseur (1982). Nonlinear analyses of the original Veronis (1963) problem in Straughan (1985) and Payne & Straughan (1987) obtain stability thresholds below which convection will not occur. More recently the penetrative effect of buoyancy term (1.1) has been applied in two geophysical models. Payne *et al.* (1988) use a modified form of (1.1) in determining criteria for the onset of salt convection in the layer of thawing permafrost beneath the sea around parts of the Earth's coast. George *et al.* (1989) apply the effect of (1.1) to the formation of patterned ground above 11,000 feet. Chapters 6–8 expand on this analysis and consider new models for polygonal ground formation. Alternatively, Whitehead & Chen (1970) and Whitehead (1971) propose another point of view to penetrative convection by employing a nonlinear basic density in the upward variable with the convective system occupying a half space.

Deardorff *et al.* (1969) examine penetrative convection experimentally by mimicking the situation where solar radiation ground heating replaces atmospheric inversion. Walden & Ahlers (1981) model convective motions of liquid ^{4}He at temperatures close to its density maximum of 2.178K. Azouni (1981b) analyses the formation of helical clouds of solute, gas bubbles or particles caused

by penetrative convection above an ice-water interface. The analysis of Veronis (1963) has also inspired many other experiments, e.g. Azouni (1981a) and Azouni & Normand (1983a,b).

Recently, however, several studies have questioned whether the quadratic equation (1.1) is accurate enough for detailed comparison with field studies and experiments. Moore & Weiss (1973) remark that it is preferable to model the situation found in stars, where an unstable layer is bounded above and below by a stable layer, by a *cubic* equation of state. In general though, writers adopt a higher order equation of state to obtain a better curve fit for the density. Wu & Cheng (1976) employ a cubic equation of state to study the linear instability of a plane layer where the free upper surface is subject to surface tension gradients. The same buoyancy model is employed by Sun *et al.* (1969). Inaba & Fukuda (1984) and Vasseur *et al.* (1983) use another model to study convection in an inclined square region and cylindrical annulus, respectively. Polynomial density models proposed by Merker *et al.* (1979) and their applications are discussed in chapter 4.

Another model for penetrative convection is that which involves fluid motions driven by internal heat generation. In general, work based on this model concentrates on an internally heated plane layer of fluid with a fixed upper surface temperature and thermally insulated lower surface. Such a system is inspired by cloud physics where the unstable layer of fluid is often bounded by stable fluid layers rather than rigid walls. Alternatively, the model of the Earth's atmosphere expounded earlier may be theoretically described in the above manner. One of the first studies of this problem is that of Roberts (1967), where he performs a linear instability analysis for a horizontal fluid layer with constant heat source. The work of Roberts (1967) is closely associated with corresponding experimental work in Tritton & Zarraga (1967). Other examples of work associated with the Roberts problem may be found in chapters 5 and 9. Heat sources have also been employed more recently in other geophysical contexts. Matthews & Heaney (1987) and Matthews (1988) discuss penetrative convection which occurs

beneath ice in an ice covered lake. To model solar radiation they employ heat sources which are a function of the vertical ordinate. Ghosal & Spiegel (1991) study the instability of a He^3 layer in the sun. They consider convection in a lower He^3 layer with internal heat generation, overlaid by a semi-infinite radiative layer with no heat generation. There are many other practical applications of internal heat source models. Schubert *et al.* (1969) consider a fluid layer which has variable viscosity and an internal heat source, with physical applications to the interiors of planets. Akopyan & Zel'dovich (1985) consider heat sources which vary sinusoidally in the horizontal directions; such heating might be produced by laser beams focussed on a fluid layer. Many of the above aspects of penetrative convection and those mentioned later may be found in a forthcoming book by Straughan (1992b).

Several of the nonlinear analyses of penetrative convection (some of which have been cited above) involve the use of the nonlinear *energy method*. This technique allows us to obtain sufficient conditions for the nonlinear stability of some base solution. In general, this condition takes the form of a critical Rayleigh number; for Rayleigh numbers below this critical value no convective motions will occur. We may compare stability conditions with those of linear instability theory. Linear theory provides sufficient conditions for instability; however, any linear analysis is only valid for infinitesimal disturbances. It is possible that subcritical instabilities may occur in penetrative convection problems (Veronis 1963). So in general we calculate both the energy and linear results so that we may compare the stability predictions obtained from each method. Extensive accounts of the energy method and its applications may be found in Joseph (1976) and Straughan (1992a).

It is the aim of this thesis to discuss and analyse penetrative convection problems which are the result of the density maximum and/or internal heat generation. Where possible we consider and compare results from both linear and nonlinear systems. In chapter 2 we consider a heat-conducting viscous fluid, the density of which is a cubic function of temperature. We show that the solution to

a boundary-initial value problem for this fluid depends continuously on changes in the heat supply both forward and backward in time. Chapter 3 uses the same methods to show continuous dependence of a solution on a boundary heat flux. In this case the fluid density is a quadratic function of temperature and the region we consider is a plane layer.

We begin chapter 4 by comparing and discussing the density models for water proposed by Merker *et al.* (1979). We then develop a nonlinear analysis for penetrative convection for each model. A conditional stability limit is obtained by using the method of coupling parameters, and an unconditional limit is also obtained by constructing a suitable weighted energy. Chapter 5 uses a similar energy analysis to discuss the stability of an internally heated fluid layer, with prescribed heat flux on the lower surface and constant upper surface temperature. In the buoyancy term we assume a cubic dependence on temperature.

Chapter 6 introduces patterned ground formation and gives an account of the processes involved in polygon formation. A theoretical analysis is presented with a model based on the onset of convection in a saturated soil below which is a cold permafrost layer. Darcy's law is adopted and we assume the equation of state proposed by Merker *et al.* (1979). Predictions, particularly those for the width-to-depth ratio of the patterned ground, are reported. In chapter 7 we present the analysis for the onset of cellular convection in a saturated, horizontal porous layer which is subject to a *time–periodic* boundary condition. We apply this to the formation of patterned ground where the soil surface is subject to periodic solar radiation heating and examine the effect varying frequency and modulation amplitude have on our predictions. In chapter 8 we discuss an analysis appropriate to the formation of patterned ground under water. We perform a linear stability analysis for a fluid layer overlying a saturated porous layer of finite depth, and present predictions for the critical Rayleigh numbers and width-to-depth ratios of the polygons. In addition, we plot eigenfunctions and streamlines for the fluid motions at the onset of convection.

Finally, chapter 9 presents a generalized energy analysis for rotating fluid

layer which is subject to internal heating. We demonstrate that rotation has a stabilizing effect even when a heat source is present. The material in chapters 2, 5 and 7 are taken from articles by McKay (1990, 1991, 1992). Similarly, chapters 4, 6 and 8 may be found in McKay & Straughan (1991, 1992a,b).

Chapter 2

Continuous dependence on the heat supply for the Boussinesq equations with a cubic density law

2.1 Introduction

In this chapter we consider the solution to the equations of motion for an incompressible, heat conducting, viscous fluid under a Boussinesq approximation, although the equation of state adopted is given by the cubic model

$$\rho = \rho_0(1 + AT - BT^2 + CT^3), \tag{2.1}$$

where ρ is density of the fluid, ρ_0 is the density at $0°C$, T is the temperature of the fluid, and A, B and C are constants. In particular we shall establish continuous dependence of the solution on the heat source both forward and backward in time. In Merker *et al.* (1979) the writers studied convection in a horizontal water layer. They calculated that a cubic law similar to (2.1) above, for particular constants A, B and C, predicted the onset of convection 8% more accurately than the quadratic model suggested by Veronis (1963). As a result we adopt a cubic model in our more general problem. (The use of relation (2.1) in more general convection problems is discussed in chapter 4.)

A number of writers have produced continuous dependence results for several different problems. Knops & Payne (1968) established continuous dependence on the initial data for the Navier-Stokes equations backward in time. Galdi & Rionero (1983) and Galdi & Straughan (1988) considered similar forward and backward problems for exterior domains. In addition Song (1988) produced inequalties establishing continuous dependence on density and on the coefficient of kinematic viscosity. As mentioned in chapter 1, Roberts (1967)

and Tritton & Zarraga (1967) studied convection in a plane layer of Boussinesq fluid with internal heating. However, they did not discuss continuous dependence upon an arbitrary, bounded heat source. Such continuous dependence is of importance in several practical contexts, e.g. geothermal reservoir engineering, where the current data and equations are used in order to extrapolate back to previous times.

In section 2.2 we shall study the forward in time dependence. An ordinary energy argument is used to establish continuous dependence on the heat supply. However this argument fails in section 2.3 which studies the backward in time dependence. If we use an energy method in the backward in time example, then we are unable to produce dependence upon the heat supply alone. In addition, the backward in time problem is improperly posed because the solution does not depend continuously upon the final data, unless the set of solutions is restricted. As a result the backward problem is more complicated than the forward one. In order to overcome this difficulty we employ a logarithmic convexity argument. This argument has been used in several papers, e.g. Knops & Payne (1968), Payne (1971), Lavrentiev (1967), and involves twice differentiating a functional $F(t)$ (to be defined in section 2.3) and obtaining an estimate for its log. This inequality can then be integrated in order to establish a continuous dependence result.

2.2 Continuous dependence on the heat supply forward in time

The equations of motion for a heat conducting, linear, viscous fluid, with a cubic density law, forward in time are:

$$v_{i,t} + v_j v_{i,j} = -p_{,i} + \Delta v_i + b_i(1 + AT - BT^2 + CT^3), \tag{2.2}$$

$$v_{i,i} = 0, \tag{2.3}$$

$$T_{,t} + v_i T_{,i} = \Delta T + Q\,, \tag{2.4}$$

where $\mathbf{v}$, $\mathbf{b}$ are the velocity and body force, p is pressure, T is temperature, $Q(\mathbf{x},t)$ is heat supply, and standard indicial notation is employed. Without loss of generality we have set the viscosity, thermal diffusivity and density equal to unity, and the body force is taken constant.

Equations (2.2)–(2.4) are defined on the domain $\Omega \times (0,\mathcal{T}]$ where $\Omega \subset \mathbf{R}^3$ is a bounded domain representing the volume occupied by the fluid. Let Γ denote the boundary of Ω which is assumed sufficiently smooth to allow applications of the divergence theorem.

The boundary conditions we consider are

$$\begin{aligned} v_i(\mathbf{x},t) &= \bar{v}_i(\mathbf{x},t) \qquad \text{on} \qquad \Gamma \times [0,\mathcal{T}], \\ T(\mathbf{x},t) &= T_1(\mathbf{x},t) \qquad \text{on} \qquad \Gamma \times [0,\mathcal{T}]. \end{aligned} \tag{2.5}$$

If $\bar{\mathbf{v}} \cdot \mathbf{n} = 0$ on Γ_2 then we may consider an alternative boundary condition on Γ, where $(2.5)_2$ holds on $\Gamma_1 \times [0,\mathcal{T}]$ and

$$\frac{\partial T}{\partial \mathbf{n}}(\mathbf{x},t) = T_2(\mathbf{x},t) \qquad \text{on} \qquad \Gamma_2 \times [0,\mathcal{T}], \tag{2.6}$$

where $\mathbf{n}$ is the unit normal to Γ, $\Gamma_1 \cup \Gamma_2 = \Gamma$ and $\Gamma_1 \cap \Gamma_2 = \emptyset$.

The initial conditions are

$$\left.\begin{aligned} v_i(\mathbf{x},0) &= v_i^0(\mathbf{x}) \\ T(\mathbf{x},0) &= T_0(\mathbf{x}) \end{aligned}\right\} \qquad \text{in} \qquad \Omega \times \{0\}, \tag{2.7}$$

where $\bar{\mathbf{v}}$, $\mathbf{v}^0$, T_0, T_1 and T_2 are prescribed functions of the arguments indicated.

Let $\chi = (\mathbf{v}, T, p)$ and $\chi^* = (\mathbf{v}^*, T^*, p^*)$ be two classical solutions to equations (2.2)–(2.4) with boundary-initial values (2.5)–(2.7); the unstarred quantities

denote the base flow and the starred quantities the perturbed flow. Assume χ, χ^* satisfy (2.2)–(2.7) for the same data $\bar{\mathbf{v}}$, $\mathbf{v}^0$, T_0, T_1, T_2 and the same body force $\mathbf{b}$, but different heat sources $Q(\mathbf{x},t)$, $Q^*(\mathbf{x},t)$. Also we assume $\mathbf{v}$, $\mathbf{v}^*$, T, T^* are $C^2(\Omega \times [0,\mathcal{T}])$.

Define

$$u_i = v_i^* - v_i\,, \qquad \theta = T^* - T, \qquad \pi = p^* - p, \qquad q = Q^* - Q.$$

Then these variables satisfy

$$u_{i,t} + v_j^* u_{i,j} + u_j v_{i,j} = -\pi_{,i} + \Delta u_i - B_i\theta\,, \tag{2.8}$$

$$u_{i,i} = 0\,, \tag{2.9}$$

$$\theta_{,t} + v_i^*\theta_{,i} + u_i T_{,i} = \Delta\theta + q\,, \tag{2.10}$$

where

$$B_i = -Ab_i + Bb_i(T^* + T) - Cb_i({T^*}^2 + T^*T + T^2),$$

and

$$\begin{aligned} u_i &= 0 \qquad \text{on} \qquad \Gamma \times [0,\mathcal{T}], \\ \theta &= 0 \qquad \text{on} \qquad \Gamma_1 \times [0,\mathcal{T}], \\ \frac{\partial\theta}{\partial\mathbf{n}} &= 0 \qquad \text{on} \qquad \Gamma_2 \times [0,\mathcal{T}], \end{aligned} \tag{2.11}$$

where $\Gamma_2 = \emptyset$ unless $\bar{\mathbf{v}}\cdot\mathbf{n} = 0$ on $\Gamma_2 \times [0,\mathcal{T}]$.

We say a vector $\mathbf{w}$ is of class $\mathcal{V}$, if for some prescribed constant a,

$$\sup_{\Omega\times[0,\mathcal{T}]} w_i w_i \le a^2\,.$$

A scalar R is of class $\mathcal{W}$, if for some prescribed constant m,

$$\sup_{\Omega\times[0,\mathcal{T}]} R^2 \le m^2\,.$$

In terms of the above, we are interested in a function $(\mathbf{u},\theta) \in (C^2(\bar{\Omega}\times[0,\mathcal{T}]))^4$, with $\mathbf{v} \in \mathcal{V}$ and T, $T^* \in \mathcal{W}$. By boundedness of T, T^* we also have a bound

$$\sup_{\Omega\times[0,\mathcal{T}]} B_i B_i \le D^2$$

for some constant D.

To establish continuous dependence our energy analysis begins by multiplying (2.8) by u_i and integrating over Ω to give

$$\frac{1}{2}\frac{d}{dt}\|\mathbf{u}\|^2 + <v_j^* u_{i,j} u_i> + <u_i u_j v_{i,j}> = -<\pi_{,i} u_i> + <u_i \Delta u_i> - <B_i \theta u_i>, \tag{2.12}$$

where

$$<f> = \int_\Omega f(\mathbf{x})\, d\mathbf{x}$$

and $\|.\|$ is the $L^2(\Omega)$ norm.

Next, multiply (2.10) by θ and integrate over Ω to give

$$\frac{1}{2}\frac{d}{dt}\|\theta\|^2 + <v_i^* \theta \theta_{,i}> + <\theta u_i T_{,i}> = <\theta \Delta \theta> + <q\theta>\ . \tag{2.13}$$

Expressions (2.12) and (2.13) may be simplified using (2.9), (2.11) and the divergence theorem:

$$\begin{aligned} <v_j^* u_{i,j} u_i> &= <\left(v_j^* u_i u_i\right)_{,j}> - <v_{j,j}^* u_i u_i> - <v_j^* u_{i,j} u_i> \\ &= -<v_j^* u_{i,j} u_i>\ . \end{aligned}$$

Therefore

$$<v_j^* u_{i,j} u_i> = 0\,.$$

Similarly

$$<v_i^* \theta \theta_{,i}> = 0\,.$$

Using the Cauchy-Schwarz inequality we may show that, for α, β, γ and $\delta > 0$ to be chosen,

$$-<u_i u_j v_{i,j}> = <u_{i,j} u_j v_i> \leq \frac{a^2}{2\alpha}\|\mathbf{u}\|^2 + \frac{\alpha}{2}\|\nabla \mathbf{u}\|^2\,;$$

$$-<u_i T_{,i} \theta> = <u_i T \theta_{,i}> \leq \frac{m^2}{2\beta}\|\mathbf{u}\|^2 + \frac{\beta}{2}\|\nabla \theta\|^2\,;$$

$$<q\theta> \leq \frac{1}{2\delta}\|q\|^2 + \frac{\delta}{2}\|\theta\|^2\,;$$

$$-<B_i u_i \theta> \leq \frac{D}{2\gamma}\|\mathbf{u}\|^2 + \frac{D\gamma}{2}\|\theta\|^2\,;$$

$$<\pi_{,i} u_i> = <(\pi u_i)_{,i}> - <\pi u_{i,i}> = 0\,;$$

and finally

$$< u_i \Delta u_i > = -\|\nabla \mathbf{u}\|^2 , \qquad < \theta \Delta \theta > = -\|\nabla \theta\|^2 .$$

Let

$$E(t) = \frac{1}{2}\|\mathbf{u}\|^2 + \frac{1}{2}\|\theta\|^2.$$

Then from equations (2.12), (2.13) and the above equalities/inequalities,

$$\begin{aligned} \frac{dE}{dt} \leq & -\|\nabla \mathbf{u}\|^2 - \|\nabla \theta\|^2 + \left(\frac{a^2}{2\alpha} + \frac{m^2}{2\beta} + \frac{D}{2\gamma}\right)\|\mathbf{u}\|^2 \\ & + \frac{\alpha}{2}\|\nabla \mathbf{u}\|^2 + \frac{\beta}{2}\|\nabla \theta\|^2 + \frac{D\gamma}{2}\|\theta\|^2 + \frac{1}{2\delta}\|q\|^2 + \frac{\delta}{2}\|\theta\|^2 . \end{aligned} \tag{2.14}$$

Choose $\alpha = \beta = 2$ to remove $\|\nabla \mathbf{u}\|^2, \|\nabla \theta\|^2$ terms; and choose $\delta = \frac{1}{2}, \gamma = 1$. Then (2.14) becomes

$$\frac{dE}{dt} \leq \left(\frac{a^2}{4} + \frac{m^2}{4} + \frac{D}{2}\right)\|\mathbf{u}\|^2 + \left(\frac{D}{2} + \frac{1}{4}\right)\|\theta\|^2 + \|q\|^2 .$$

Let $c_3 = \max\left\{\frac{a^2}{2} + \frac{m^2}{2} + D, D + \frac{1}{2}\right\}$ so that

$$\frac{dE}{dt} \leq c_3 E + \|q\|^2.$$

If we define

$$M = \sup_{[0,T]} \|q\|^2,$$

upon integration we find

$$E(t) \leq e^{c_3 t} E(0) + \frac{1}{c_3} M \left(e^{c_3 t} - 1\right).$$

Since we are primarily interested in continuous dependence on the heat source, we may choose the initial data such that $E(0) = 0$. So if we set

$$K(t) = \frac{1}{c_3}\left(e^{c_3 t} - 1\right),$$

we obtain

$$E(t) \leq K(t) M . \tag{2.15}$$

Inequality (2.15) establishes continuous dependence, forward in time, on the heat supply in energy measure.

2.3 Continuous dependence on the heat supply backward in time

The equations of motion for a heat-conducting, linear, viscous fluid with the cubic density law, backward in time, are:

$$v_{i,t} = v_i v_{i,j} + p_{,i} - \Delta v_i - b_i(1 + AT - BT^2 + CT^3)\,, \tag{2.16}$$

$$v_{i,i} = 0\,, \tag{2.17}$$

$$T_{,t} = v_i T_{,i} - \Delta T - Q\,. \tag{2.18}$$

Equations (2.16)–(2.18) are defined on the domain $\Omega \times (0, \mathcal{T}]$ as described in section 2.2. Once again, without loss of generality, we have set the viscosity, thermal diffusivity and density equal to unity, and the body force is taken constant.

Boundary condition (2.5) is chosen as before. Boundary condition (2.6) becomes

$$\frac{\partial T}{\partial \mathbf{n}} = T_2(\mathbf{x}, t) \qquad \text{on} \quad \Gamma_2 \times [0, \mathcal{T}] \text{ if } \bar{v}_i \equiv 0 \text{ on } \Gamma_2\,, \tag{2.19}$$

where $\mathbf{n}$ is unit normal to Γ, $\Gamma_1 \cup \Gamma_2 = \Gamma$ and $\Gamma_1 \cap \Gamma_2 = \emptyset$. The "initial" condition we consider is (2.7).

Classical solutions χ, χ^* are once again the unperturbed and perturbed solutions as described in the previous section. Both solutions correspond to the same data $\bar{\mathbf{v}}$, $\mathbf{v}^0$, T_0, T_1, T_2 and heat sources $Q(\mathbf{x}, t)$, $Q^*(\mathbf{x}, t)$.

Define

$$u_i = v_i^* - v_i\,, \qquad \theta = T^* - T\,, \qquad \pi = p^* - p\,, \qquad q = Q^* - Q\,.$$

Then from (2.16)–(2.19), (2.6) and (2.7) these variables satisfy

$$u_{i,t} = v_j^* u_{i,j} + u_j v_{i,j} + \pi_{,i} - \Delta u_i + B_i \theta\,, \tag{2.20}$$

$$u_{i,i} = 0\,, \tag{2.21}$$

$$\theta_{,t} = v_i^* \theta_{,i} + u_i T_{,i} - \Delta\theta - q \tag{2.22}$$

where

$$B_i(\mathbf{x}, t) = -[Ab_i - Bb_i(T^* + T) + Cb_i(T^{*2} + T^* T + T^2)].$$

The boundary and initial conditions are

$$\begin{aligned} u_i &= 0 \quad \text{on} \quad \Gamma \times [0,\mathcal{T}]\,, \\ \theta &= 0 \quad \text{on} \quad \Gamma_1 \times [0,\mathcal{T}]\,, \\ \frac{\partial \theta}{\partial \mathbf{n}} &= 0 \quad \text{on} \quad \Gamma_2 \times [0,\mathcal{T}]\,, \\ u_i = \theta &= 0 \quad \text{at} \quad t = 0, \end{aligned} \tag{2.23}$$

where $\Gamma_2 = \emptyset$ unless $\bar{v}_i \equiv 0$ on Γ_2.

We say a vector $\mathbf{w}$ is of class $\mathcal{A}$ if for some prescribed constant a,

$$\sup_{\Omega \times [0,\mathcal{T}]} w_i w_i \leq a^2\,,$$

and of class $\mathcal{B}$ if for some prescribed constant b,

$$\sup_{[0,\mathcal{T}]} \left\{ \|w_{i,t} w_{i,t}\|_{\frac{3}{2}} + \|w_{[i,j]} w_{[i,j]}\|_{\frac{3}{2}} \right\} \leq b^2,$$

where $\|.\|_p$ denotes the norm on $L^p(\Omega)$ and $a_{[i,j]} = \frac{1}{2}(a_{i,j} - a_{j,i})$. A scalar S is of class $\mathcal{M}$ or $\mathcal{N}$ respectively, if for prescribed constants m and n,

$$\sup_{\Omega \times [0,\mathcal{T}]} S^2 + \sup_{\Omega \times [0,\mathcal{T}]} |\nabla S|^2 \leq m^2 \tag{2.24}$$

or

$$\sup_{\Omega \times [0,\mathcal{T}]} |\nabla S|^2 + \sup_{[0,\mathcal{T}]} \|S_{,t} S_{,t}\|_{\frac{3}{2}} \leq n^2. \tag{2.25}$$

We also make the unrestrictive assumption that a bound

$$\sup_{\Omega \times [0,\mathcal{T}]} (|\mathbf{B}| + |Q + Q^*|) \leq \beta \tag{2.26}$$

is known for the body force and the sum of heat sources for some prescribed constant β. (Essentially we are assuming Q, Q^*, T and T^* are bounded in modulus on $\Omega \times [0,\mathcal{T}]$, and using the fact that $\mathbf{b}$ is constant to produce bounds for $|\mathbf{B}|$ and $|Q + Q^*|$.)

We are interested in a function $(\mathbf{u}, \theta) \in (C^2(\bar{\Omega} \times [0,\mathcal{T}]))^4$ with $\mathbf{v}^* \in \mathcal{A}$, $\mathbf{v} \in \mathcal{A} \cap \mathcal{B}$, $T^* \in \mathcal{M}$ and $T \in \mathcal{M} \cap \mathcal{N}$.

Define the functional $F(t)$ by

$$F(t) = \int_0^t \left(\|\mathbf{u}\|^2 + \|\theta\|^2\right) d\eta + \int_0^{\mathcal{T}} \left(\|q\|^2 + \|q_{,t}\|^2\right) dt\,. \tag{2.27}$$

Then using (2.20) and (2.22),

$$\begin{aligned} F'(t) &= 2\int_0^t \left(< u_i u_{i,\eta} > + < \theta\theta_{,\eta} >\right) d\eta \\ &= 2\int_0^t < u_i(u_j v_{i,j} - \Delta u_i + B_i\theta) > \; d\eta \\ &\qquad + 2\int_0^t < \theta(u_i T_{,i} - \Delta\theta - q) > \; d\eta\,. \end{aligned} \tag{2.28}$$

Using the conditions of (2.23) and the divergence theorem we obtain

$$< u_i \Delta u_i > = -\|\nabla \mathbf{u}\|^2\,, \qquad < \theta\Delta\theta > = -\|\nabla\theta\|^2\,.$$

So from (2.28),

$$\begin{aligned} -\int_0^t \left(\|\nabla\mathbf{u}\|^2 + \|\nabla\theta\|^2\right) d\eta &= -\frac{1}{2}F'(t) + \int_0^t < u_i u_j v_{i,j} > \; d\eta + \int_0^t < B_i u_i \theta > \; d\eta \\ &\qquad + \int_0^t < \theta u_i T_{,i} > \; d\eta - \int_0^t < q\theta > \; d\eta\,. \end{aligned} \tag{2.29}$$

Furthermore, differentiating (2.28) we have

$$\begin{aligned} F''(t) &= 2\int_0^t \left(< u_{i,s}u_{i,s} > + < \theta_{,s}\theta_{,s} > + < u_i u_{i,ss} > + < \theta\theta_{,ss} >\right) ds \\ &= 2\int_0^t \left(\|\mathbf{u}_{,s}\|^2 + \|\theta_{,s}\|^2\right) ds + 2\int_0^t < \theta\frac{\partial}{\partial s}(v_i^*\theta_{,i} + u_i T_{,i} - \Delta\theta - q) > \; ds \\ &\qquad + 2\int_0^t < u_i\frac{\partial}{\partial s}(v_j^* u_{i,j} + u_j v_{i,j} + \pi_{,i} - \Delta u_i + B_i\theta) > \; ds \end{aligned}$$

$$= 2\int_0^t \left(\|\mathbf{u}_{,s}\|^2 + \|\theta_{,s}\|^2\right) ds + 2\int_0^t < u_i(v^*_{j,s}u_{i,j} + v^*_j u_{i,js} + u_{j,s}v_{i,j}$$
$$+ u_j v_{i,js} + \pi_{,is} - \Delta u_{i,s} + B_{i,s}\theta + B_i\theta_{,s}) > \, ds$$
$$+ 2\int_0^t < \theta(v^*_i\theta_{,is} + v^*_{i,s}\theta_{,i} + u_{i,s}T_{,i} + u_i T_{,is} - \Delta\theta_{,s} - q_{,s}) > \, ds. \qquad (2.30)$$

Using the divergence theorem, equations (2.20)–(2.22) and boundary conditions (2.23) we can derive the following integrals:-

$$< \theta v^*_{i,s}\theta_{,i} > = < (\theta v^*_{i,s}\theta)_{,i} - \theta_{,i}v^*_{i,s}\theta > = \, - < \theta_{,i}v^*_{i,s}\theta > \, .$$

Therefore

$$< \theta v^*_{i,s}\theta_{,i} > = \, 0 \, .$$

Similarly

$$< u_i v^*_{j,s}u_{i,j} > = \, 0 \, ; \qquad < u_i\pi_{,is} > = \, 0 \, ;$$
$$< \theta(\Delta\theta)_{,s} > = < \Delta\theta\theta_{,s} > = \, - < \theta_{,s}(\theta_{,s} - v^*_i\theta_{,i} - u_i T_{,i} + q) > \, ;$$
$$< u_i\Delta u_{i,s} > = \, - < u_{i,s}(u_{i,s} - v^*_j u_{i,j} - u_j v_{i,j} + B_i\theta) > \, ;$$
$$< u_i v^*_j u_{i,js} > = \, - < u_{i,j}v^*_j u_{i,s} > \, ; \qquad < u_i u_j v_{i,js} > = \, - < u_{i,j}u_j v_{i,s} >$$

and

$$< \theta u_i T_{,is} > = \, - < \theta_{,i}u_i T_{,s} > \, .$$

These integrals may now be employed to rearrange (2.30) so that we find

$$F''(t) = 4\int_0^t \left(\|\mathbf{u}_{,s}\|^2 + \|\theta_{,s}\|^2\right) ds - 4\int_0^t < v^*_j(u_{i,j}u_{i,s} + \theta_{,j}\theta_{,s}) > \, ds$$
$$+ 2\int_0^t < u_i\theta B_{i,s} > \, ds - 4\int_0^t < u_{i,s}u_j v_{[i,j]} > \, ds$$
$$- 2\int_0^t < u_j(v_{i,s}u_{i,j} + T_{,s}\theta_{,j}) > \, ds + 2\int_0^t \left(< q\theta_{,s} > - < \theta q_{,s} >\right) ds$$
$$+ 2\int_0^t < (u_i\theta_{,s} - \theta u_{i,s})(B_i - T_{,i}) > \, ds \, . \qquad (2.31)$$

Next, let

$$\chi_i = u_{i,t} - \frac{1}{2} v_k^* u_{i,k} - \frac{1}{2} u_k v_{[i,k]} ,$$

$$\Phi = \theta_{,t} - \frac{1}{2} v_m^* \theta_{,m} .$$

Then

$$\|\chi_i\|^2 = \|\mathbf{u}_{,t}\|^2 + \frac{1}{4} < (v_k^* u_{i,k} + u_k v_{[i,k]})(v_j u_{i,j} + u_j v_{[i,j]}) >$$
$$- < v_k^* u_{i,t} u_{i,k} > - < u_k u_{i,t} v_{[i,k]} > ,$$

$$\|\Phi\|^2 = \|\theta_{,t}\|^2 + \frac{1}{4} < v_m^* \theta_{,m} v_j^* \theta_{,j} > - < \theta_{,t} v_m^* \theta_{,m} >$$

and

$$< u_i \chi_i > = < u_i (u_{i,t} - \frac{1}{2} v_k^* u_{i,k} - \frac{1}{2} u_k v_{[i,k]}) > = < u_i u_{i,t} >$$

using the divergence theorem and conditions (2.23). Similarly

$$< \theta \Phi > = < \theta \theta_{,t} > .$$

Therefore

$$\int_0^t \left(< u_i \chi_i > + < \theta \Phi > \right) ds = \frac{1}{2} F' .$$

In order to employ a logarithmic convexity technique, we first calculate $FF'' - (F')^2$. The result is

$$FF'' - (F')^2 = 4S^2 + \sum_{i=1}^{4} I_i + \sum_{i=1}^{3} J_i$$
$$+ 4 \left(\int_0^T \left(\|q\|^2 + \|q_{,t}\|^2 \right) dt \right) \left(\int_0^t \left(\|\chi_i\|^2 + \|\Phi\|^2 \right) ds \right) , \tag{2.32}$$

where

$$S^2 = \left(\int_0^t \left(\|\mathbf{u}\|^2 + \|\theta\|^2 \right) ds \right) \left(\int_0^t \left(\|\chi_i\|^2 + \|\Phi\|^2 \right) ds \right) - \left[\int_0^t \left(< u_i \chi_i > + < \theta \Phi > \right) ds \right]^2$$

is non-negative due to the Cauchy-Schwarz inequality; and

$$I_1 = -2F \int_0^t < u_j(v_{i,s}u_{i,j} + T_{,s}\theta_{,j}) > \, ds \,,$$

$$I_2 = -F \int_0^t < (v_j^* u_{i,j} + u_j v_{[i,j]})(v_k^* u_{i,k} + u_k v_{[i,k]}) + v_j^* v_m^* \theta_{,j}\theta_{,m} > \, ds \,,$$

$$I_3 = -2F \int_0^t < \theta q_{,s} > \, ds \,,$$

$$I_4 = 2F \int_0^t < u_i \theta B_{i,s} > \, ds \,,$$

$$J_1 = 2F \int_0^t < (B_i - T_{,i}) u_i \theta_{,s} > \, ds \,,$$

$$J_2 = -2F \int_0^t < (B_i - T_{,i}) \theta u_{i,s} > \, ds \,,$$

$$J_3 = 2F \int_0^t < q\theta_{,s} > \, ds.$$

We shall now bound I_1, I_2, J_1 and J_2 using Hölder's inequality, the Cauchy-Schwarz inequality and the arithmetic-geometric mean inequality. In addition, the Sobolev inequality

$$\|\mathbf{u}\|_6 \leq \gamma \|\nabla \mathbf{u}\| \,,$$

for a positive constant γ, will also be used. Let $k^2 = b^2 + n^2$. Then

$$\begin{aligned} I_1 &\geq -F \int_0^t < u_j u_j v_{i,s} v_{i,s} + u_{i,j} u_{i,j} + u_j u_j T_{,s} T_{,s} + \theta_{,j}\theta_{,j} > \, ds \\ &\geq -F \int_0^t < (u_j u_j)^3 >^{\frac{1}{3}} \left\{ < (v_{i,s} v_{i,s})^{\frac{3}{2}} >^{\frac{2}{3}} + < (T_{,s})^3 >^{\frac{2}{3}} \right\} ds \\ &\qquad - F \int_0^t \left(\|\nabla \mathbf{u}\|^2 + \|\nabla \theta\|^2 \right) ds \end{aligned}$$

$$\geq -F \int_0^t \left((1+k^2\gamma^2)\|\nabla \mathbf{u}\|^2 + \|\nabla\theta\|^2\right) ds\,. \tag{2.33}$$

Using the following inequalities in the interval $[0,\mathcal{T}]$,

$$\begin{aligned}
&< (v_j^* u_{i,j} + u_j v_{[i,j]})(v_k^* u_{i,k} + u_k v_{[i,k]}) > \\
&\qquad \leq 2a^2\|\nabla \mathbf{u}\|^2 + 2 < u_j u_k v_{[i,j]} v_{[i,k]} > \\
&\qquad \leq 2a^2\|\nabla \mathbf{u}\|^2 + 2 < (u_i u_i)^3 >^{\frac{1}{3}} < \left(v_{[i,j]} v_{[i,j]}\right)^{\frac{3}{2}} >^{\frac{2}{3}} \\
&\qquad \leq 2(a^2 + b^2\gamma^2)\|\nabla \mathbf{u}\|^2\,,
\end{aligned}$$

it follows that

$$I_2 \geq -2(a^2+b^2\gamma^2)F \int_0^t \|\nabla \mathbf{u}\|^2\, ds - a^2 F \int_0^t \|\nabla\theta\|^2\, ds\,. \tag{2.34}$$

Set

$$\xi_i = B_i - T_{,i} = -Ab_i + Bb_i(T^* + T) - Cb_i(T^{*2} + T^*T + T^2) - T_{,i}\,.$$

Using the bounds on $\mathbf{B}$, T and T^* given in (2.24)–(2.26), we may assume that

$$\sup_{\Omega\times[0,\mathcal{T}]} \xi_i\xi_i \leq 2D^2\,, \qquad \text{where} \qquad D^2 = \beta^2 + n^2\,.$$

This inequality may now be used in order to bound J_1 and J_2.

$$\begin{aligned}
J_1 &= 2F \int_0^t < \xi_i u_i (\Phi + \frac{1}{2} v_m^* \theta_{,m}) > \, ds \\
&\geq -\frac{F}{2} \int_0^t < \xi_i \xi_i u_i u_i > \, ds - \frac{F}{2} \int_0^t < v_m^* v_m^* \theta_{,m} \theta_{,m} > \, ds \\
&\qquad\qquad - 2F(2D^2)^{\frac{1}{2}} \left(\int_0^t \|\Phi\|^2\, ds \int_0^t \|\mathbf{u}\|^2\, ds \right)^{\frac{1}{2}} \\
&\geq -D^2 F \int_0^t \|\mathbf{u}\|^2\, ds - \frac{1}{2} F a^2 \int_0^t \|\nabla\theta\|^2\, ds - 2^{\frac{3}{2}} FD \left(\int_0^t \|\Phi\|^2\, ds \int_0^t \|\mathbf{u}\|^2\, ds \right)^{\frac{1}{2}},
\end{aligned} \tag{2.35}$$

$$J_2 = -2F \int_0^t <\xi_i \theta(\chi_i + \frac{1}{2} v_k^* u_{i,k} + \frac{1}{2} u_k v_{[i,k]})> \, ds$$

$$\geq -2^{\frac{3}{2}} DF \Big(\int_0^t \|\theta\|^2 \, ds \int_0^t \|\chi_i\|^2 \, ds \Big)^{\frac{1}{2}} - 2FD^2 \int_0^t \|\theta\|^2 \, ds$$

$$- \frac{1}{2}(a^2 + b^2\gamma^2) F \int_0^t \|\nabla \mathbf{u}\|^2 \, ds \, . \tag{2.36}$$

Using the Cauchy-Schwarz inequality, for positive constants α and λ to be chosen,

$$J_3 = 2F \int_0^t <q\Phi> \, ds + F \int_0^t <q v_m^* \theta_{,m}> \, ds$$

$$\geq -2F \Big(\int_0^{\mathcal{T}} \|q\|^2 \, dt \int_0^t \|\Phi\|^2 \, ds \Big)^{\frac{1}{2}}$$

$$- F \Big(\frac{1}{2\alpha} \int_0^{\mathcal{T}} <q v_m^* q v_m^*> \, dt + \frac{\alpha}{2} \int_0^t \|\nabla \theta\|^2 \, ds \Big)$$

$$\geq -\frac{F^2 a^2}{2\alpha} - \frac{F\alpha}{2} \int_0^t \|\nabla \theta\|^2 \, ds - \frac{F^2}{\lambda} - \lambda \int_0^{\mathcal{T}} \|q\|^2 \, dt \int_0^t \|\Phi\|^2 \, ds \, .$$

Choose $\alpha = 2$, $\lambda = 4$ to give

$$J_3 \geq -\frac{F^2}{4}(1 + a^2) - F \int_0^t \|\nabla \theta\|^2 \, ds - 4 \int_0^{\mathcal{T}} \|q\|^2 \, dt \int_0^t \|\Phi\|^2 \, ds \, . \tag{2.37}$$

Similarly,

$$I_3 \geq -F \int_0^t \|\theta\|^2 \, ds - F \int_0^{\mathcal{T}} \|q_{,t}\|^2 \, dt \, . \tag{2.38}$$

In order to produce an estimate for I_4 we must first consider the $B_{i,s}$ term which occurs in its definition:

$$B_{i,s} = B b_i (T^* + T)_{,s} - C b_i [(2T^* + T) T^*_{,s} + (2T + T^*) T_{,s}]$$

$$= b_i [B - C(2T + T^*)] T_{,s} + b_i [B - C(2T^* + T)] T^*_{,s} .$$

Since T^*, T are bounded in modulus, we shall assume there exists positive constants K, L and M say, such that

$$K = \sup_{\Omega\times[0,T]} |[B - C(2T + T^*)]|,$$
$$L = \sup_{\Omega\times[0,T]} |[B - C(2T^* + T)]|,$$

and

$$M = \max\{K, L\}.$$

We can also assume, without loss of generality, that b_i is bounded by the same bound as B_i,

$$\text{i.e.} \qquad \sup_{\Omega\times[0,T]} |b_i| \leq \beta\,.$$

Using the Cauchy-Schwarz inequality and boundary condition (2.23) we can derive an estimate for I_4:

$$\begin{aligned}
I_4 &= 2F \int_0^t < u_i\theta B_{i,s} > \, ds \\
&= 2F \int_0^t < u_i\theta b_i(B - C[2T + T^*])(v_iT_{,i} - \Delta T - Q) \\
&\qquad + u_i\theta b_i(B - C[2T^* + T])(v_i^*T_{,i}^* - \Delta T^* - Q^*) > \, ds \\
&\geq -4\beta MmF \int_0^t \left(\|\nabla\theta\|\|\mathbf{u}\| + \|\theta\|\|\nabla\mathbf{u}\|\right) ds - 2F\beta M(2am + \beta) \int_0^t \|\theta\|\|\mathbf{u}\| \, ds \\
&\geq -2\beta M(am + \beta)F \int_0^t \left(\|\theta\|^2 + \|\mathbf{u}\|^2\right) ds \\
&\qquad - 4M\beta m^2 F \int_0^t \left(\|\nabla\theta\|^2 + \|\nabla\mathbf{u}\|^2\right) ds\,. \qquad (2.39)
\end{aligned}$$

Having produced bounds for I_α and J_β, we now derive

$$\begin{aligned}
FF'' - (F')^2 \geq 4S^2 - c_1F \int_0^t \|\nabla\mathbf{u}\|^2 \, ds - c_2F \int_0^t \|\nabla\theta\|^2 \, ds \\
- c_3F^2 - 2^{3/2}DFH\,,
\end{aligned} \qquad (2.40)$$

where we have defined

$$c_1 = 1 + k^2\gamma^2 + \frac{5}{2}(a^2 + b^2\gamma^2) + 4M\beta m^2 ,$$
$$c_2 = 2 + \frac{3}{2}a^2 + 4M\beta m^2 ,$$
$$c_3 = 2\beta M(am + \beta) + \frac{1}{4}a^2 + 2D^2 + \frac{5}{4}$$

and

$$H = \left(\int_0^t \|\Phi\|^2 \, ds \int_0^t \|\mathbf{u}\|^2 \, ds\right)^{\frac{1}{2}} + \left(\int_0^t \|\theta\|^2 \, ds \int_0^t \|\chi_i\|^2 \, ds\right)^{\frac{1}{2}} .$$

It was shown earlier that

$$S^2 + \frac{1}{4}(F')^2 = \left(\int_0^t (\|\mathbf{u}\|^2 + \|\theta\|^2) \, ds\right)\left(\int_0^t (\|\chi_i\|^2 + \|\Phi\|^2) \, ds\right) .$$

So if we utilize the inequality $(a+b) \leq \sqrt{2}(a^2+b^2)^{1/2}$, we may show that

$$\begin{aligned} S^2 + \frac{1}{4}(F')^2 &\geq \int_0^t \|\mathbf{u}\|^2 \, ds \int_0^t \|\Phi\|^2 \, ds + \int_0^t \|\theta\|^2 \, ds \int_0^t \|\chi_i\|^2 \, ds \\ &\geq \frac{1}{2}\left[\left(\int_0^t \|\mathbf{u}\|^2 \, ds \int_0^t \|\Phi\|^2 \, ds\right)^{\frac{1}{2}} + \left(\int_0^t \|\theta\|^2 \, ds \int_0^t \|\chi_i\|^2 \, ds\right)^{\frac{1}{2}}\right]^2 \\ &\geq \frac{1}{2}H^2 . \end{aligned}$$

Therefore

$$-H \quad \geq \quad -2^{1/2}\left(S + \frac{F'}{2}\right) \quad = \quad -2^{1/2}S - 2^{-1/2}F' .$$

Thus

$$-2^{3/2}DHF \geq -4DFS - 2DFF' . \tag{2.41}$$

Using (2.29), integration by parts and the arithmetic-geometric mean inequality

we can obtain

$$-\int_0^t \left(\|\nabla \mathbf{u}\|^2 + \|\nabla\theta\|^2\right) ds$$

$$\geq -\frac{1}{2}F' - \frac{1}{2}\int_0^t \left(\|\nabla \mathbf{u}\|^2 + \|\nabla\theta\|^2\right) ds - \left(\frac{a^2}{2} + \frac{m^2}{2} + \frac{\beta}{2}\right)\int_0^t \|\mathbf{u}\|^2 \, ds$$

$$- \left(\frac{\beta}{2} + \frac{1}{2}\right)\int_0^t \|\theta\|^2 \, ds - \frac{1}{2}\int_0^{\mathcal{T}} \|q\|^2 \, dt$$

which in turn gives

$$-\int_0^t \left(\|\nabla \mathbf{u}\|^2 + \|\nabla\theta\|^2\right) ds \geq -F' - c_4 F\,, \tag{2.42}$$

where $c_4 = \max\{a^2 + m^2 + \beta, 1 + \beta\}$. Estimates (2.33)–(2.39), (2.41) and (2.42) are now employed in (2.32) so that we may derive

$$\begin{aligned} FF'' - (F')^2 &\geq 4S^2 - c_5 F'F - c_4 c_5 F^2 - c_3 F^2 - 4DFS - 2DFF' \\ &= 4(S - 2^{-1}DF)^2 - D^2F^2 - c_5 F'F - c_4 c_5 F^2 - c_3 F^2 - 2DFF' \\ &\geq -k_1 FF' - k_2 F^2\,, \end{aligned} \tag{2.43}$$

where

$$c_5 = \max\{c_1, c_2\}, \quad k_1 = c_5 + 2D, \qquad k_2 = D^2 + c_4 c_5 + c_3.$$

Inequality (2.43) is now integrated, see e.g. Payne (1971), to yield

$$F(t) \leq [F(0)]^{(\sigma-\sigma_1)/(1-\sigma_1)} \left[F(\mathcal{T})e^{\mu\mathcal{T}}\right]^{(1-\sigma)/(1-\sigma_1)} e^{-\mu t} \tag{2.44}$$

where

$$\sigma = e^{-k_1 t}\,, \qquad \sigma_1 = e^{-k_1 \mathcal{T}} \qquad \text{and} \qquad \mu = \frac{k_2}{k_1}.$$

If we now define

$$K(\mathcal{T}) = \left[F(\mathcal{T})e^{\mu\mathcal{T}}\right]^{(1-\sigma)/(1-\sigma_1)}$$

(for which an a *priori* estimate is known), and use the original definition of $F(t)$ in (2.27), then we find that

$$\int_0^t \left(\|\mathbf{u}\|^2 + \|\theta\|^2\right) ds \leq K(\mathcal{T}) e^{-\mu t} \left[\int_0^{\mathcal{T}} \left(\|q\|^2 + \|q_{,t}\|^2\right) dt\right]^{(\sigma-\sigma_1)/(1-\sigma_1)} - \int_0^{\mathcal{T}} \left(\|q\|^2 + \|q_{,t}\|^2\right) dt \tag{2.45}$$

This inequality thus establishes continuous dependence upon the heat supply, backward in time, on compact subintervals of $[0, \mathcal{T})$.

Chapter 3

Continuous dependence on a boundary heat flux for the Boussinesq equations

3.1 Introduction

In this chapter we consider a *plane layer* of fluid and establish continuous dependence of the solution to the equations of motion upon a heat flux at the lower boundary. We consider an incompressible, heat conducting, viscous fluid which has a quadratic equation of state as proposed by Veronis (1963),

$$\rho = \rho_m[1 - \alpha(T - T_m)^2], \tag{3.1}$$

where α is a constant, ρ is density and ρ_m is the maximum value of ρ attained at $T = T_m$. (The choice of density law for a fluid is discussed in chapters 1 and 4.)

As with the analysis in the previous chapter, Roberts (1967), Tritton & Zarraga (1967) and Straughan (1990) studied convection in a plane layer of fluid with internal heating and a heat flux at the lower boundary. However they did not establish continuous dependence on any *boundary data*, such as a heat flux. The boundary conditions chosen here, with a flux at the lower boundary and fixed upper surface temperature, are appropriate to the situation which arises in the Earth's atmosphere. Predictions for stability/instability in such a system are given in chapter 5.

In section 3.2 (as in section 2.2) we study forward in time dependence using an ordinary energy analysis. Since the backward in time problem is once again improperly posed (in an unrestricted class of solutions the solution does not depend continuously on the initial data), in section 3.3 we re-employ the logarithmic convexity argument to produce backward in time dependence.

3.2 Continuous dependence on boundary data forward in time

In standard indicial notation, the equations of motion for a heat-conducting linear viscous fluid, forward in time, are:

$$v_{i,t} + v_j v_{i,j} = -p_{,i} + \Delta v_i + b_i[1 - \alpha(T - T_m)^2]\,, \tag{3.2}$$

$$v_{i,i} = 0\,, \tag{3.3}$$

$$T_{,t} + v_i T_{,i} = \Delta T + Q\,, \tag{3.4}$$

where $\mathbf{v}$, $\mathbf{b}$ are the velocity and body force, p is pressure, T is temperature and $Q(\mathbf{x}, t)$ is the heat supply. As before, without loss of generality, we have set the viscosity, thermal diffusivity and density equal to unity, and the body force is taken constant.

Equations (3.2)–(3.4) are defined on the domain $\Omega \times (0, \mathcal{T}]$ where $\Omega = \mathbf{R}^2 \times (0, 1)$ represents the volume of the fluid. The boundary conditions we consider are

$$\mathbf{v}(\mathbf{x}, t) = \mathbf{0} \qquad \text{on} \quad z = 0, 1; \tag{3.5}$$

$$T(\mathbf{x}, t) = T_1(\mathbf{x}, t) \qquad \text{on} \quad z = 1; \tag{3.6}$$

$$\frac{\partial T}{\partial \mathbf{n}}(\mathbf{x}, t) = \gamma_0(\mathbf{x}, t) \qquad \text{on} \quad z = 0; \tag{3.7}$$

where γ_0 is the boundary heat flux and $\mathbf{n}$ is the unit normal to the surface $z = 0$. In addition, we assume that the p, $\mathbf{v}$, T fields are periodic in the x and y directions. The Cartesian product of a cell in the (x, y) plane with $(0, 1)$ is the period cell V. The boundary of V on the plane $z = 0$ shall be denoted by ∂V. Conditions (3.5)–(3.7) are defined for $t \in (0, \mathcal{T}]$. The initial conditions are

$$\left.\begin{aligned} v_i(\mathbf{x}, 0) &= v_i^0(\mathbf{x}) \\ T(\mathbf{x}, 0) &= T_0(\mathbf{x}) \end{aligned}\right\} \qquad \text{in} \quad \Omega \times \{0\}, \tag{3.8}$$

where $\mathbf{v}^0$, T_0, T_1 and γ_0 are prescribed functions of the arguments indicated.

Following the method employed in chapter 2, we let $\chi = (\mathbf{v}, T, p)$, $\chi^* = (\mathbf{v}^*, T^*, p^*)$ be two classical solutions to equations (3.2)–(3.4); the unstarred quantities denote the base flow and the starred quantities the perturbed flow. Assume

χ, χ^* satisfy (3.2)–(3.4) and boundary-initial conditions (3.5), (3.6) and (3.8) for the same data Q, $\mathbf{v}^0$, $\bar{\mathbf{v}}$, T_0, T_1 and body force $\mathbf{b}$, but χ will satisfy condition (3.7) for boundary heat flux $\gamma_1(\mathbf{x},t)$ and χ^* for heat flux $\gamma_2(\mathbf{x},t)$. Also we assume v_i, v_i^*, T, T^* are $C^2(\Omega\times[0,\mathcal{T}])$.

Define

$$u_i = v_i^* - v_i, \qquad \theta = T^* - T, \qquad \pi = p^* - p, \qquad \gamma = \gamma_2 - \gamma_1.$$

Then from equations (3.2)–(3.8) these variables satisfy

$$u_{i,t} + v_j^* u_{i,j} + u_j v_{i,j} = -\pi_{,i} + \Delta u_i - B_i\theta\,, \tag{3.9}$$

$$u_{i,i} = 0\,, \tag{3.10}$$

$$\theta_{,t} + v_i^*\theta_{,i} + u_i T_{,i} = \Delta\theta\,, \tag{3.11}$$

where $B_i = (\alpha(T^*+T) - 2T_m)b_i$. The boundary conditions become, for $t\in(0,\mathcal{T}]$,

$$\begin{aligned} u_i &= 0 && \text{on} \quad z = 0,1\,,\\ \theta &= 0 && \text{on} \quad z = 1\,,\\ \frac{\partial\theta}{\partial\mathbf{n}} &= \gamma(\mathbf{x},t) && \text{on} \quad z = 0\,. \end{aligned} \tag{3.12}$$

The initial conditions become for $\mathbf{x}\in\Omega$,

$$\mathbf{u}(\mathbf{x},0) = \theta(\mathbf{x},0) = 0\,. \tag{3.13}$$

In terms of the classes of functions defined in section 2.2, we are interested in a function $(\mathbf{u},\theta)\in(C^2(\bar{\Omega}\times[0,\mathcal{T}]))^4$, with $\mathbf{v}\in\mathcal{V}$ and T, $T^*\in\mathcal{W}$. By boundedness of T and T^*, there exists a constant D such that

$$\sup_{\Omega\times[0,\mathcal{T}]} B_i B_i \le D^2\,.$$

To establish continuous dependence we begin our analysis by multiplying (3.9) by u_i and integrating over V to give (after applications of the divergence theorem)

$$\frac{1}{2}\frac{d}{dt}\|\mathbf{u}\|^2 + <u_i u_j v_{i,j}> = -\|\nabla\mathbf{u}\|^2 - <B_i\theta u_i>\,, \tag{3.14}$$

where $\|.\|$ is the $L^2(V)$ norm and $<f>=\int_V f\,dV$. Next multiply (3.11) by θ and integrate over V to give

$$\frac{1}{2}\frac{d}{dt}\|\theta\|^2+<\theta u_i T_{,i}>=<\theta\Delta\theta>\ . \tag{3.15}$$

Our energy analysis requires that we find upper bounds for the time derivatives in (3.14) and (3.15). To this end using the Cauchy-Schwarz inequality we may show that

$$-<u_i u_j v_{i,j}>=<u_{i,j}u_j v_i>\leq \frac{a^2}{4}\|\mathbf{u}\|^2+\|\nabla\mathbf{u}\|^2\,;$$

$$-<u_i T_{,i}\theta>=<u_i\theta_{,i}T>\leq \frac{m^2}{2}\|\mathbf{u}\|^2+\frac{1}{2}\|\nabla\theta\|^2;$$

$$-<B_i\theta u_i>\leq \frac{D}{2}\|\mathbf{u}\|^2+\frac{D}{2}\|\theta\|^2\,.$$

Furthermore, Hölder's inequality and boundary condition (3.12) give

$$\begin{aligned}\theta(x,y,0)&=\theta(x,y,1)-\int_0^1\theta_{,z}(x,y,z)\,dz\\&=-\int_0^1\theta_{,z}(x,y,z)\,dz\\&\leq\left(\int_0^1\theta_{,z}^2(x,y,z)\,dz\right)^{1/2}.\end{aligned}$$

Thus

$$\begin{aligned}\oint_{\partial V}\theta^2(x,y,z)\,dA&\leq\oint_{\partial V}\left(\int_0^1\theta_{,z}^2\,dz\right)dA\\&=\int_V\theta_{,z}^2\,dV\\&\leq\|\nabla\theta\|^2\,,\end{aligned}\tag{3.16}$$

where $\oint_{\partial V}.\,dA$ denotes integration over the boundary plane ∂V. Hence from inequality (3.16), Hölder's inequality and the divergence theorem we may produce

the following:

$$\begin{aligned}
<\theta\Delta\theta> &= <(\theta\theta_{,j})_{,j}> - <\theta_{,j}\theta_{,j}> \\
&= -\oint_{\partial V} \gamma\theta \, dA - \|\nabla\theta\|^2 \\
&\leq \left(\oint_{\partial V} \gamma^2 \, dA\right)^{1/2} \left(\oint_{\partial V} \theta^2(x,y,z) \, dA\right)^{1/2} - \|\nabla\theta\|^2 \\
&\leq \Gamma - \frac{1}{2}\|\nabla\theta\|^2,
\end{aligned}$$

where $\Gamma = \frac{1}{2}\oint_{\partial V} \gamma^2 \, dA$.

We may now define the "energy" $E(t)$ by

$$E(t) = \frac{1}{2}\|\mathbf{u}\|^2 + \frac{1}{2}\|\theta\|^2.$$

Then from equations (3.14), (3.15) and the above equalities/inequalities,

$$\frac{dE}{dt} \leq \left(\frac{a^2}{4} + \frac{D}{2} + \frac{m^2}{2}\right)\|\mathbf{u}\|^2 + \frac{D}{2}\|\theta\|^2 + \Gamma\,.$$

If we define

$$c = \frac{a^2}{2} + D + m^2 \quad (\neq 0), \qquad \hat{\Gamma} = \sup_{[0,T]} \Gamma,$$

we have

$$\frac{dE}{dt} \leq \frac{c}{2}(\|\mathbf{u}\|^2 + \|\theta\|^2) + \hat{\Gamma} = cE + \hat{\Gamma}.$$

Upon integration we find

$$E(t) \leq e^{ct}E(0) + \frac{\hat{\Gamma}}{c}(e^{ct} - 1)\,.$$

Using initial conditions (3.13) we can show that

$$\begin{aligned}
E(0) &= \frac{1}{2}\left(\int_V \mathbf{u}^2(\mathbf{x},0) \, dV\right)^{1/2} + \frac{1}{2}\left(\int_V \theta^2(\mathbf{x},0) \, dV\right)^{1/2} \\
&= 0.
\end{aligned}$$

So if we set

$$K(t) = \frac{1}{c}(e^{ct} - 1)\,,$$

we obtain

$$E(t) \leq \hat{\Gamma}K(t). \tag{3.17}$$

Inequality (3.17) establishes continuous dependence, forward in time, on the lower boundary heat flux in energy measure.

3.3 Continuous dependence on the boundary data backward in time

Assuming the viscosity, density and thermal diffusivity are unity, and the body force is constant, the equations of motion for a heat-conducting linear viscous fluid, backward in time are:

$$v_{i,t} = v_j v_{i,j} + p_{,i} - \Delta v_i - b_i[1 - \alpha(T - T_m)^2]\,, \tag{3.18}$$

$$v_{i,i} = 0\,, \tag{3.19}$$

$$T_{,t} = v_i T_{,i} - \Delta T + Q\,. \tag{3.20}$$

Equations (3.18)–(3.20) are defined on the domain $\Omega \times (0, \mathcal{T}]$ as described in section 3.2. The boundary/"initial"conditions chosen are (3.5)–(3.8). Classical solutions χ, χ^* are once again the unperturbed and perturbed solutions described in the previous section; χ corresponds to heat flux $\gamma_1(\mathbf{x}, t)$ on the lower boundary and χ^* corresponds to heat flux $\gamma_2(\mathbf{x}, t)$.

Define

$$u_i = v_i^* - v_i, \qquad \theta = T^* - T, \qquad \pi = p^* - p, \qquad \gamma = \gamma_2 - \gamma_1.$$

Then from (3.18)–(3.20),

$$u_{i,t} = v_j^* u_{i,j} + u_j v_{i,j} + \pi_{,i} - \Delta u_i + B_i \theta\,, \tag{3.21}$$

$$u_{i,i} = 0\,, \tag{3.22}$$

$$\theta_{,t} = v_i^* \theta_{,i} + u_i T_{,i} - \Delta\theta\,, \tag{3.23}$$

where $B_i = (\alpha(T^* + T) - 2T_m)b_i$. The boundary-initial conditions which these variables must satisfy are (3.12) and (3.13).

In terms of the classes defined in section 2.3 we are interested in a function $(\mathbf{u}, \theta) \in \left(C^2(\bar{\Omega} \times [0, \mathcal{T}])\right)^4$ with $\mathbf{v}^* \in \mathcal{A}$, $\mathbf{v} \in \mathcal{A} \cap \mathcal{B}$, $T^* \in \mathcal{M}$ and $T \in \mathcal{M} \cap \mathcal{N}$. Since T, $T^* \in \mathcal{M}$ (i.e. T and T^* are bounded in modulus in $\Omega \times [0, \mathcal{T}]$), we may also assume that there exist constants p, $\beta > 0$ such that

$$\oint_{\partial V} \theta^2 \, dA \le p^2, \qquad \sup_{\Omega \times [0,\mathcal{T}]} |\mathbf{B}| \le \beta\,.$$

In order to establish continuous dependence we must first define the functional $F(t)$ by

$$F(t) = \int_0^t \left(\|\mathbf{u}\|^2 + \|\theta\|^2 \right) d\eta + \mathcal{Q}\,, \tag{3.24}$$

where

$$\mathcal{Q} = \int_0^{\mathcal{T}} \left(\oint_{\partial V} \gamma^2 \, dA + \oint_{\partial V} {\gamma_{,t}}^2 \, dA \right) dt + \sup_{[0,\mathcal{T}]} \left(\oint_{\partial V} \gamma^2 \, dA \right)^{1/2}.$$

Differentiating (3.24) we have, using (3.21) and (3.23),

$$\begin{aligned} F'(t) = 2 \int_0^t &< u_i(u_j v_{i,j} - \Delta u_i + B_i\theta) > \, d\eta \\ &+ 2 \int_0^t < \theta(u_i T_{,i} - \Delta\theta) > \, d\eta\,. \end{aligned} \tag{3.25}$$

From conditions (3.12) and the divergence theorem we obtain

$$\begin{aligned} < u_i \Delta u_i > &= -\|\nabla \mathbf{u}\|^2\,, \\ < \theta \Delta \theta > &= -\|\nabla\theta\|^2 - \oint_{\partial V} \gamma\theta \, dA\,. \end{aligned}$$

and via these equations and (3.25) it can be shown that

$$\begin{aligned} -\int_0^t \left(\|\nabla \mathbf{u}\|^2 + \|\nabla\theta\|^2 \right) d\eta = -\frac{1}{2} F'(t) &+ \int_0^t < u_i u_j v_{i,j} > \, d\eta + \int_0^t < B_i u_i \theta > \, d\eta \\ &+ \int_0^t < \theta u_i T_{,i} > \, d\eta + \int_0^t \left(\oint_{\partial V} \gamma\theta \, dA \right) d\eta\,. \end{aligned} \tag{3.26}$$

Furthermore, twice differentiating (3.24) we have

$$\begin{aligned} F''(t) = 2 \int_0^t \left(\|\mathbf{u}_{,s}\|^2 + \|\theta_{,s}\|^2 \right) ds + 2 \int_0^t &< u_i(v^*_{j,s} u_{i,j} + v^*_j u_{i,js} + u_{j,s} v_{i,j} + u_j v_{i,js} \\ &+ \pi_{,is} - \Delta u_{i,s} + B_{i,s}\theta + B_i \theta_{,s}) > \, ds \\ + 2 \int_0^t &< \theta(v^*_i \theta_{,is} + v^*_{i,s} \theta_{,i} + u_{i,s} T_{,i} + u_i T_{,is} - \Delta\theta_{,s}) > \, ds\,. \end{aligned} \tag{3.27}$$

Using the divergence theorem, equation (3.23) and boundary conditions (3.12) we can derive the following equivalent form for the integral $< \theta\Delta\theta_{,s} >$ which occurs in (3.27):

$$< \theta\Delta\theta_{,s} >= - < \theta_{,s}(\theta_{,s} - v_i^*\theta_{,i} - u_i T_{,i}) > + \oint_{\partial V} \left(\gamma\theta_{,s} - \gamma_{,s}\theta\right) dA\,.$$

This integral may now be employed along with the divergence theorem and the equations of motion to rearrange (3.27) to give:

$$\begin{aligned} F''(t) = 4\int_0^t \left(\|\mathbf{u}_{,s}\|^2 + \|\theta_{,s}\|^2\right) ds - 4\int_0^t < v_j^*(u_{i,j}u_{i,s} + \theta_{,j}\theta_{,s}) > \, ds \\ + 2\int_0^t < u_i\theta B_{i,s} > \, ds - 4\int_0^t < u_{i,s}u_j v_{[i,j]} > \, ds \\ - 2\int_0^t < u_j(v_{i,s}u_{i,j} + T_{,s}\theta_{,j}) > \, ds + 2\int_0^t < (u_i\theta_{,s} - \theta u_{i,s})(B_i - T_{,i}) > \, ds \\ + 2\int_0^t \left(\oint_{\partial V} \gamma_{,s}\theta - \gamma\theta_{,s}\, dA \right) ds. \end{aligned}$$

In order to employ a logarithmic convexity technique, we first calculate $FF'' - (F')^2$. This produces

$$\begin{aligned} FF'' - (F')^2 = 4S^2 + \sum_{i=1}^{4} I_i + \sum_{i=1}^{3} J_i \\ + 4\int_0^T \left(\oint_{\partial V} \gamma^2\, dA + \oint_{\partial V} {\gamma_{,t}}^2\, dA \right) dt \int_0^t \left(\|\chi_i\|^2 + \|\Phi\|^2\right) ds, \end{aligned}$$

where

$$\chi_i = u_{i,t} - \frac{1}{2}v_k^* u_{i,k} - \frac{1}{2}u_k v_{[i,k]}\,,$$

$$\Phi = \theta_{,t} - \frac{1}{2}v_m^*\theta_{,m}\,,$$

$$I_3 = 2F\int_0^t \left(\oint_{\partial V} \theta\gamma_{,s}\, dA \right) ds\,,$$

$$J_3 = -2F\int_0^t \left(\oint_{\partial V} \gamma\theta_{,s}\, dA \right) ds\,,$$

$$S^2 = \int_0^t \left(\|\mathbf{u}\|^2 + \|\theta\|^2\right) ds \int_0^t \left(\|\chi_i\|^2 + \|\Phi\|^2\right) ds - \left(\int_0^t \left(< u_i \chi_i > + < \theta \Phi >\right) ds\right)^2$$

(which is non-negative by the Cauchy-Schwarz inequality), and all other I_α, J_β are as defined in section 2.3.

The integrals I_1, I_2, J_1 and J_2 are bounded using using Hölder's inequality, the Cauchy-Schwarz inequality, the arithmetic-geometric mean inequality, and the Sobolev inequality

$$\|\mathbf{u}\|_6 \leq \xi \|\nabla \mathbf{u}\|,$$

for a positive constant ξ, to give the following bounds:

$$I_1 \geq -F \int_0^t \left((1 + k^2\xi^2)\|\nabla \mathbf{u}\|^2 + \|\nabla\theta\|^2\right) ds\,, \tag{3.28}$$

$$I_2 \geq -2(a^2 + b^2\xi^2)F \int_0^t \|\nabla \mathbf{u}\|^2 \, ds - a^2 F \int_0^t \|\nabla\theta\|^2 \, ds\,, \tag{3.29}$$

$$\begin{aligned} J_1 \geq -D^2 F \int_0^t \|\mathbf{u}\|^2 \, ds - \frac{1}{2} a^2 F \int_0^t \|\nabla\theta\|^2 \, ds \\ - 2^{\frac{3}{2}} DF \left(\int_0^t \|\Phi\|^2 \, ds \int_0^t \|\mathbf{u}\|^2 \, ds\right)^{\frac{1}{2}}, \end{aligned} \tag{3.30}$$

$$\begin{aligned} J_2 \geq -2^{\frac{3}{2}} DF \left(\int_0^t \|\theta\|^2 \, ds \int_0^t \|\chi_i\|^2 \, ds\right)^{\frac{1}{2}} - 2D^2 F \int_0^t \|\theta\|^2 \, ds \\ - \frac{1}{2}(a^2 + b^2\xi^2)F \int_0^t \|\nabla \mathbf{u}\|^2 \, ds\,, \end{aligned} \tag{3.31}$$

where $k^2 = b^2 + n^2$, and having set

$$\lambda_i = B_i - T_{,i} = \alpha(T^* + T)b_i - 2T_m b_i - T_{,i},$$

we have incorporated the bounds on B_i, T and T^* discussed earlier to produce

$$\sup_{\Omega \times [0,T]} \lambda_i \lambda_i \leq 2D^2, \qquad \text{where} \qquad D^2 = \beta^2 + n^2\,.$$

Utilizing inequality (3.16) obtained in section 3.2 along with Hölder's inequality and the Cauchy-Schwarz inequality, we may bound I_3 as follows:

$$\begin{aligned} I_3 &= 2F \int_0^t \left(\oint_{\partial V} \theta \gamma_{,s} \, dA \right) ds \\ &\geq -2F \left[\int_0^{\mathcal{T}} \left(\oint_{\partial V} {\gamma_{,s}}^2 \, dA \right) dt \int_0^t \left(\oint_{\partial V} \theta^2 \, dA \right) d\eta \right]^{1/2} \\ &\geq -F \int_0^{\mathcal{T}} \left(\oint_{\partial V} {\gamma_{,s}}^2 \, dA \right) dt - F \int_0^t \|\nabla \theta\|^2 \, ds \,. \end{aligned} \tag{3.32}$$

Similarly,

$$\begin{aligned} J_3 &= -2F \int_0^t \left(\oint_{\partial V} \gamma \theta_{,s} \, dA \right) ds \\ &= -2F \int_0^t \left[\frac{\partial}{\partial s} \left(\oint_{\partial V} \theta \gamma \, dA \right) - \oint_{\partial V} \theta \gamma_{,s} \, dA \right] ds \\ &= -2F \oint_{\partial V} \theta \gamma \, dA + I_3 \\ &\geq -2F \left(\oint_{\partial V} \gamma^2 \, dA \right)^{1/2} \left(\oint_{\partial V} \theta^2 \, dA \right)^{1/2} \\ &\quad - F \int_0^{\mathcal{T}} \left(\oint_{\partial V} {\gamma_{,s}}^2 \, dA \right) dt - F \int_0^t \|\nabla \theta\|^2 \, ds \\ &\geq -F \int_0^{\mathcal{T}} \left(\oint_{\partial V} {\gamma_{,s}}^2 \, dA \right) dt - F \int_0^t \|\nabla \theta\|^2 \, ds \\ &\quad - 2pF \sup_{[0,\mathcal{T}]} \left(\oint_{\partial V} \gamma^2 \, dA \right)^{1/2} . \end{aligned} \tag{3.33}$$

In order to produce an estimate for I_4, we first consider

$$B_{i,s} = \alpha b_i (T + T^*)_{,s} \,.$$

Without loss of generality, we can assume that b_i is bounded by the same bound as B_i, i.e.

$$\sup_{\Omega\times[0,T]} |b_i| \leq \beta\,.$$

So using the Cauchy-Schwarz inequality and boundary condition (3.12) we may obtain the following estimate for I_4:

$$\begin{aligned} I_4 &= 2F\int_0^t < u_i\theta B_{i,s} > \, ds \\ &= 2F\int_0^t < b_i\alpha u_i\theta(v_i^*T_{,i}^* + v_iT_{,i} - \Delta T^* - \Delta T) > \, ds \\ &\geq -4\alpha m^2 F\int_0^t \left(\|\nabla\mathbf{u}\|^2 + \|\nabla\theta\|^2\right) ds \\ &\qquad - (2am+\beta)\alpha\beta F\int_0^t \left(\|\theta\|^2 + \|\mathbf{u}\|^2\right) ds\,. \end{aligned} \tag{3.34}$$

The bounds we have produced for I_α, J_β are now utilized in order to produce the following inequality,

$$\begin{aligned} FF'' - (F')^2 \geq 4S^2 &- c_1F\int_0^t \|\nabla\mathbf{u}\|^2\, ds - c_2F\int_0^t \|\nabla\theta\|^2\, ds \\ &- c_3F^2 - 2^{3/2}DFH, \end{aligned} \tag{3.35}$$

where

$$\begin{aligned} c_1 &= 1 + k^2\xi^2 + \frac{5}{2}(a^2 + b^2\xi^2) + 4\alpha m^2\,, \\ c_2 &= 3 + \frac{3}{2}a^2 + 4\alpha m^2\,, \\ c_3 &= 2(p+1) + 2D^2 + \alpha\beta(2am+\beta)\,, \end{aligned}$$

and

$$H = \left(\int_0^t \|\Phi\|^2\, ds \int_0^t \|\mathbf{u}\|^2\, ds\right)^{1/2} + \left(\int_0^t \|\theta\|^2\, ds \int_0^t \|\chi_i\|^2\, ds\right)^{1/2}.$$

From equation (2.41) we know that

$$-2^{3/2}DHF \geq -4DFS - 2DFF'\,. \tag{3.36}$$

Using (3.26), integration by parts and the arithmetic-geometric mean inequality we can also obtain

$$-\int_0^t \left(\|\nabla \mathbf{u}\|^2 + \|\nabla\theta\|^2\right) ds \geq -\frac{1}{2}F' - \frac{1}{2}\int_0^t \|\nabla \mathbf{u}\|^2 \, ds - \frac{3}{4}\int_0^t \|\nabla\theta\|^2 \, ds$$
$$- \frac{\beta}{2}\int_0^t \|\theta\|^2 \, ds - \frac{1}{2}(a^2+\beta+m^2)\int_0^t \|\mathbf{u}\|^2 \, ds - \int_0^{\mathcal{T}} \left(\oint_{\partial V} \gamma^2 \, dA\right) dt \,,$$

from which we derive the bound

$$-\int_0^t \left(\|\nabla \mathbf{u}\|^2 + \|\nabla\theta\|^2\right) ds \geq -2F' - c_4 F \,, \tag{3.37}$$

where $c_4 = \max\{2\beta, 2(a^2+m^2+\beta), 4\}$. Estimates (3.28)–(3.34), (3.36), (3.37) are now employed in (3.35) in order to obtain

$$\begin{aligned} FF'' - (F')^2 &\geq 4(S - 2^{-1}DF)^2 - D^2F^2 - 2c_5FF' - c_4c_5F^2 - c_3F^2 - 2DFF' \\ &\geq -k_1FF' - k_2F^2 \,, \end{aligned} \tag{3.38}$$

where

$$c_5 = \max\{c_1, c_2\}, \qquad k_1 = 2c_5 + 2D, \qquad k_2 = D^2 + c_4c_5 + c_3.$$

Inequality (3.38) is now integrated to yield

$$\int_0^t \left(\|\mathbf{u}\|^2 + \|\theta\|^2\right) ds \leq K(\mathcal{T}) e^{-\mu t} \mathcal{Q}^{(\sigma-\sigma_1)/(1-\sigma_1)} - \mathcal{Q}$$

where $\sigma = e^{-k_1 t}$, $\sigma_1 = e^{-k_1 \mathcal{T}}$, $\mu = \frac{k_2}{k_1}$ and

$$K(\mathcal{T}) = [F(\mathcal{T}) e^{\mu \mathcal{T}}]^{(1-\sigma)/(1-\sigma_1)}$$

(for which an *a priori* estimate is known). This inequality thus establishes continuous dependence upon the boundary heat flux, backward in time, on compact subintervals of $[0, \mathcal{T})$.

Chapter 4

Nonlinear energy stability and convection near the density maximum

4.1 Introduction

We now turn attention to the analysis of penetrative convection in fluid layers, and in particular conditions for the onset of fluid motions. Penetrative convection and its application to geophysical fluid dynamics and convection in stars is described in chapter 1. In particular, we discussed the weakly nonlinear finite amplitude analysis of Veronis (1963) for two stress free boundaries. Veronis' (1963) analysis is based on adopting for the density law in the body force term the form

$$\rho = \rho_4[1 - \alpha(T-4)^2], \tag{4.1}$$

where $\rho(T)$ is density, T temperature, ρ_4 the density at 4°C, and $\alpha \simeq 7.68 \times 10^{-6}(^\circ\mathrm{C}^{-2})$.

However, as mentioned in chapter 1 it has been suggested by some authors that density law (4.1) is not accurate enough for comparison with experiments, see e.g. Merker *et al.* (1979) and the references therein. Merker *et al.* (1979) suggest using a density law like

$$\rho = \rho_0[1 + AT - BT^2 + CT^3], \tag{4.2}$$

or even like

$$\rho = \rho_0[1 + AT - BT^2 + CT^3 - DT^4 + ET^5], \tag{4.3}$$

where ρ_0 is the density of water at 0°C and the coefficients A–E are constants obtained by curve fitting to data points. Merker *et al.* (1979) suggest for water

values in (4.2) of

$$\begin{aligned} A &= 6.85650 \times 10^{-5}(^{\circ}\mathrm{C}^{-1}), \\ B &= 8.82063 \times 10^{-6}(^{\circ}\mathrm{C}^{-2}), \\ C &= 4.16668 \times 10^{-8}(^{\circ}\mathrm{C}^{-3}), \end{aligned} \tag{4.4}$$

while in (4.3),

$$\begin{aligned} A &= 6.79939 \times 10^{-5}(^{\circ}\mathrm{C}^{-1}), \\ B &= 9.10749 \times 10^{-6}(^{\circ}\mathrm{C}^{-2}), \\ C &= 1.00543 \times 10^{-7}(^{\circ}\mathrm{C}^{-3}), \\ D &= 1.12689 \times 10^{-9}(^{\circ}\mathrm{C}^{-4}), \\ E &= 6.59285 \times 10^{-12}(^{\circ}\mathrm{C}^{-5}); \end{aligned} \tag{4.5}$$

where Merker *et al.* (1979) further regard (4.3) together with (4.5) "exact" in the range 0°C to 40°C. It is important to note that for highly accurate predictions on the onset of convection Merker *et al.* (1979) suggest (*on the basis of linear theory*) that (4.2) is about 10% more accurate than (4.1), whereas (4.3) yields approximately a 3% improvement over (4.2). The analysis presented in this chapter would indicate that it is preferable to employ (4.2), but (4.3) for such a small gain in accuracy leads to much greater mathematical complications. Relation (4.2) has been employed by Niedrauer & Martin (1979) in their investigation of the convective motion of brine in channels formed in sea ice; they extrapolated from the analysis of Wooding (1959) who employed the classical linear temperature density relation. Equation (4.2) has also been advocated by Ruddick & Shirtcliffe (1979). Legros *et al.* (1974) compare experimental results for thermal convection with values calculated using a *sixth order* equation of state.

Since Merker *et al.* (1979) give only linear instability results and it is clear from the analytical methods of Veronis' (1963) work that subcritical instabilities will exist also for (4.2) and (4.3), we here concentrate on determining a nonlinear threshold below which there is stability. To achieve our aim we employ nonlinear energy methods. A nonlinear energy analysis will produce a critical Rayleigh number below which convection will not occur. By also calculating the critical

Rayleigh number of linear theory we are able to show that the parameter region of possible subcritical instability is small.

In section 4.2 we derive conditional, i.e. initial amplitude dependent, nonlinear stability results using the cubic density law (4.2). This is followed in section 4.3 by a new weighted energy technique which yields unconditional results, albeit weaker than the conditional ones. In section 4.4 it is shown how a conditional result may be established for quintic relation (4.3) since the previous method fails. The penultimate section indicates how one may develop a weighted energy analysis for (4.3) and the chapter is completed in section 4.6 with some numerical results which compare the conditional and weighted energy critical Rayleigh numbers with the corresponding linear ones.

4.2 Conditional energy stability for the cubic density relation

The equations of momentum, continuity and energy in the fluid are:

$$\dot{u}_i = -\frac{1}{\rho_0} p_{,i} - g\frac{\rho}{\rho_0} k_i + \nu \Delta u_i \,, \tag{4.6}$$

$$u_{i,i} = 0 \,, \tag{4.7}$$

$$\dot{T} = \kappa \Delta T \,, \tag{4.8}$$

where standard indicial notation is employed, $\mathbf{u}$, p, g, ν, κ, Δ are, respectively, velocity, pressure, gravity constant, kinematic viscosity, thermal diffusivity, the Laplace operator and $\mathbf{k} = (0, 0, 1)$. In this chapter and throughout the remainder of the thesis we shall interchange $\mathbf{u}$ and $\mathbf{x}$ with (u, v, w) and (x, y, z), respectively.

We suppose the fluid is contained in the layer $z \in (0, d)$ with

$$T = T_1 \ \text{ at } \ z = 0 \,, \qquad T = T_2 \quad (> T_1) \ \text{ at } \ z = d \,; \tag{4.9}$$

where T_1 and T_2 are constants with $0 \leq T_1 \leq 4$. In this and subsequent sections in the chapter, the density $\rho(T)$ in (4.6) will be replaced by either (4.2) or (4.3).

Equations (4.6)–(4.8) possess the motionless solution

$$\bar{\mathbf{u}} \equiv \mathbf{0}, \qquad \bar{T} = T_1 + \beta z, \qquad \beta = \frac{T_2 - T_1}{d} \,, \tag{4.10}$$

with the pressure $\bar{p}$ determined from

$$\frac{d\bar{p}}{dz} = -g\rho(\bar{T}) \,. \tag{4.11}$$

The object of this chapter is to study the *nonlinear* stability of this solution.

In this and the next section we study the stability of solution (4.10), (4.11) with ρ given by (4.2). Thus, suppose u_i, θ, π are perturbations to the steady solution (4.10), (4.11) with $\rho(T)$ given by (4.2), i.e.

$$u_i = \bar{u}_i + u_i, \qquad T = \bar{T} + \theta, \qquad p = \bar{p} + \pi.$$

Then if we introduce the non-dimensionalization

$$x_i = x_i^* d, \quad u_i = u_i^* U, \quad \theta = \theta^* T^\sharp, \quad \pi = \pi^* P,$$

$$U = \frac{\nu}{d}, \quad T^\sharp = U\left(\frac{Pr\beta}{Ag}\right)^{1/2}, \quad P = \frac{U\rho_0\nu}{d},$$

$$R^2 = \frac{Ag\beta d^4}{\kappa\nu}, \quad t = t^*\frac{d^2}{\nu}, \quad Pr = \frac{\nu}{\kappa}, \quad \Delta T = T_2 - T_1,$$

$$\xi = \frac{T_1}{\Delta T}, \quad a_1 = \frac{B}{A}\Delta T, \quad a_2 = \frac{C}{A}(\Delta T)^2,$$

the equations governing the non-dimensionalized perturbation variables are (after dropping all stars):

$$u_{i,t} + u_j u_{i,j} = -\pi_{,i} + \Delta u_i - R f_1 \theta k_i + Pr k_i f_2 \theta^2 - k_i a_2 \frac{Pr^2}{R}\theta^3\,, \tag{4.12}$$

$$u_{i,i} = 0, \tag{4.13}$$

$$Pr(\theta_{,t} + u_i\theta_{,i}) = -Rw + \Delta\theta, \tag{4.14}$$

where f_1 and f_2 are given by

$$\begin{aligned} f_1(z) &= 1 - 2a_1(\xi + z) + 3a_2(\xi + z)^2, \\ f_2(z) &= a_1 - 3a_2(\xi + z). \end{aligned} \tag{4.15}$$

R is related to the Rayleigh number and Pr is a Prandtl number. We suppose the two surfaces are fixed and so the boundary conditions are

$$\begin{gathered} u_i = \theta = 0 \quad \text{on} \quad z = 0, 1, \ \text{and} \\ u_i,\ \theta,\ \pi \ \text{are periodic in} \ x, y. \end{gathered} \tag{4.16}$$

The linear instability problem follows from (4.12)–(4.14) by assuming a time dependence like $e^{\sigma t}$ and dropping all nonlinear contributions. Merker *et al.* (1979) assume $\sigma \in \mathbf{R}$. Since the linearized system of (4.12)–(4.14) is not symmetric it is not likely that $\sigma \in \mathbf{R}$. However, it is likely that it is good enough to look at the instability boundary on which $\sigma = 0$. For completeness we write down the relevant linearized system for stationary convection ($\sigma = 0$):

$$\pi_{,i} = \Delta u_i - R f_1 \theta k_i\,, \tag{4.17}$$

$$Rw = \Delta\theta\,, \tag{4.18}$$

where $\mathbf{u}$ is again solenoidal. Employing normal modes, e.g. $u_i = u_i(z)\phi(x,y)$ where

$$\Delta^*\phi = -a^2\phi,$$

ϕ is the cell shape function, a is the wavenumber and

$$\Delta^* = \frac{\partial^2}{\partial x^2} + \frac{\partial^2}{\partial y^2},$$

(4.17), (4.18) may be reduced to

$$\begin{aligned} (D^2 - a^2)^2 W &= -R\, a^2 f_1 \Theta, \\ (D^2 - a^2)\Theta &= RW, \end{aligned} \tag{4.19}$$

where $W(z) = u_3(z)$, $\Theta(z) = \theta(z)$ and $D = d/dz$. The minimum over a^2 of the smallest eigenvalue R is now sought and this yields the instability boundary, which was also computed by Merker *et al.* (1979).

The nonlinear stability analysis of (4.10), (4.11) commences by deriving energy relations from (4.12) and (4.14) as follows:

$$\begin{aligned} \frac{1}{2}\frac{d}{dt}\|\mathbf{u}\|^2 &= -R < f_1\theta w > -\|\nabla \mathbf{u}\|^2 \\ &\quad + Pr < f_2\theta^2 w > -a_2\frac{Pr^2}{R} < w\theta^3 >, \end{aligned} \tag{4.20}$$

$$\frac{1}{2}Pr\frac{d}{dt}\|\theta\|^2 = -R < w\theta > -\|\nabla\theta\|^2, \tag{4.21}$$

where $w = u_3$, and $\|\cdot\|$ and $< \cdot >$ denote the $L^2(V)$ norm and integration over V respectively. To dominate the last term in (4.20) (arising from the cubic term in the density) by means of the stabilizing terms $\|\nabla\mathbf{u}\|^2$ and $\|\nabla\theta\|^2$ in (4.20), (4.21) we find it necessary to introduce a piece of the L^4 integral of θ to control the relevant destabilizing term. Thus, we calculate

$$\frac{1}{4}Pr\frac{d}{dt}\|\phi\|^2 = -R < w\theta^3 > -\frac{3}{4}\|\nabla\phi\|^2, \tag{4.22}$$

where we have set $\phi = \theta^2$.

Next define a generalized energy, $E(t)$, by

$$E(t) = \frac{1}{2}\|\mathbf{u}\|^2 + \frac{1}{2}\lambda Pr\|\theta\|^2 + \frac{\mu}{4}Pr\|\phi\|^2, \tag{4.23}$$

for λ and μ, positive coupling parameters to be chosen. Define now

$$I = -\big[\lambda < w\theta > + < f_1\theta w >\big], \tag{4.24}$$

$$\mathcal{D} = \|\nabla \mathbf{u}\|^2 + \lambda\|\nabla\theta\|^2, \tag{4.25}$$

and then differentiating (4.23) and using (4.20)–(4.22) we show that

$$\begin{aligned}\frac{dE}{dt} =& RI - \mathcal{D} - \frac{3\mu}{4}\|\nabla\phi\|^2 \\ &- \Big(\frac{a_2 Pr^2}{R} + R\mu\Big) < w\theta^3 > + Pr < f_2\theta^2 w > .\end{aligned} \tag{4.26}$$

We next define R_E by

$$R_E^{-1} = \max_{\mathcal{H}} \frac{I}{\mathcal{D}}, \tag{4.27}$$

where $\mathcal{H}$ is the space of admissible solutions. Upon making use of the Sobolev inequality (see Gilbarg & Trudinger, 1977)

$$< \theta^4 >^{1/4} \leq c_1\|\nabla\theta\|,$$

for some constant c_1, in (4.26) we may derive

$$\begin{aligned}\frac{dE}{dt} \leq& -\mathcal{D}\Big(\frac{R_E - R}{R_E}\Big) - \frac{3\mu}{4}\|\nabla\phi\|^2 + PrF_2c_1^2\|\nabla\theta\|^2\,\|w\| \\ &+ \Big(\frac{a_2Pr^2}{R} + R\mu\Big)\sqrt{2}c_1^2E^{1/2}\|\nabla\phi\|\,\|\nabla\theta\|,\end{aligned} \tag{4.28}$$

where we have put $F_2 = a_1 + 3a_2\xi$. To see how nonlinear stability ensues put $\alpha = (R_E - R)/R_E$ and suppose $R < R_E$ so that $\alpha > 0$. Next, employ the arithmetic-geometric mean inequality on the last term in (4.28) to obtain for $\omega(> 0)$ at our disposal:

$$\begin{aligned}\frac{dE}{dt} \leq& -\alpha\mathcal{D} - \frac{3\mu}{4}\|\nabla\phi\|^2 \\ &+ \Big\{\Big(PrF_2c_1^2\sqrt{2} + \Big[\frac{a_2Pr^2}{R} + R\mu\Big]\frac{\omega}{\sqrt{2}}c_1^2\Big)\|\nabla\theta\|^2 \\ &+ \Big(\frac{a_2Pr^2}{R} + R\mu\Big)\frac{c_1^2}{\omega\sqrt{2}}\|\nabla\phi\|^2\Big\}E^{1/2}\,.\end{aligned} \tag{4.29}$$

Choose now ω and μ such that

$$\frac{4\lambda\alpha}{3\mu\omega} = \frac{2RPrF_2}{a_2Pr^2 + \mu R^2} + \omega, \tag{4.30}$$

after λ has been chosen as described below. We thus find immediately from (4.29) that for constants k_1, k_2, computable from (4.29), (4.30),

$$\frac{dE}{dt} \leq -(k_1 - k_2E^{1/2})(\alpha\|\nabla\mathbf{u}\|^2 + \alpha\lambda\|\nabla\theta\|^2 + \frac{3}{4}\mu\|\nabla\phi\|^2). \tag{4.31}$$

If now $E^{1/2}(0) < k_1/k_2$ then it is easy to show $E(t) \to 0$ as $t \to \infty$. So, provided $E^{1/2}(0) < k_1/k_2$ and $R < R_E$ nonlinear stability follows. The *conditional* threshold R_E is determined from (4.27).

The Euler-Lagrange equations arising from (4.27) are calculated by first setting $\psi = \lambda^{1/2}\theta$ to find:

$$\begin{aligned} 2\Delta u_i - R_E M(z)\psi k_i &= \pi_{,i}\,, \\ 2\Delta\psi - R_E M(z)w &= 0, \end{aligned} \tag{4.32}$$

where $M(z) = (f_1 + \lambda)/\lambda^{1/2}$ and π is a Lagrange multiplier. These equations are solved numerically, but first we may obtain useful information by employing the parametric differentiation technique of Joseph, c.f. Joseph & Shir (1966). We show for $k = a_1, a_2, \lambda$ or ξ,

$$< \Big(R_E\frac{\partial M}{\partial k} + M\frac{\partial R_E}{\partial k}\Big)\psi w >= 0, \tag{4.33}$$

$$\|\nabla\mathbf{u}\|^2 + \|\nabla\psi\|^2 = -R_E < M\psi w > . \tag{4.34}$$

Hence there follows

$$\begin{aligned} R_E < \frac{\partial M}{\partial k}\psi w > &= -\frac{\partial R_E}{\partial k} < M\psi w > \\ &= R_E^{-1}\frac{\partial R_E}{\partial k}(\|\nabla\mathbf{u}\|^2 + \|\nabla\psi\|^2). \end{aligned} \tag{4.35}$$

This immediately yields two useful relations:

$$\frac{\partial R_E}{\partial\xi} = \frac{R_E^2}{\mathcal{D}} < \psi w\Big[\frac{-2a_1 + 6a_2(\xi + z)}{\sqrt{\lambda}}\Big] >, \tag{4.36}$$

and

$$\frac{\partial R_E}{\partial a_2} = 3\frac{R_E^2}{\mathcal{D}\sqrt{\lambda}} < \psi w(\xi + z)^2 >, \tag{4.37}$$

where $\mathcal{D} = \|\nabla \mathbf{u}\|^2 + \|\nabla \psi\|^2$. Experience with numerical eigenvalue problems of this type suggests the product ψw is often one-signed and so (4.36) and (4.37) yield an indication of the type of result to be found numerically.

Another useful relation is found by selecting $k = \lambda$ in (4.33). For, at the best value of λ, $\partial R_E/\partial\lambda = 0$ and so

$$< \psi w \frac{\partial M}{\partial \lambda} >= 0. \tag{4.38}$$

Equation (4.38) is very useful as it *suggests* that

$$\tilde{\lambda} = f_1 \text{ average}$$

will be a good "guess" when searching numerically. Values of $f^* = f_1(1/2)$ and $\bar{f} = \int_0^1 f_1 dz$ are compared in section 4.6 with the best value of λ found numerically.

The Euler-Lagrange equations are solved numerically by adopting normal modes in (4.32). The resulting eigenvalue problem has form

$$\begin{aligned} D^4 W &= 2a^2 D^2 W - a^4 W - \frac{1}{2} R_E M a^2 \Psi, \\ D^2 \Psi &= a^2 \Psi + \frac{1}{2} R_E M W, \end{aligned} \tag{4.39}$$

where $D = d/dz$. For two fixed surfaces the boundary conditions are

$$W = DW = \Psi = 0 \quad \text{on} \quad z = 0, 1. \tag{4.40}$$

We use the compound matrix method, see Drazin & Reid (1981), and the golden search technique to find

$$\max_{\lambda} \min_{a^2} R_E^2(a^2; \lambda).$$

A brief comparison of the Merker *et al.* (1979) and Veronis (1963) models is useful. To facilitate this we rewrite equation (4.1) as

$$\rho = \rho_4(1 - 16\alpha)\Big[1 + \Big(\frac{8\alpha}{1 - 16\alpha}\Big)T - \Big(\frac{\alpha}{1 - 16\alpha}\Big)T^2\Big]. \tag{4.41}$$

Thus,

$$\rho_0 \,(\text{Veronis}) \equiv \rho_4(1 - 16\alpha) = 999.8491234$$

whereas

$$\rho_0 \,(\text{Merker } et\ al.) = 999.8396,$$

i.e. 9.5×10^{-4} % difference. Merker *et al.* (1979) also consider a quadratic model

$$\rho = \rho_0[1 + AT - BT^2], \tag{4.42}$$

where

$$A = 6.62105 \times 10^{-5}(^\circ\mathrm{C}^{-1}), \qquad B = 8.27631 \times 10^{-6}(^\circ\mathrm{C}^{-2}).$$

We are here mainly concerned with their cubic and fifth order models. However, for direct comparison between the various models, the coefficients in the Veronis model and the cubic model (4.2) are:

Veronis

$$A = 6.14476 \times 10^{-5}(^\circ\mathrm{C}^{-1}), \qquad B = 7.68094 \times 10^{-6}(^\circ\mathrm{C}^{-2}),$$

Equation (4.2)

$$A = 6.85650 \times 10^{-5}(^\circ\mathrm{C}^{-1}), \qquad B = 8.82063 \times 10^{-6}(^\circ\mathrm{C}^{-2}),$$

$$C = 4.16668 \times 10^{-8}(^\circ\mathrm{C}^{-3}).$$

4.3 Unconditional (weighted energy) stability for the cubic density

Payne & Straughan (1987) showed that by employing a weighted energy one could recover unconditional nonlinear stability, i.e. for all initial amplitudes, for the quadratic density relation (4.1). The nonlinearities which arise due to relation (4.2) are evidently too complicated to allow that method work and so we devise another generalized energy function $E(t)$ as follows:

$$E(t) = \frac{1}{2}\|\mathbf{u}\|^2 + \frac{1}{2}Pr\mu_1\|\theta\|^2 + \frac{1}{3}Pr < \mu_2(z)\theta^3 > + \frac{\lambda}{4R^2}Pr\|\phi\|^2. \tag{4.44}$$

Here λ and μ_1 are positive coupling parameters to be selected while $\mu_2(z)$ is a linear function in z we choose later. Of course, λ, μ_1 and μ_2 must be such that $E(t)$ is positive definite.

We differentiate E and use equations (4.12)–(4.14) to find, after a little integration by parts,

$$\begin{aligned}\frac{dE}{dt} =& - R[< f_1\theta w > + \mu_1 < \theta w >] \\ & - \Big\{\|\nabla\mathbf{u}\|^2 + \mu_1\|\nabla\theta\|^2 + < \mu_2\nabla\theta\cdot\nabla\phi > + \frac{3\lambda}{4R^2}\|\nabla\phi\|^2\Big\} \\ & + Pr < f_2 w\theta^2 > - R < \mu_2\theta^2 w > \\ & + < w\theta^3 > \Big\{-a_2\frac{Pr^2}{R} - \frac{\lambda}{R} + \frac{1}{3}Pr\mu_2'\Big\}.\end{aligned} \tag{4.45}$$

Now choose

$$\mu_2 = \frac{3}{PrR}(\lambda + a_2Pr^2)z, \tag{4.46}$$

so that the last term in (4.45) vanishes. Further, set $R\psi = \phi$ which reduces (4.45) to

$$\begin{aligned}\frac{dE}{dt} =& R\{< r\theta w > + < s\psi w >\} \\ & - \Big\{\|\nabla\mathbf{u}\|^2 + \mu_1\|\nabla\theta\|^2 + b < z\nabla\theta\cdot\nabla\psi > + c\|\nabla\psi\|^2\Big\},\end{aligned} \tag{4.47}$$

where we have put

$$\begin{aligned} r &= -(f_1 + \mu_1), \\ s &= Pr(a_1 - 3a_2\xi) - \Big(\frac{3\lambda}{Pr} + 6a_2Pr\Big)z, \\ b &= \frac{3}{Pr}(\lambda + a_2Pr^2), \\ c &= \frac{3\lambda}{4}. \end{aligned}$$

Select λ now such that

$$\lambda = \Big(\frac{\mu_1 - 6a_2}{6}\Big) Pr^2$$

and restrict μ_1 so that $\mu_1 > 12a_2$. Although this is not a unique choice it has the effect of ensuring E is positive definite and likewise the dissipative term in (4.47) can dominate the production term and hence lead to a meaningful maximum problem. Thus, if we define in (4.47)

$$I = < r\theta w > + < sw\psi >,$$

$$\mathcal{D} = \|\nabla \mathbf{u}\|^2 + \mu_1 \|\nabla\theta\|^2 + b < z\nabla\theta \cdot \nabla\psi > + c\|\nabla\psi\|^2,$$

we find

$$\frac{dE}{dt} \leq -\mathcal{D}R\Big(\frac{1}{R} - \frac{1}{R_1}\Big)$$

where

$$R_1^{-1} = \max_{\mathcal{H}} \frac{I}{\mathcal{D}}. \tag{4.48}$$

For $R < R_1$ we may then show there exists $k(> 0)$ such that

$$\frac{dE}{dt} \leq -kE,$$

and so $R < R_1$ is a sufficient condition to guarantee nonlinear *unconditional* stability. In (4.48) $\mathcal{H}$ is the space of admissible solutions. If we further define

$$R_w^{-1} = \max_{\mathcal{H}^*} \frac{I}{\mathcal{D}}, \tag{4.49}$$

where $\mathcal{H}^*$ is the space of competitors in which ψ and θ are unconnected, then clearly $R_1^{-1} \leq R_w^{-1}$. Hence, if $R < R_w$ this too is a sufficient condition for unconditional nonlinear stability. The Euler-Lagrange equations corresponding to (4.49) are:

$$\begin{aligned} &R_w r w + 2\mu_1 \Delta\theta + b\nabla\cdot(z\nabla\psi) = 0, \\ &R_w s w + 2c\Delta\psi + b\nabla\cdot(z\nabla\theta) = 0, \\ &R_w k_i(r\theta + s\psi) + 2\Delta u_i = \pi_{,i}\,, \end{aligned} \tag{4.50}$$

where π is again a Lagrange multiplier and given the way λ is chosen,

$$
\begin{aligned}
b &= \frac{1}{2}\mu_1 Pr, \quad c = \frac{1}{8}(\mu_1 - 6a_2)Pr^2, \\
s &= Pr\{a_1 - 3a_2\xi - (\frac{1}{2}\mu_1 + 3a_2)z\}, \\
r &= -\mu_1 - 1 + 2a_1(\xi + z) - 3a_2(\xi + z)^2.
\end{aligned} \tag{4.51}
$$

To determine $R_w(a^2;\mu_1)$, equations (4.50) are reduced by normal modes to

$$
\begin{aligned}
&(D^2 - a^2)^2 W - \frac{1}{2}R_w(ra^2\Theta + sa^2\Psi) = 0, \\
&(D^2 - a^2)\Theta + \frac{\mu_1 Pr}{2\gamma}D\Psi - \frac{b^2}{2c\gamma}zD\Theta \\
&\qquad\qquad + \frac{R_w}{\gamma}\Big(r - \frac{bzs}{2c}\Big)W = 0, \\
&(D^2 - a^2)\Psi + \frac{b}{\hat{\gamma}}D\Theta - \frac{b^2}{2\mu_1\hat{\gamma}}zD\Psi \\
&\qquad\qquad + \frac{R_w}{\hat{\gamma}}\Big(s - \frac{bzr}{2\mu_1}\Big)W = 0,
\end{aligned} \tag{4.52}
$$

where

$$
\gamma = \Big(\frac{\mu_1}{\mu_1 - 6a_2}\Big)(2\mu_1 - 12a_2 - \mu_1 z^2)\ (> 0)
$$

and

$$
\hat{\gamma} = \frac{1}{4}Pr^2(\mu_1 - \frac{1}{2}\mu_1 z^2 - 6a_2)\ (> 0).
$$

Numerical output for the *constrained* optimization-eigenvalue problem,

$$
\max_{\mu_1}\min_{a^2} R_w^2(a^2;\mu_1),
$$

where $\mu_1 > 12a_2$, is given in tables 4.1 and 4.2.

We remark again that the choice of λ is not unique. Another approach to unconditional nonlinear stability is to employ the energy

$$
E(t) = \frac{1}{2}\|\mathbf{u}\|^2 + \frac{1}{2}Pr < \mu_1\theta^2 > + \frac{1}{3}Pr < \mu_2\theta^3 > + \frac{\lambda}{4}Pr < \theta^4 >,
$$

and a choice which leads to the removal of cubic (or higher) terms is

$$
\begin{aligned}
\mu_2(z) &= \zeta_2 + 3\Big(\frac{\lambda R}{Pr} + \frac{a_2 Pr}{R}\Big)z, \\
\mu_1(z) &= \zeta_1 - 2\Big(a_1 - 3a_2\xi - \frac{\zeta_2 R}{Pr}\Big)z + 3\Big(2a_2 + \frac{\lambda R^2}{Pr^2}\Big)z^2,
\end{aligned}
$$

ζ_1, ζ_2 being positive constants at our disposal. We only include details for our former energy.

4.4 Conditional energy stability for the fifth order relation

Suppose now the buoyancy term in the momentum equation has density defined by (4.3) with the coefficients given by (4.5). The conduction solution whose stability we investigate is again defined by (4.10), (4.11), but where $\rho(\bar{T})$ in (4.11) is determined from (4.3). The perturbation equations for u_i, θ, π are found by non-dimensionalizing with the scalings before (4.12)–(4.14), although here we additionally need

$$a_3 = \frac{D}{A}(\Delta T)^3, \quad a_4 = \frac{E}{A}(\Delta T)^4,$$

and we further introduce $f_1(z), ..., f_4(z)$ by

$$\begin{aligned} f_1(z) &= 1 - 2a_1(\xi + z) + 3a_2(\xi + z)^2 \\ &\qquad - 4a_3(\xi + z)^3 + 5a_4(\xi + z)^4, \\ f_2(z) &= a_1 - 3a_2(\xi + z) + 6a_3(\xi + z)^2 - 10a_4(\xi + z)^3, \\ f_3(z) &= a_2 - 4a_3(\xi + z) + 10a_4(\xi + z)^2, \\ f_4(z) &= a_3 - 5a_4(\xi + z). \end{aligned} \tag{4.53}$$

The non-dimensional system of perturbation equations becomes:

$$\begin{aligned} u_{i,t} + u_j u_{i,j} &= -\pi_{,i} + \Delta u_i - R f_1 \theta k_i + Pr k_i f_2 \theta^2 \\ &\qquad - k_i f_3 \frac{Pr^2}{R}\theta^3 + k_i f_4 \frac{Pr^3}{R^2}\theta^4 - k_i a_4 \frac{Pr^4}{R^3}\theta^5, \\ u_{i,i} &= 0, \\ Pr(\theta_{,t} + u_i \theta_{,i}) &= -Rw + \Delta\theta, \end{aligned} \tag{4.54}$$

with the spatial domain of (4.54) being the layer $z \in (0, 1)$. We investigate with boundary conditions for two fixed surfaces.

Again, a combination of L^2 integrals of $\mathbf{u}$ and θ is insufficient to develop a nonlinear energy analysis. Moreover, the addition of an L^4 integral of θ appears inadequate. We construct, therefore, a generalized energy which involves the L^2, L^4 and L^6 integrals of θ, namely:

$$E(t) = \frac{1}{2}\|\mathbf{u}\|^2 + \frac{1}{2}\lambda Pr\|\theta\|^2 + \frac{\mu}{4} Pr\|\phi\|^2 + \frac{\gamma}{6} Pr\|\psi\|^2, \tag{4.55}$$

where λ, μ, γ are three (positive) coupling parameters at our disposal, and $\phi = \theta^2$, $\psi = \theta^3$.

The new energy identity is:

$$\begin{aligned}\frac{dE}{dt} =& RI - \mathcal{D} - \frac{3\mu}{4}\|\nabla\phi\|^2 - \frac{5\gamma}{9}\|\nabla\psi\|^2 \\ &+ Pr < f_2\theta^2 w > - < w\theta^3\Big(\frac{f_3 Pr^2}{R} + R\Big) > \\ &+ \frac{Pr^3}{R^2} < f_4\theta^4 w > - < w\theta^5\Big(\frac{a_4 Pr^4}{R^3} + R\Big) >,\end{aligned} \tag{4.56}$$

where I and $\mathcal{D}$ have the same form as in (4.24), (4.25), namely:

$$I = - < (f_1 + \lambda)\theta w >, \quad \mathcal{D} = \|\nabla \mathbf{u}\|^2 + \lambda\|\nabla\theta\|^2,$$

but f_1 is now given by (4.53).

We denote the last four terms in (4.56) by $J_1, ..., J_4$ and denote by $\bar{f}_2$, $\bar{f}_3$, $\bar{f}_4$ the maximum values of f_2, f_3, f_4 in $[0, 1]$. The quantities $J_1, ..., J_4$ are estimated as follows:

$$\begin{aligned}J_1 = Pr < f_2 w\theta^2 > &\leq Pr\bar{f}_2\|\phi\|\|w\|, \\ &\leq Pr\bar{f}_2 c_1\|\nabla\theta\|^2\|w\|,\end{aligned} \tag{4.57}$$

where the Cauchy-Schwarz inequality, and the Sobolev inequality

$$< \theta^4 >^{1/2} \leq c_1\|\nabla\theta\|^2,$$

have been used. By similar use of the Cauchy-Schwarz and Sobolev inequalities:

$$\begin{aligned}J_2 = & - < w\theta^3\big(\frac{f_3 Pr^2}{R} + R\big) > \\ &\leq \Big(\frac{Pr^2}{R}\bar{f}_3 + R\Big)\|w\|\|\theta\phi\| \\ &\leq \Big(\frac{Pr^2}{R}\bar{f}_3 + R\Big)c_1\|w\|\|\nabla\theta\|\|\nabla\phi\|,\end{aligned} \tag{4.58}$$

$$\begin{aligned}J_3 = & \frac{Pr^3}{R^2} < f_4 w\theta^4 > \\ &\leq \frac{Pr^3}{R^2}\bar{f}_4\|w\|\|\phi^2\| \\ &\leq \frac{Pr^3}{R^2}c_1\bar{f}_4\|w\|\|\nabla\phi\|^2,\end{aligned} \tag{4.59}$$

$$
\begin{aligned}
J_4 &= - < w\theta^5 \Big(\frac{a_4 Pr^4}{R^3} + R\Big) > \\
&\leq \Big(\frac{a_4 Pr^4}{R^3} + R\Big)\|w\|\|\phi\psi\| \\
&\leq \Big(\frac{a_4 Pr^4}{R^3} + R\Big) c_1 \|w\|\|\nabla\phi\|\|\nabla\psi\|. \qquad (4.60)
\end{aligned}
$$

Estimates (4.57)–(4.60) are utilized in (4.56) and we then define

$$
R_E^{-1} = \max_{\mathcal{H}} \frac{I}{\mathcal{D}}, \qquad (4.61)
$$

and conclude

$$
\begin{aligned}
\frac{dE}{dt} \leq & - \mathcal{D}\Big(\frac{R_E - R}{R_E}\Big) - \frac{3\mu}{4}\|\nabla\phi\|^2 - \frac{5\gamma}{9}\|\nabla\psi\|^2 \\
& + Pr\bar{f}_2 c_1 \|\nabla\theta\|^2\|w\| + \Big(\frac{Pr^2}{R}\bar{f}_3 + R\Big) c_1 \|w\|\|\nabla\theta\|\|\nabla\phi\| \qquad (4.62) \\
& + \frac{Pr^3}{R^2} c_1 \bar{f}_4 \|w\|\|\nabla\phi\|^2 + \Big(\frac{a_4 Pr^4}{R^3} + R\Big) c_1 \|w\|\|\nabla\phi\|\|\nabla\psi\|.
\end{aligned}
$$

Provided $R < R_E$ we may now utilize in (4.62) a procedure, *mutatis mutandis*, analogous to that adopted in (4.28) in order to obtain inequality (4.29), where now the dissipation is a linear combination of $\|\nabla\mathbf{u}\|^2, \|\nabla\theta\|^2, \|\nabla\phi\|^2$ and $\|\nabla\psi\|^2$. From the resulting inequality, it is straightforward to establish conditional nonlinear stability. However, the expression for R_E will still only involve the terms I and $\mathcal{D}$.

The nonlinear stability threshold is determined by calculating R_E for which Euler-Lagrange equations are (4.32), although f_1 is in this case given by (4.53). The critical Rayleigh number is again found by the optimization

$$
\max_{\lambda} \min_{a^2} R_E^2(a^2; \lambda).
$$

Numerical results for the fifth order equation of state are contained in tables 4.4–4.6.

4.5 Unconditional energy stability for the quintic density relation

The analysis in this chapter is completed by sketching a heuristic weighted energy approach to unconditional stability when the density relation (4.3) holds.

To develop an unconditional nonlinear stability analysis analogous to that presented earlier for the cubic density relation, but when perturbation equations (4.54) hold, we commence with a generalized (weighted) energy of form:

$$\begin{aligned} E(t) = \frac{1}{2}\|\mathbf{u}\|^2 + \frac{1}{2}Pr\mu_1\|\theta\|^2 + \frac{\mu_2 Pr}{3R} < \theta^3 > \\ + \frac{Pr}{4R^2} < \mu_3\theta^4 > + \frac{Pr}{5} < \mu_4\theta^5 > + \frac{Pr\mu_5}{6R^4} < \theta^6 >, \end{aligned} \tag{4.63}$$

where μ_1, μ_2, μ_5 are coupling parameters at our disposal and $\mu_3(z)$ is a quadratic function of z while $\mu_4(z)$ is linear in z. The extra weights in (4.63) are apparently necessary due to the extra nonlinearities in $(4.54)_1$.

The energy identity for (4.63) is found to be:

$$\begin{aligned} \frac{dE}{dt} = & -R[< f_1\theta w > + \mu_1 < \theta w >] \\ & - \|\nabla\mathbf{u}\|^2 - \mu_1\|\nabla\theta\|^2 - \frac{\mu_2}{R} < \nabla\theta\cdot\nabla\phi > - \frac{3}{4R^2} < \mu_3|\nabla\phi|^2 > \\ & + Pr < f_2\phi w > - \frac{Pr^2}{R} < f_3\psi w > - \mu_2 < w\phi > - \frac{1}{R} < \mu_3 w\psi > \\ & + \frac{\mu_3''}{4R^2}\|\phi\|^2 - \frac{2}{3} < \mu_4\nabla\phi\cdot\nabla\psi > - \frac{5\mu_5}{9R^4}\|\nabla\psi\|^2 \\ & + \left\{ \frac{Pr^3}{R^2} < f_4 w\theta^4 > + \frac{Pr}{4R^2} < \mu_3' w\theta^4 > - R < \mu_4\theta^4 w > \right\} \\ & + \left(\frac{Pr\mu_4'}{5} - \frac{\mu_5}{R^3} - \frac{Pr^4 a_4}{R^3} \right) < w\theta^5 > . \end{aligned} \tag{4.64}$$

The last two groups of terms are removed with the choice

$$\mu_4 = \frac{5}{PrR^3}(\mu_5 + a_4 Pr^4)z, \tag{4.65}$$

and

$$\mu_3 = \left(\frac{10\mu_5}{Pr^2} + 20a_4 Pr^2\right)z^2 - Pr^2(4a_3 - 20a_4\xi)z. \tag{4.66}$$

Introduce now $\chi = \phi R^{-1}$ and $\eta = \psi R^{-2}$ and define I, $\mathcal{D}$ by:

$$\begin{aligned} I =& - < (f_1 + \mu_1)\theta w > - < (\mu_2 - Prf_2)w\chi > \\ & - < (Pr^2 f_3 + \mu_3)w\eta >, \end{aligned} \tag{4.67}$$

$$\begin{aligned} \mathcal{D} =& \|\nabla \mathbf{u}\|^2 + \mu_1 \|\nabla\theta\|^2 + \mu_2 < \nabla\theta \cdot \nabla\chi > \\ & + \frac{3}{4} < \mu_3 |\nabla\chi|^2 > + \frac{2}{3} < \hat{\mu}_4 \nabla\chi \cdot \nabla\eta > + \frac{5\mu_5}{9} \|\nabla\eta\|^2, \end{aligned} \tag{4.68}$$

where $\hat{\mu}_4 = R^3 \mu_4$. Employing (4.65) and (4.66), (4.64) may be rewritten:

$$\frac{dE}{dt} = RI - \mathcal{D} + \frac{\mu_3''}{4} \|\chi\|^2. \tag{4.69}$$

To remove the $\|\chi\|^2$ term we set *at the outset*

$$\mu_3(z) = \hat{\mu}_3 + \tilde{\mu}_3(z),$$

where $\tilde{\mu}_3$ is defined by (4.66). We now select $\hat{\mu}_3$ such that

$$3\hat{\mu}_3 \pi^2 \geq \frac{20\mu_5}{Pr^2} + 40 a_4 Pr^2,$$

and obtain instead of (4.69):

$$\frac{dE}{dt} \leq RI - \mathcal{D}. \tag{4.70}$$

An energy analysis may be developed from (4.70) in a similar manner to that indicated earlier for the cubic density relation.

The numerical results, especially the conditional nonlinear energy ones, for the equation of state (4.2) appear to fit the practical situation very accurately. Since equation (4.2) would appear to yield results which from a practical point of view are likely to be as useful as those of (4.3), the extra complexity introduced (evidently necessarily) by the above analysis and the extra numerical effort involved would seem to be unnecessary and hence we do not report numerical details here. It is important, however, that we have been able to show how a suitable weighted energy may be constructed to establish nonlinear unconditional stability for the fifth order density-temperature relation (4.3).

4.6 Numerical results and conclusions

4.6.1 Numerical results

It needs care with the interpretation of the Rayleigh number. Initially we calculate it as

$$R^2 = \frac{Ag\beta d^4}{\kappa\nu}.$$

For direct comparison with earlier results in Straughan (1985), we should use

$$R_B^2 = \frac{Bg\beta^2 d^5}{\kappa\nu} = R^2\left(\frac{B}{A}\Delta T\right).$$

However, Veronis (1963) and Straughan (1985) also prefer to use a Rayleigh number based on the depth of the *destabilizing layer*. So the Rayleigh number which we choose is, therefore,

$$Ra = \begin{cases} R_B^2, & \text{if} \quad T_2 \leq 4°\text{C}, \\ \left(\frac{4-T_1}{T_2-T_1}\right)^5 R_B^2, & \text{if} \quad T_2 > 4°\text{C}. \end{cases} \tag{4.71}$$

The Rayleigh number for the quintic relation (4.3) has the same form as above except the B value is given by (4.5). If we denote this number by $\hat{R}_B^2$ then the values in tables 4.4–4.6 are in terms of

$$R_B^2 = \hat{R}_B^2 \frac{B_{\text{cubic}}}{B_{\text{quintic}}},$$

where the values are again adjusted for depth when T_2 exceeds 4°C in an analogous manner to (4.71). This choice of R_B^2 allows us to compare our cubic and quintic results directly.

T_2	1	2	3	4	5	6	7	8
Ra_L	251.96	589.51	1062.64	1767.71	954.47	661.69	584.34	606.53
Ra_E	251.89	588.72	1058.18	1747.93	927.68	615.35	488.01	438.31
Ra_w	241.54	505.70	761.44	992.66	391.76	180.63	92.90	51.83
a_L^2	9.714	9.719	9.737	9.780	9.888	10.232	11.577	15.885
a_E^2	9.715	9.723	9.751	9.815	9.966	10.348	11.268	13.055
a_w^2	9.654	9.648	9.652	9.660	9.673	9.682	9.693	9.705
$\bar{\lambda}$	.873	.748	.627	.512	.406	.316	.252	.221
$\bar{f}_1$	.872	.745	.620	.495	.372	.250	.129	.010
f_1^*	.872	.745	.618	.493	.368	.245	.122	.000
$\bar{\mu}_1$	1.073	1.227	1.449	1.712	2.002	2.307	2.622	2.945
μ_{1L}	.007	.029	.066	.117	.182	.262	.357	.467

Table 4.1 Critical Rayleigh and wavenumbers $Ra_L, Ra_E, Ra_w, a_L, a_E, a_w$.
The subscript $L \equiv$linear, $E \equiv$conditional energy,
$w \equiv$unconditional weighted energy.
Equation of state (4.2) holds, and $T_1 = 0°C$.
$\bar{\lambda}$ denotes the optimal value of λ; $\bar{f}_1$, f_1^* are estimates of λ.
$\bar{\mu}_1$ is the best value of μ_1, while μ_{1L} $(= 12a_2)$ is a lower threshold for μ_1.

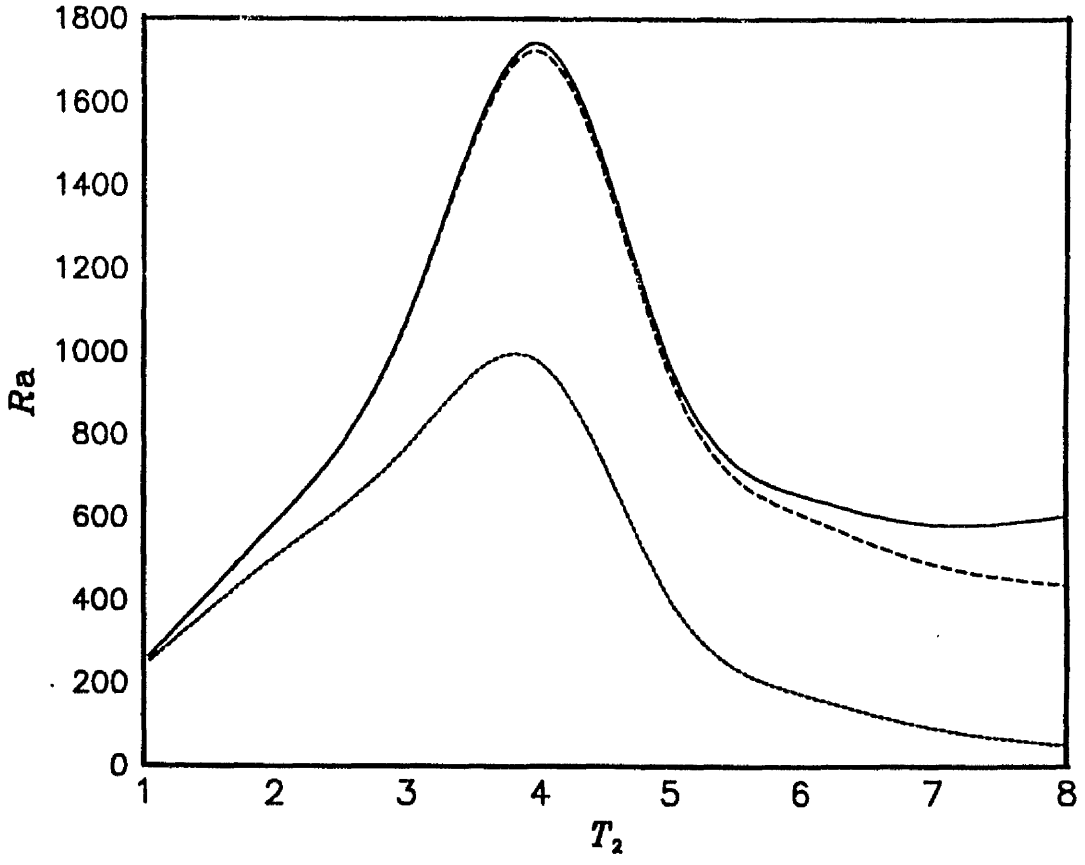

Figure 4.1 Critical Rayleigh numbers Ra_L, Ra_E and Ra_w versus surface temperature T_2.
Equation of state (4.2) holds and $T_1 = 0°C$.
Ra_L: ——, Ra_E: ----, Ra_w:· · · ·

T_2	2	3	4	5	6	7	8
Ra_L	355.32	890.01	1773.04	825.12	595.84	609.42	619.69
Ra_E	355.14	887.38	1735.41	793.98	520.11	440.26	403.07
Ra_w	331.10	683.42	1000.51	300.76	115.74	52.27	26.41
a_L^2	9.716	9.731	9.770	9.958	10.907	15.910	22.783
a_E^2	9.717	9.741	9.804	10.055	10.874	13.060	15.771
a_w^2	9.650	9.650	9.660	9.674	9.689	9.706	9.718
$\bar{\lambda}$	.619	.498	.382	.279	.202	.165	.181
$\bar{f}_1$	.618	.493	.370	.247	.126	.005	-.113
f_1^*	.618	.493	.368	.245	.122	.000	-.121
$\bar{\mu}_1$	.829	1.016	1.268	1.555	1.860	2.175	2.498
μ_{1L}	.007	.029	.066	.117	.182	.262	.357

Table 4.2 Critical Rayleigh and wavenumbers $Ra_L, Ra_E, Ra_w, a_L, a_E, a_w$.
The subscript $L \equiv$linear, $E \equiv$conditional energy,
$w \equiv$unconditional weighted energy.
Equation of state (4.2) holds, and $T_1 = 1°C$.

T_2	3	4	5	6	7	8
Ra_L	595.73	1781.01	666.77	612.44	620.19	619.19
Ra_E	595.61	1762.31	619.89	442.14	371.08	238.61
a_L^2	9.711	9.773	10.232	15.934	25.956	37.141
a_E^2	9.728	9.811	10.346	13.072	16.365	16.646
$\bar{\lambda}$	.370	.254	.157	.110	.145	.254
$\bar{f}_1$	.368	.245	.123	.002	-.117	-.235
f_1^*	.368	.245	.122	.000	-.121	-.241

Table 4.3 Critical Rayleigh and wavenumbers Ra_L, Ra_E, a_L, a_E.
The subscript $L \equiv$linear, $E \equiv$conditional energy.
Equation of state (4.2) holds, and $T_1 = 2°C$.

T_2	1	2	3	4	5	6	7	8
Ra_L	255.37	600.46	1087.30	1819.37	987.68	688.82	610.05	633.28
Ra_E	255.30	599.62	1082.58	1798.19	958.90	638.78	507.47	456.44
a_L^2	9.705	9.705	9.716	9.781	9.896	10.255	11.640	15.990
a_E^2	9.706	9.710	9.730	9.818	9.977	10.376	11.303	13.101
$\bar{\lambda}$	.868	.740	.618	.502	.397	.308	.246	.215

Table 4.4 Critical Rayleigh and wavenumbers Ra_L, Ra_E, a_L, a_E.
The subscript $L \equiv$linear, $E \equiv$conditional energy.
Equation of state (4.3) holds, and $T_1 = 0°C$.
$\bar{\lambda}$ denotes the optimal value of λ.

T_2	2	3	4	5	6	7	8
Ra_L	363.94	917.63	1842.03	863.68	628.82	645.61	655.36
Ra_E	363.76	914.83	1820.76	829.45	546.45	464.30	425.66
a_L^2	9.693	9.729	9.780	9.974	10.973	16.121	22.997
a_E^2	9.695	9.739	9.817	10.074	10.919	13.146	15.953
$\bar{\lambda}$	.609	.487	.372	.271	.195	.160	.172

Table 4.5 Critical Rayleigh and wavenumbers Ra_L, Ra_E, a_L, a_E.
The subscript $L \equiv$linear, $E \equiv$conditional energy.
Equation of state (4.3) holds, and $T_1 = 1°C$.

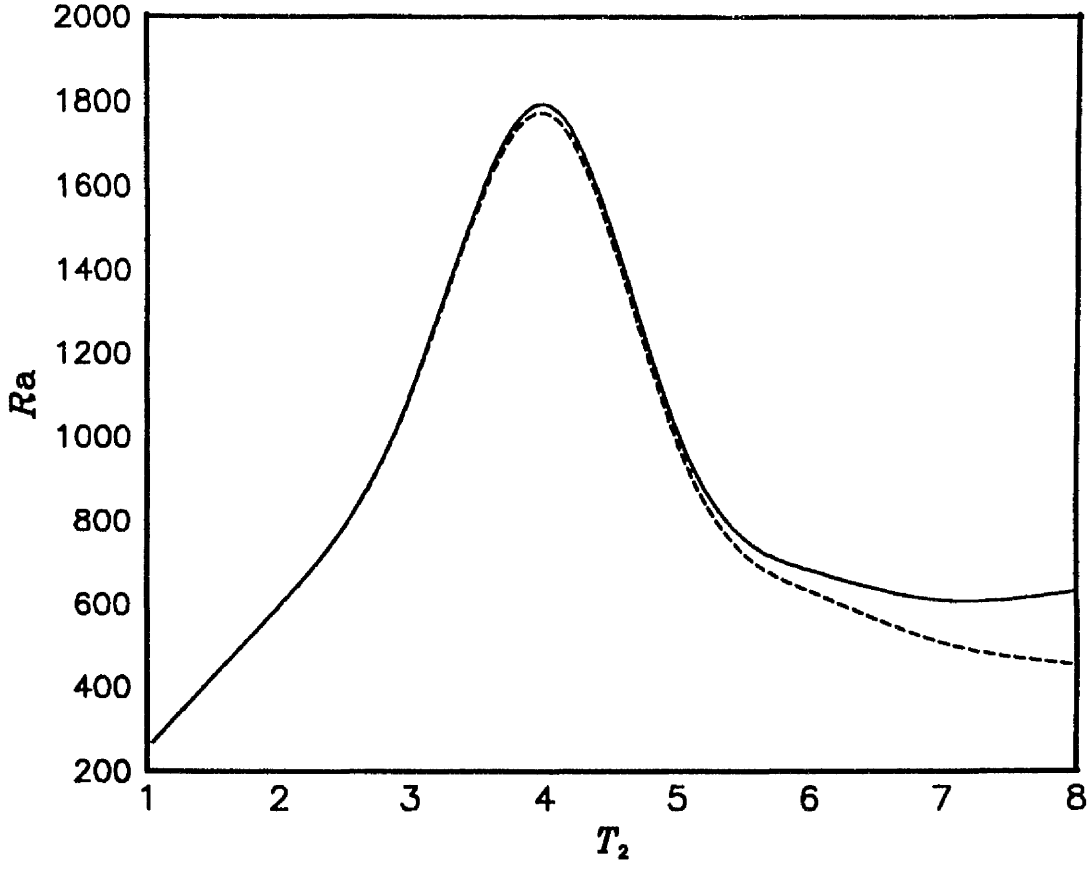

Figure 4.2 Critical Rayleigh numbers Ra_L and Ra_E
versus surface temperature T_2.
Equation of state (4.3) holds and $T_1 = 0°C$.
Ra_L: ——, Ra_E: ----

T_2	3	4	5	6	7	8
Ra_L	619.93	1871.34	711.60	663.99	670.33	669.48
Ra_E	619.01	1849.75	659.11	475.61	335.55	445.91
a_L^2	9.719	9.782	10.269	16.324	26.391	37.804
a_E^2	9.723	9.818	10.383	13.224	16.605	27.202
$\bar{\lambda}$	.359	.244	.150	.106	.110	.108

Table 4.6 Critical Rayleigh and wavenumbers Ra_L, Ra_E, a_L, a_E.
The subscript $L \equiv$linear, $E \equiv$conditional energy.
Equation of state (4.3) holds, and $T_1 = 2°C$.
$\bar{\lambda}$ denotes the optimal value of λ.

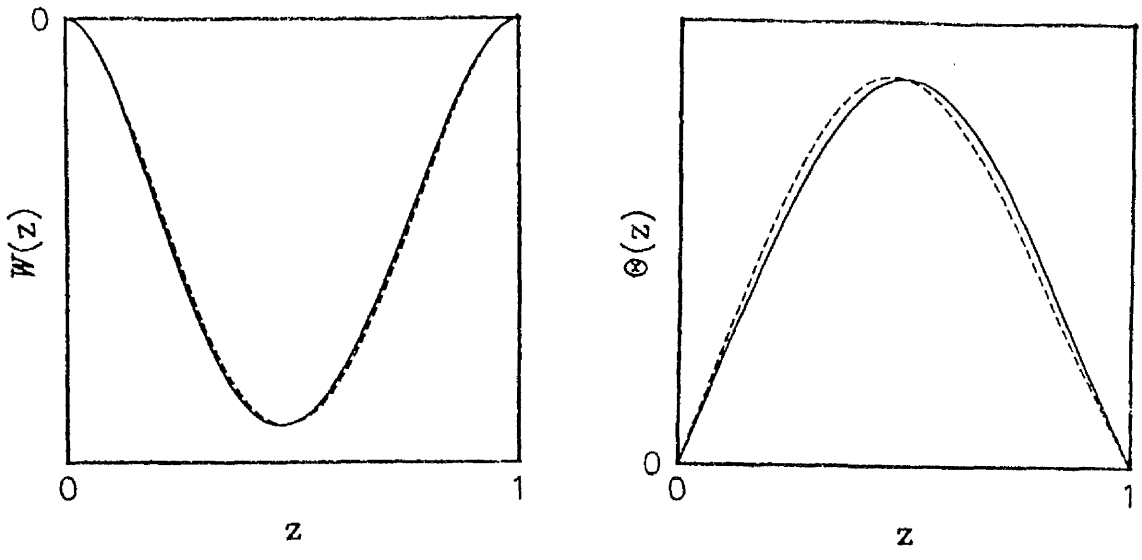

Figure 4.3 Normalized perturbation eigenfunctions $W(z)$, $\Theta(z)$.
$T_1 = 0°\text{C}$, $T_2 = 4°\text{C}$. $Ra_L = 1767.71$, $Ra_E = 1747.93$, $a_L^2 = 9.780$, $a_E^2 = 9.815$.
Linear: ——, Energy: ----

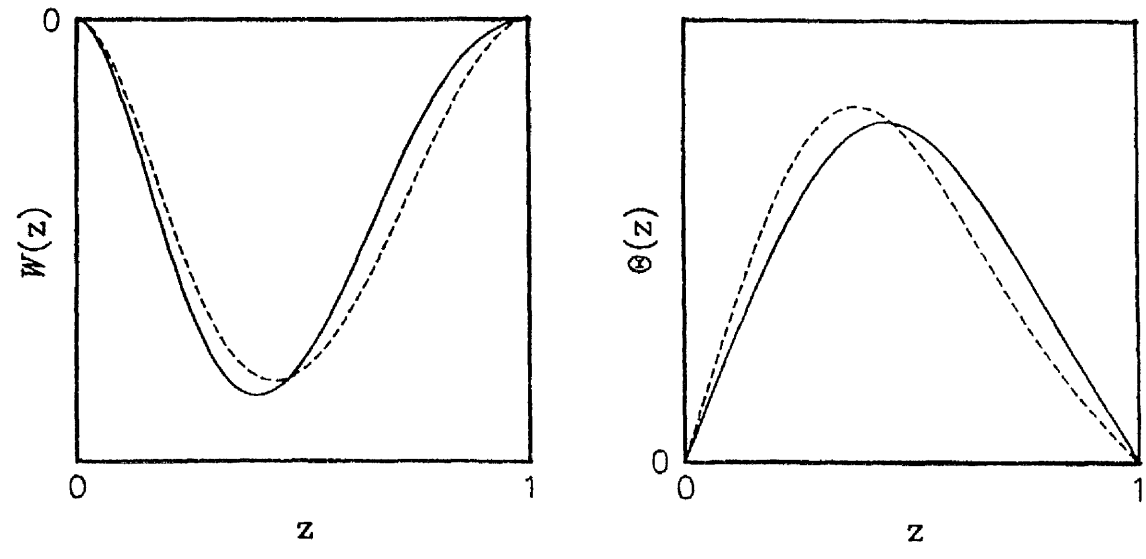

Figure 4.4 $T_1 = 1°\text{C}$, $T_2 = 6°\text{C}$. $Ra_L = 595.84$, $Ra_E = 520.11$,
$a_L^2 = 10.907$, $a_E^2 = 10.874$. Linear: ——, Energy: ----

4.6.2 Discussion

We may now compare the results in tables 4.1 and 4.4 with those given in Straughan (1985). The linear and conditional energy critical Rayleigh numbers given in tables 4.1 and 4.4 are *higher* than those given in Straughan (1985), contradicting the predictions of Merker *et al.* (1979). However, as explained earlier, the different values of B used by Veronis (1963) and Merker *et al.* (1979) lead to different Ra. If the same value for B were adopted in Straughan (1985) and here, then we would find that the critical Rayleigh numbers using the cubic density relation (4.2) are approximately 10% smaller than those using the quadratic relation. A quintic density relation (4.3) produces critical Rayleigh numbers which are 8% smaller than those in Straughan (1985). The corresponding critical wavenumbers in all three cases differ by less than 1%. The wavenumbers also exhibit the same behaviour in each case. The Rayleigh numbers decrease as the upper surface temperature is increased beyond 4°C. The linear Rayleigh numbers in each case decrease to a minimum value at approximately 7°C before approaching a constant asymptotic value. Critical wavenumbers increase as upper surface temperature increases.

Tables 4.1–4.6 and figures 4.1 and 4.2 show that the critical Rayleigh numbers increase as the upper temperature is increased from 1°C to 4°C. This increase is a result of the definition of Ra. The water layer itself becomes more unstable as this temperature is increased. As the lower surface temperature is increased, the critical Rayleigh numbers decrease (provided $1 \leq T_2 \leq 6$).

For upper surface temperatures less than 4°C the difference between the energy and linear results is small (less than 1% in some cases). This suggests that subcritical instabilities are unlikely to occur in this situation. However as the upper surface temperature increases, the difference between linear and energy Rayleigh numbers increases. Therefore, as predicted by Veronis (1963), subcritical instabilities are likely to occur in this region. In figures 4.3 and 4.4 we compute the normalized perturbation eigenfunctions $W(z)$, $\Theta(z)$ which occur at the onset of convection, as predicted by *linear theory*. For comparison we also include

the corresponding eigenfunctions which occur at the critical conditional Rayleigh number in energy theory. However, as the energy method only gives information about *stability* in the layer and not instability, the energy eigenfunctions do not represent physical instabilities in the fluid. Nevertheless, figure 4.3 shows that when the critical Rayleigh numbers of linear and energy theory are close the corresponding eigenfunctions are almost identical. Figure 4.4 suggests that the eigenfunctions are less alike when the difference between Rayleigh numbers is greater.

As mentioned earlier the linear and conditional energy results of tables 4.1–4.3 are very close to those given in tables 4.4–4.6. Indeed, in general, they support the predictions made by Merker *et al.* (1979) regarding the size of the critical Rayleigh number. The critical Rayleigh numbers of the quintic relation (4.3) are slightly higher than those of the cubic case, contradicting Merker *et al.* (1979). This is partially due to the definition of conditional stability. The bounds on the initial energy given in the cubic example are different from those given in the quintic case. This will naturally lead to difficulties when comparing the Rayleigh numbers. Comparing the critical wavenumbers we also observe that the cubic and quintic relations produce wavenumbers which are in very good agreement. In general there is no more than a 2% difference between the numbers.

Tables 4.1 and 4.2 and figure 4.1 also show the results obtained for *unconditional energy stability.* The large discrepancies between these Rayleigh numbers and other corresponding results demonstrate the effect restricting the initial energy will have on the fluid stability and any numerical calculations.

Finally, we shall consider the numerically calculated values of the coupling parameters – in particular $\bar{\lambda}$ given in tables 4.1–4.3. $\bar{\lambda}$ decreases as the upper surface temperature increases. It reaches a minimum at approximately 7°C before starting to increase. Furthermore, the values of $\bar{f}_1$ and f_1^* are close to those of $\bar{\lambda}$ for $1 \leq T_2 \leq 6$. This suggests that the parametric differentiation technique of Joseph is indeed useful when searching numerically for $\bar{\lambda}$.

4.6.3 Conclusion

The cubic density relation (4.2) produces critical Rayleigh numbers which exhibit the same behaviour as those produced using a quadratic model. As predicted by Merker *et al.* (1979), the former results are lower and more accurate. The quintic density model (4.3) will produce Rayleigh numbers even more accurately. However, the small gain in accuracy and the increase in mathematical analysis required for the quintic model make it preferable to use the cubic density relation (4.2) when discussing penetrative convection. Furthermore, the increase in analysis and extra numerical computation required in order to produce (weaker) *unconditional* stability bounds make it more practical to obtain *conditional* stability results when employing this cubic density model.

Chapter 5

Convection with internal heat generation near the density maximum

5.1 Introduction

In this chapter we shall employ the cubic density law for water advocated by Merker *et al.* (1979) when studying a convection problem similar to that of Roberts (1967) and Tritton & Zarraga (1967), related to the system described in chapters 2 and 3. We shall consider the problem of penetrative convection in an internally heated plane layer of water whose lower surface is subject to a given heat flux, while the upper surface is held at a constant temperature.

In one of the first articles on this problem Roberts (1967) derives the linear instability boundary for a horizontal fluid layer which is subject to uniform heating, and studies the resulting solution behaviour after the onset of convection. The results obtained are compared with experimental observations of the same problem made by Tritton & Zarraga (1967). This lead Thirlby (1970) to study cell structures as the Rayleigh number varied. The numerical analysis of Thirlby (1970) found the critical values of the Rayleigh number at which the size and shape of the convection cells altered. Similarly, the papers of Lennie *et al.* (1988) and Travis *et al.* (1990) perform numerical analyses of internally heated systems. In particular, Travis *et al.* (1990) perform a benchmark comparison of the different numerical schemes which have been used to model the convection system. McKenzie *et al.* (1974) also perform numerical analyses on a number of convection problems, including convection due to internal heating, with applications to convection in the Earth's mantle.

Here we deal with the problem of finding linear instability estimates and

the analagous (conditional) nonlinear stability estimates. The latter is achieved by employing energy theory. In Roberts (1967) the writer observes that in the experiments of Tritton & Zarraga (1967) it may be inappropriate to have the heat source constant. As a result we discuss the possibility of a non-uniform heat supply. A nonlinear energy analysis will produce a critical Rayleigh number below which convection will not occur. However, due to the fact that subcritical instabilities may occur in an internal heating convection problem (Joseph & Shir 1966), we shall also calculate a linear critical Rayleigh number above which convection will occur. The parameter region of possible subcritical instability is small.

5.2 Convection in a horizontal layer

We shall consider a layer of water satisfying the cubic equation of state (4.2). The water shall occupy the horizontal region $z \in (0, d)$, with the lower boundary $z = 0$ heated in some manner and the upper boundary $z = d$ held at a constant temperature T_u.

The equations of motion are (using standard indicial notation):

$$\begin{aligned} v_{i,t} + v_j v_{i,j} &= -\frac{1}{\rho_0} p_{,i} + \nu \Delta v_i - g k_i \left[1 + AT - BT^2 + CT^3\right], \\ v_{i,i} &= 0, \\ T_{,t} + v_i T_{,i} &= \kappa \Delta T + Q, \end{aligned} \tag{5.1}$$

where $\mathbf{v}$, T, p, g, ν, κ, Q are respectively velocity, temperature in $^\circ C$, pressure, gravitational constant, kinematic viscosity, thermal diffusivity and the heat supply. A, B, C are the constants described in chapter 4, and $\mathbf{k} = (0, 0, 1)$. Equations (5.1) are defined on the spatial region $\mathbf{R}^2 \times \{z \in (0, d)\}$ with boundary conditions

$$\mathbf{v} = \mathbf{0}, \quad z = 0, d; \qquad T = T_u, \quad z = d; \qquad \frac{\partial T}{\partial z} = \gamma, \quad z = 0. \tag{5.2}$$

We shall consider four possible heat supplies:

$$\begin{aligned} \text{I} \quad &: \quad Q = Q \quad (\text{constant} \neq 0), \\ \text{II} \quad &: \quad Q = Q(e^{z/d} - 1), \\ \text{III} \quad &: \quad Q = Q \sin \frac{2\pi z}{d}, \\ \text{IV} \quad &: \quad Q = 0. \end{aligned} \tag{5.3}$$

The remainder of this chapter shall be split into two subsections. In subsection (i) we shall discuss cases I, II and III where convection in the layer is produced by the heat flux at the lower boundary and an internal heat source. In subsection (ii) we shall discuss case IV where motion is generated solely by a flux on the lower boundary.

(i) Cases I, II, III Non-zero heat supply

The steady solutions $(\bar{\mathbf{v}}, \bar{T}(z), \bar{p})$ corresponding to boundary conditions (5.2) are in each case:

$$\begin{aligned}
&\text{I}: \quad \bar{\mathbf{v}} \equiv \mathbf{0}, \qquad \bar{T} = \frac{Q}{2\kappa}(d^2 - z^2) - \gamma(d-z) + T_u\,, \\
&\text{II}: \quad \bar{\mathbf{v}} \equiv \mathbf{0}, \qquad \bar{T} = \frac{Qd^2}{2\kappa}\left(e - \frac{3}{2} - e^{z/d} + \frac{z}{d} + \frac{z^2}{2d^2}\right) - \gamma(d-z) + T_u\,, \\
&\text{III}: \quad \bar{\mathbf{v}} \equiv \mathbf{0}, \qquad \bar{T} = \frac{Qd^2}{2\pi\kappa}\left(1 + \frac{1}{2\pi}\sin\frac{2\pi z}{d} - \frac{z}{d}\right) - \gamma(d-z) + T_u\,.
\end{aligned} \tag{5.4}$$

The hydrostatic pressure is given by equations (5.1). Now introduce perturbations $(\mathbf{u}, \theta, \pi)$ via

$$\mathbf{v} = \bar{\mathbf{v}} + \mathbf{u}, \qquad T = \bar{T} + \theta, \qquad p = \bar{p} + \pi.$$

In terms of the non-dimensional (asterisked) variables

$$t = T^+ t^*, \qquad \pi = P\pi^*, \qquad \mathbf{x} = d\mathbf{x}^*, \qquad \mathbf{u} = U\mathbf{u}^*, \qquad \theta = T^\sharp\theta^*,$$

$$T^+ = \frac{d^2}{\nu}, \qquad U = \frac{\nu}{d}, \qquad P = \frac{U\nu}{d}, \qquad T^\sharp = U\left(\frac{\nu}{dAg\kappa}\right)^{\frac{1}{2}},$$

and non-dimensional numbers

$$Pr = \frac{\nu}{\kappa}, \qquad R^2 = \frac{d^7 A Q^2 g}{\kappa^3 \nu}, \tag{5.5}$$

the Prandtl and Rayleigh numbers respectively, the perturbation equations are (dropping *'s):

$$\begin{aligned}
u_{i,t} + u_j u_{i,j} = -\pi_{,i} + \Delta u_i - R\theta k_i\left(\frac{1}{\beta} + \frac{2B}{A}M(z) + \frac{3C\beta}{A}M(z)^2\right) \\
+ 3Pr\theta^2 k_i\left(\frac{C\beta}{A}M(z) + \frac{B}{A}\right) - \frac{CPr^2\beta}{AR}\theta^3 k_i\,,
\end{aligned} \tag{5.6}$$

$$u_{i,i} = 0\,,$$

$$Pr(\theta_{,t} + u_i\theta_{,i}) = R(f(z) - \hat{\gamma})w + \Delta\theta,$$

where $w = u_3$,

$$\hat{\gamma} = \frac{\gamma\kappa}{Qd}\,, \qquad \beta = \frac{Qd^2}{\kappa}(\neq 0)\,, \qquad \delta = -\frac{T_u}{\beta}\,, \tag{5.7}$$

$$M(z) = -h(z) + \hat{\gamma}(1-z) + \delta\,,$$

and $f(z)$, $h(z)$ are defined in each case as follows:

$$\begin{aligned} &\text{I}: && f(z) = z, && h(z) = \tfrac{1}{2}(1-z^2); \\ &\text{II}: && f(z) = e^z - 1 - z, && h(z) = e - \tfrac{3}{2} - e^z + z + \tfrac{1}{2}z^2; \\ &\text{III}: && f(z) = \tfrac{1}{2\pi}(1-\cos 2\pi z), && h(z) = \tfrac{1}{2\pi}\left(1 + \tfrac{1}{2\pi}\sin 2\pi z - z\right). \end{aligned} \tag{5.8}$$

Equations (5.6) hold on the spatial region $\mathbf{R}^2 \times (0,1)$ and the boundary conditions become

$$\begin{aligned} &u_i = 0, \quad z = 0, 1; \\ &\frac{\partial \theta}{\partial z} = 0, \quad z = 0; \qquad \theta = 0, \quad z = 1; \\ &\mathbf{u}, \theta, \pi \quad \text{have a periodic structure in } x, y. \end{aligned} \tag{5.9}$$

We choose boundary conditions appropriate to two fixed surfaces.

To obtain the nonlinear stability, first multiply $(5.6)_1$ by u_i and integrate over a period cell V. Then use of equation $(5.6)_2$ together with the divergence theorem and boundary conditions (5.9) yields

$$\begin{aligned} \frac{1}{2}\frac{d}{dt}\|\mathbf{u}\|^2 = -D(\mathbf{u}) - < R\theta w \left(\frac{1}{\beta} + \frac{2B}{A}M(z) + \frac{3C\beta}{A}M(z)^2\right) > \\ + 3Pr < \theta^2 w \left(\frac{C\beta}{A}M(z) + \frac{B}{A}\right) > - \frac{CPr^2\beta}{AR} < \theta^3 w >, \end{aligned} \tag{5.10}$$

where $\|.\|$ is the $L^2(V)$ norm, $D(\mathbf{m}) = \|\nabla \mathbf{m}\|^2$ for any vector $\mathbf{m}$, and

$$< f >= \int_V f(\mathbf{x})\, d\mathbf{x}.$$

Similarly, multiplying $(5.6)_3$ by θ and integrating over V yields

$$\frac{Pr}{2}\frac{d}{dt}\|\theta\|^2 = < R\theta w\,(f(z) - \hat{\gamma}) > - D(\theta), \tag{5.11}$$

where $D(S) = \|\nabla S\|^2$ for any scalar S.

A straightforward combination of (5.10) and (5.11) is evidently unsatisfactory to produce a nonlinear stability bound for the cubic density model. We here derive another identity which involves θ^4. This allows us to estimate the necessary terms. Define $\phi = \theta^2$, multiply $(5.6)_3$ by θ^3 and integrate over V to see that

$$\frac{Pr}{4}\frac{d}{dt}\|\phi\|^2 = < R\theta^3 w\,(f(z) - \hat{\gamma}) > - \frac{3}{4}D(\phi), \tag{5.12}$$

where the divergence theorem and boundary conditions (5.9) have been employed.

We now introduce η and $\lambda(>0)$ as coupling parameters to be chosen, and define an "energy" $E(t)$ by

$$E(t) = \frac{1}{2}\|\mathbf{u}\|^2 + \frac{Pr}{2}\eta\|\theta\|^2 + \frac{Pr}{4}\lambda\|\phi\|^2 . \tag{5.13}$$

Then from (5.10)–(5.12) we may obtain,

$$\frac{dE}{dt} = -D(\mathbf{u}) - \eta D(\theta) - \frac{3}{4}\lambda D(\phi) - R < \theta w F(z) > + < \theta^2 w G(z) > + < \theta\phi w H(z) >,$$

where

$$F(z) = \frac{1}{\beta} + \frac{2B}{A}M(z) + \frac{3C\beta}{A}M(z)^2 - \eta\left(f(z) - \hat{\gamma}\right) ,$$

$$G(z) = 3Pr\left(\frac{C\beta}{A}M(z) + \frac{B}{A}\right) ,$$

$$H(z) = \lambda R\left(f(z) - \hat{\gamma}\right) - \frac{CPr^2\beta}{AR} .$$

Next, let

$$I_\eta = - < F(z)\theta w >, \qquad D_\eta = D(\mathbf{u}) + \eta D(\theta),$$

and define

$$\frac{1}{R_E} = \max_{\mathcal{H}} \frac{I_\eta}{D_\eta} ,$$

where $\mathcal{H}$ is the space of admissible functions over which we seek the maximum. Then from the energy equation first derived we find

$$\frac{dE}{dt} \leq -RD_\eta\left(\frac{1}{R} - \frac{1}{R_E}\right) + < \theta^2 w G(z) > - \frac{3}{4}\lambda D(\phi) + < \theta\phi w H(z) > . \tag{5.14}$$

Suppose now $R < R_E$. Then

$$\alpha = R\left(\frac{1}{R} - \frac{1}{R_E}\right) > 0.$$

Thus

$$\frac{dE}{dt} \leq -\alpha D_\eta + < \theta^2 w G(z) > - \frac{3}{4}\lambda D(\phi) + < \theta\phi w H(z) > .$$

If we set

$$G_m = \max_{z\in[0,1]} |G(z)|,$$

which is finite for each case I, II and III in this region, for $\tau(>0)$ to be chosen we may obtain

$$<\theta^2 wG(z)> \leq \frac{G_m}{2\tau}\|\phi\|^2 + \frac{G_m\tau}{2}\|w\|^2$$
$$\leq \frac{G_m}{2\tau c_1}D(\phi) + \frac{G_m\tau}{2c_1}D(\mathbf{u}),$$

where in the last line Poincaré's inequality $D(\mathbf{u}) + D(\phi) \geq c_1(\|\phi\|^2 + \|w\|^2)$ for some $c_1 > 0$ has been employed. Choose now τ such that

$$\tau = \frac{\alpha c_1}{G_m}.$$

This gives

$$\frac{dE}{dt} \leq -\frac{\alpha}{2}D(\mathbf{u}) - \alpha\eta D(\theta) - \left(\frac{3}{4}\lambda - \frac{{G_m}^2}{2{c_1}^2\alpha}\right)D(\phi) + <\theta\phi wH(z)>. \qquad (5.15)$$

It should be explained here how the coupling parameters η and λ are used. η is chosen in order to maximize the critical Rayleigh number of the energy theory. However, λ is chosen in order to control the cubic nonlinearities which occur in this problem due to the cubic terms in the equation of state. In order to do this, choose λ so large that

$$\lambda > \frac{2{G_m}^2}{3{c_1}^2\alpha},$$

and define

$$J = \frac{3}{4}\lambda - \frac{{G_m}^2}{2{c_1}^2\alpha} \quad (>0).$$

We then find

$$\frac{dE}{dt} \leq -\mathcal{D} + <\theta\phi wH(z)>, \qquad (5.16)$$

where

$$\mathcal{D} = \frac{\alpha}{2}D(\mathbf{u}) + \alpha\eta D(\theta) + JD(\phi).$$

If we now define the finite constant

$$H_m = \max_{z\in[0,1]}|H(z)|,$$

and utilize Hölder's inequality and the Sobolev inequality

$$\left(\int_V \phi^4 \, d\mathbf{x}\right)^{\frac{1}{4}} \leq k\left(\int_V |\nabla\phi|^2 \, d\mathbf{x}\right)^{\frac{1}{2}}$$

for some constant $k > 0$, we may show that

$$\begin{aligned} <\theta\phi w H(z)> &\leq H_m \|w\| \|\theta\phi\| \\ &\leq H_m \|w\| \left(\int_V \theta^4 \, d\mathbf{x}\right)^{\frac{1}{4}} \left(\int_V \phi^4 \, d\mathbf{x}\right)^{\frac{1}{4}} \\ &\leq k H_m \|w\| D(\phi)^{\frac{1}{2}} \|\phi\|^{\frac{1}{2}} \\ &\leq \frac{k H_m}{J^{\frac{1}{2}}} \|w\| \mathcal{D}^{\frac{1}{2}} \|\phi\|^{\frac{1}{2}}. \end{aligned}$$

However, from (5.13) we may obtain

$$\|w\| \leq (2E(t))^{\frac{1}{2}}, \qquad \|\phi\|^{\frac{1}{2}} \leq \left(\frac{4}{\lambda Pr} E(t)\right)^{\frac{1}{4}}.$$

Thus, by Poincaré's inequality where $c_2 > 0$ is some constant,

$$\begin{aligned} <\theta\phi w H(z)> &\leq 2k H_m \left(\frac{1}{\lambda J^2 c_2^2 Pr}\right)^{\frac{1}{4}} \mathcal{D} E(t)^{\frac{1}{4}} \\ &= K \mathcal{D} E(t)^{\frac{1}{4}}, \end{aligned} \tag{5.17}$$

where the constant K is defined as indicated.

Finally, from (5.16) and (5.17) we deduce

$$\frac{dE}{dt} \leq -\mathcal{D}\left(1 - K E(t)^{\frac{1}{4}}\right). \tag{5.18}$$

Hence if

$$\text{(i)} \quad R < R_E \qquad \text{and} \qquad \text{(ii)} \quad E(0)^{\frac{1}{4}} < \frac{1}{K}, \tag{5.19}$$

we may show from inequality (5.18) that $E(t) \to 0$ exponentially as $t \to \infty$. This yields conditional, nonlinear stability.

The conditional stability relates to the base solution of the flow. It is a mathematically precise and rigorous statement of (nonlinear) stability for a problem

which is subject to a determinable bound on its initial energy. In comparison, however, linear instability theory gives no indication of the initial threshold; it is being said only that it is valid for "infinitesimal" disturbances.

It now remains to find the critical Rayleigh number, Ra_E, which indicates an upper limit of stability in the fluid. Recall that

$$\frac{1}{R_E} = \max_{\mathcal{H}} -\frac{<F(z)\theta w>}{D(\mathbf{u}) + \eta D(\theta)} . \tag{5.20}$$

Define $\psi = \eta^{\frac{1}{2}}\theta$ and $S(z) = \eta^{-\frac{1}{2}}F(z)$ so that

$$\frac{1}{R_E} = \max_{\mathcal{H}} -\frac{<S(z)\psi w>}{D(\mathbf{u}) + D(\psi)} .$$

The Euler-Lagrange equations for R_E are

$$\begin{aligned} \Delta u_i - \tfrac{1}{2}R_E S(z)\psi k_i &= \varpi_{,i} , \\ \Delta\psi - \tfrac{1}{2}R_E S(z) w &= 0 , \end{aligned} \tag{5.21}$$

where ϖ is a Lagrange multiplier which appears because of the solenoidal nature of $\mathbf{u}$. If we now take curl curl $(5.21)_1$ and take the third component of the resulting equation, we obtain

$$\Delta^2 w - \frac{1}{2}R_E S(z)\Delta^*\psi = 0 , \tag{5.22}$$

where $\Delta^* = \dfrac{\partial^2}{\partial x^2} + \dfrac{\partial^2}{\partial y^2}$. Because of the periodicity of $\mathbf{u}$ and θ in the x and y directions we may now introduce normal modes, i.e.

$$w = W(z)T(x,y) , \qquad \psi = \Psi(z)T(x,y) ,$$

where $\Delta^* T = -a^2 T$ and a is the horizontal wave number.

Equations $(5.21)_2$ and (5.22) now become

$$\begin{aligned} (D^2 - a^2)^2 W + \tfrac{1}{2}a^2 R_E S(z)\Psi &= 0 , \\ (D^2 - a^2)\Psi - \tfrac{1}{2}R_E S(z) W &= 0 , \end{aligned} \tag{5.23}$$

where $D = \dfrac{\partial}{\partial z}$. Equations (5.23) are defined on the spatial region $z \in (0,1)$ with boundary conditions

$$W = DW = 0, \quad z = 0,1; \qquad \Psi = 0, \quad z = 1 ; \qquad D\Psi = 0, \quad z = 0. \tag{5.24}$$

We require to solve this system for the lowest eigenvalue $R_E(a^2;\eta)$ and then determine

$$Ra_E = \max_{\eta} \min_{a} R_E^2(a^2;\eta).$$

Here Ra_E is the critical Rayleigh number of energy theory.

We may compare this with the eigenvalue problem of linear theory for stationary convection. If we had chosen a quadratic buoyancy term in the momentum equation $(5.1)_1$, we could easily have shown that exchange of stabilities holds when our boundaries are stress free. Our nonlinear energy results are very close to those of stationary convection, suggesting that it is sufficient to consider only stationary convection for our linear theory, even though here the boundaries are fixed and the density law is cubic. The eigenvalue problem of linear theory is:

$$\begin{aligned} (D^2 - a^2)^2 W + a^2 R \left(\tfrac{1}{\beta} + \tfrac{2B}{A} M(z) + \tfrac{3C\beta}{A} M(z)^2 \right) \Theta = 0\,, \\ (D^2 - a^2)\Theta + R(f(z) - \hat{\gamma}) W = 0\,. \end{aligned} \tag{5.25}$$

(Note: $\theta = \Theta(z)T(x,y)$ in this problem.) Once again, for (5.25) we find

$$Ra_L = \min_{a} R^2(a^2).$$

Ra_L, the critical Rayleigh number of linear theory, indicates the onset of instability in the fluid. The numerical results were obtained by the compound matrix method and are given below.

Ra_L	a_L^2	Ra_E	a_E^2	η_c	$\bar{\eta}$	$\hat{\gamma}$	δ	β
82936.4	7.247	82670.0	7.256	0.067	0.060	0	-0.1	200
40332.1	6.767	39474.0	6.802	0.145	0.126	0	-0.1	100
53474.9	6.879	52717.6	6.927	0.107	0.095	0	-0.1	150
55930.9	7.040	55482.2	7.067	0.101	0.093	0	-0.2	150
54368.3	6.804	53450.8	6.867	0.107	0.091	0	- 0.05	150
68274.9	6.956	66564.8	7.018	0.134	0.119	0.1	- 0.1	150
96953.7	7.152	92653.0	7.245	0.170	0.154	0.2	- 0.1	150
48271.3	6.891	46985.1	6.990	0.191	0.173	0.1	- 0.2	100
69639.9	7.155	66555.3	7.245	0.236	0.219	0.2	- 0.2	100

Table 5.1 Critical Rayleigh numbers of linear theory, Ra_L, and energy theory, Ra_E, together with the respective critical wavenumbers a_L, a_E.

Case I : $f(z) = z, \quad h(z) = \frac{1}{2}(1 - z^2)$.

(η_c denotes the optimum coupling parameter η found numerically, and $\bar{\eta}$ is defined later in (5.28).)

Ra_L	a_L^2	Ra_E	a_E^2	η_c	$\bar{\eta}$	$\hat{\gamma}$	δ	β
219871	7.256	208807	7.402	0.222	0.166	0	-0.1	200
175834	7.133	165638	7.306	0.283	0.206	0	-0.1	100
191691	7.190	181268	7.349	0.257	0.190	0	-0.1	150
163191	7.269	155252	7.426	0.297	0.229	0	-0.2	150
221355	7.112	208331	7.295	0.225	0.161	0	- 0.05	150
547036	9.557	444001	9.158	0.375	0.303	0.1	- 0.1	150
1198767	14.705	830582	11.660	0.413	0.474	0.15	- 0.1	150
375774	9.625	307020	9.202	0.539	0.448	0.1	- 0.2	100
798370	14.767	556253	11.231	0.550	0.723	0.15	- 0.2	100

Table 5.2 Critical Rayleigh numbers of linear theory, Ra_L, and energy theory, Ra_E, together with the respective critical wavenumbers a_L, a_E .

Case II: $f(z) = e^z - 1 - z, \quad h(z) = e - \frac{3}{2} - e^z + z + \frac{1}{2}z^2.$

Ra_L	a_L^2	Ra_E	a_E^2	η_c	$\hat{\gamma}$	δ	β
179483	6.513	177768	6.546	0.123	0	-0.1	200
169472	6.444	166942	6.492	0.132	0	-0.1	100
169738	6.482	167724	6.520	0.131	0	-0.1	150
120838	6.576	120028	6.596	0.181	0	-0.2	150
231392	6.388	226722	6.462	0.098	0	-0.05	150
400620	6.590	391405	6.650	0.158	0.1	-0.1	150
242529	7.444	215306	7.612	0.228	0.2	-0.1	150
226385	6.455	222857	6.725	0.275	0.1	-0.2	100
965533	7.530	867691	7.689	0.560	0.2	-0.2	100

Table 5.3 Critical Rayleigh numbers of linear theory, Ra_L, and energy theory, Ra_E, together with the respective critical wavenumbers a_L, a_E.

Case III: $f(z) = \frac{1}{2\pi}(1 - \cos 2\pi z), \quad h(z) = \frac{1}{2\pi}\left(1 + \frac{1}{2\pi}\sin 2\pi z - z\right).$

The data presented in tables 5.1–5.3 show that the energy theory gives predictions which are close to those of the linear theory. This suggests that linear theory is of practical use. The definitions of $R, \hat{\gamma}, \delta$ and β make it difficult to draw conclusions directly from the data. However, the data will be of use if employed with experimental results. Three of the variables $Q, d, \hat{\gamma}$ or T_u would be fixed in an experiment and the fourth varied until its critical value is found.

The results in tables 5.1–5.3 suggest that the critical Rayleigh number increases with increasing $\hat{\gamma}$ (δ and β fixed) in both linear and energy theory. This increase is unexpected when we consider the definitions of R and $\hat{\gamma}$. We may try and explain this phenomenon using a heuristic argument. It can be shown using parametric differentiation and equations (5.21),

$$\frac{\partial R_E}{\partial \hat{\gamma}}(\|\nabla \mathbf{u}\|^2 + \|\nabla \psi\|^2) = 2R_E^2 < \frac{\partial S}{\partial \hat{\gamma}} w\psi > \ . \tag{5.26}$$

We may now calculate $\dfrac{\partial S}{\partial \hat{\gamma}}$ and take its average over z (by integrating over z from 0 to 1). For the data which we have chosen in tables 5.1–5.3, this average is always positive. Experience with similar eigenvalue problems has also shown that, in general, $< w\psi >$ is positive. This in turn *suggests* that $\dfrac{\partial R_E}{\partial \hat{\gamma}}$ is positive, i.e. R_E is increasing with increasing $\hat{\gamma}$.

This method may also be employed in order to estimate the best value of the coupling parameter η, η_c. A parametric differentiation similar to the one used above produces

$$\frac{\partial R_E}{\partial \eta}(\|\nabla \mathbf{u}\|^2 + \|\nabla \psi\|^2) = R_E^2 < \left(\frac{\eta K(z) - F(z)}{2\eta^{\frac{3}{2}}}\right) w\psi > . \tag{5.27}$$

Since the best value of η occurs when $\dfrac{\partial R_E}{\partial \eta} = 0$, (5.27) suggests that the optimum η, η_c, is close to

$$\bar{\eta} = \frac{\int_0^1 F(z)\, dz}{\int_0^1 K(z)\, dz}. \tag{5.28}$$

Values for $\bar{\eta}$ in cases I and II are given in tables 5.1 and 5.2. The predictions for $\bar{\eta}$ are close to the critical values, η_c, calculated numerically. This agreement between the two approaches emphasizes that the heuristic argument used

to demonstrate how R_E will vary with $\hat{\gamma}$, while not mathematically precise, gives a good indication of the behaviour we expect the critical Rayleigh number to exhibit.

It should be noted however that the heuristic approach is unsuccessful in case III. The choice of a heat source which heats part of the layer while the rest is cooled internally produces cancellations which make the approach impractical.

(ii) Case IV No internal heat generation

In subsection (ii) the analysis is in many ways similar to that of subsection (i). As a result we shall refer back to subsection (i) and the results proved therein on several occasions. In case IV, where $Q = 0$, the steady solution $(\bar{\mathbf{v}}, \bar{T}(z), \bar{p})$ corresponding to equations (5.1) and boundary conditions (5.2) is

$$\bar{\mathbf{v}} \equiv 0, \qquad \bar{T} = T_u - \gamma(d - z)\,,$$

with the hydrostatic pressure given by (5.1). If we introduce the perturbation $(\mathbf{u}, \theta, \pi)$ as in subsection (i), we may non-dimensionalize in a similar way. However, in this subsection we define the Rayleigh number

$$R^2 = \frac{d^5 \gamma^2 A g}{\kappa \nu},$$

and introduce the additional definitions

$$\hat{\beta} = \gamma d\,, \qquad \hat{\delta} = \frac{-T_u}{\hat{\beta}}\,, \qquad \hat{M}(z) = \hat{\delta} + (1 - z)\,.$$

The corresponding perturbation equations are:

$$\begin{aligned} u_{i,t} + u_j u_{i,j} &= -\pi_{,i} + \Delta u_i - R\theta k_i \left(\frac{1}{\hat{\beta}} + \frac{2B}{A}\hat{M}(z) + \frac{3C\hat{\beta}}{A}\hat{M}(z)^2 \right) \\ &\quad - 3Pr\theta^2 k_i \left(\frac{C}{A}\hat{\beta}\hat{M}(z) + \frac{B}{A} \right) - \frac{CPr^2\hat{\beta}}{AR}\theta^3 k_i\,, \qquad (5.29) \\ u_{i,i} &= 0\,, \\ Pr(\theta_{,t} + u_i\theta_{,i}) &= -Rw + \Delta\theta\,. \end{aligned}$$

The boundary conditions adopted are (5.9).

If we now compare equations (5.29) with (5.6) in subsection (i) then it is obvious that the two systems are very similar. If we replace $M(z)$, β, $H(z)$ and R defined in subsection (i) with, respectively, $\hat{M}(z)$, $\hat{\beta}$, $H(z) = -1$ and R defined in subsection (ii), then the analysis to prove nonlinear conditional stability in (i) will also apply in this case to prove a similar nonlinear conditional stability. The only differences between the two situations will occur when defining the constants G_m, H_m and J.

Having verified the nonlinear analysis in subsection (ii), it now remains to find R_E where

$$\frac{1}{R_E} = \max_{\mathcal{H}} \frac{I_\eta}{D_\eta},$$

and

$$I_\eta = - < \Big(\frac{1}{\hat{\beta}} + \frac{2B}{A}\hat{M}(z) + \frac{3C\hat{\beta}}{A}\hat{M}(z)^2 + \eta \Big) \theta w >,$$
$$D_\eta = D(\mathbf{u}) + \eta D(\theta).$$

So if we set $\psi = \eta^{\frac{1}{2}}\theta$ and

$$\hat{S}(z) = \eta^{-\frac{1}{2}} \Big(\frac{1}{\hat{\beta}} + \frac{2B}{A}\hat{M}(z) + \frac{3C\hat{\beta}}{A}\hat{M}(z)^2 + \eta \Big),$$

then following the corresponding analysis in subsection (i), we require to solve the eigenvalue problem

$$\begin{aligned} (D^2 - a^2)^2 W + \tfrac{1}{2}a^2 R_E \hat{S}(z)\Psi = 0, \\ (D^2 - a^2)\Psi - \tfrac{1}{2}R_E \hat{S}(z) W = 0, \end{aligned} \tag{5.30}$$

where $w = W(z)T(x,y)$ etc. This system is solved subject to boundary conditions (5.24) in order to find the lowest eigenvalue $R_E(a^2;\eta)$. We then determine

$$Ra_E = \max_{\eta} \min_{a} R_E^2(a^2;\eta)$$

as in subsection (i). We may compare this with the linear equations for stationary convection. The eigenvalue problem in this case is

$$\begin{aligned} (D^2 - a^2)^2 W + a^2 R \left(\tfrac{1}{\hat{\beta}} + \tfrac{2B}{A}\hat{M}(z) + \tfrac{3C\hat{\beta}}{A}\hat{M}(z)^2 \right) \Theta = 0, \\ (D^2 - a^2)\Theta = RW. \end{aligned} \tag{5.31}$$

Once more we obtain

$$Ra_L = \min_a R^2(a^2),$$

the critical Rayleigh number of linear theory. The numerical results for both the energy and linear theory were calculated using the compound matrix method and are given below.

Ra_L	a_L^2	Ra_E	a_E^2	η_c	$\bar{\eta}$	$\hat{\beta}$	$\hat{\gamma}$
6823.5	6.305	6785.6	6.349	0.193	0.180	10	-0.2
9076.3	6.287	8981.8	6.314	0.147	0.134	20	-0.2
10506.3	6.234	10332.8	6.282	0.129	0.115	40	-0.2
5971.7	6.352	5941.2	6.447	0.219	0.207	10	-0.1
7567.5	6.318	7508.3	6.327	0.175	0.162	20	-0.1
8385.3	6.282	8285.7	6.301	0.159	0.146	40	-0.1
11667.2	6.246	11509.1	6.299	0.115	0.102	10	-0.5
20757.0	6.130	19887.1	6.267	0.069	0.053	20	-0.5
32672.0	6.109	29810.4	6.372	0.050	0.031	40	-0.5

Table 5.4 Critical Rayleigh numbers of linear theory, Ra_L, and energy theory, Ra_E, together with the respective critical wavenumbers a_L, a_E.

Case IV: $Q = 0$.

The conclusions we can make from table 5.4 are similar to those of tables 5.1–5.3. The results for linear and energy theory are again very close, emphasizing that linear theory is a valuable guide to the processes behind the onset of convection. The calculated values of the optimum coupling parameter η, η_c, are close to those of $\bar{\eta}$, where

$$\bar{\eta} = \int_0^1 \left(\frac{1}{\hat{\beta}} + \frac{2B}{A}\hat{M}(z) + \frac{3C\hat{\beta}}{A}\hat{M}(z)^2 \right) dz \tag{5.32}$$

is found using parametric differentiation. (Expression (5.32) is a useful guide when searching numerically for η_c.) The Ra against $\hat{\beta}$ and Ra against $\hat{\gamma}$ graphs may be employed by fixing two of the three variables T_u, d or γ in an experiment and finding the critical value of the third.

Chapter 6

The influence of a cubic density law on patterned ground formation

6.1 Introduction to patterned ground formation

In this and the following two chapters we present a theoretical analysis for the formation of polygonal ground via a geophysical process which involves penetrative convection. Polygonal (or patterned) ground is a most striking and curious geological phenomenon. In general polygonal ground is found in the high mountains of the temperate zone or in remote locations far beyond the tree–line in the Arctic and Antarctic. Typically the polygons consist of stone borders with soil centres. Unlike most geological features the stone nets show an unusual regularity in size and shape. The stone borders usually form regular hexagons which are all about the same size at a single location, while between different sites polygonal stone nets vary from about 10cm in width to more than 4m. The phenomenon has been the subject of discussion for over a century but until recently no-one had advanced a satisfactory theory explaining the polygons' origin. However, the regularity in size and shape suggest that their formation involves some type of stability phenomenon. Three conditions are believed essential for the formation of stone polygons. The first requirement is the existence of alternate freeze–thaw cycles within the soil. These may be annual cycles or diurnal cycles with thawing during daytime and freezing at night. Secondly the soil must be saturated with water during at least part of the year. Finally, a frozen soil barrier must underlie the active layer. The active layer is the layer of soil which is alternately freezing and thawing. For annual cycles permafrost must be present to form the impermeable frozen soil barrier. During the spring there may be a period when

the surface has started to thaw during the daytime but most of the ground is still frozen. The diurnal cycle will allow patterned ground to form even if the soil doesn't completely thaw out during the summer.

Once the three conditions just described are satisfied, the formation of polygonal ground follows a five step process. The first three steps have been discussed in Ray *et al.* (1983), while George *et al.* (1989) added steps (iv) and (v). R. D. Gunn has actually succeeded in growing stone polygons in the laboratory by reproducing these five steps. The stages are:

(i) *Permeability enhancement as a result of the formation of needle ice and frost heaving in the soil.* A certain critical permeability must be attained in the soil before polygonal ground can form and usually only sand or gravel attain permeabilities sufficiently high. However step (iv) of the process requires frost heaving of rocks, which hardly ever happens in sands or gravel (if at all). Silty soils produce frost heaving but have small permeabilities. The required permeability is produced by the formation of needle-ice and ice-lenses which are found in soils subject to freeze/thaw cycles. The elongation of the ice-crystals perpendicular to the permafrost surface thrusts aside soil and rocks, and in so doing increases the volume of the soil. When the soil thaws the melting crystals leave the ground with a larger porosity, which in turn produces an enhanced permeability. A silty soil will increase in permeability with each freeze/thaw cycle until the critical permeability is attained and step (ii) of the process begins.

(ii) *The onset of buoyancy–driven natural convection in the water saturated soil.* During the summer water in the active layer near the permafrost interface remains close to 0°C. Water closer to the surface is considerably warmer. However, because the maximum density of water occurs at 4°C rather than its freezing point, this system is gravitationally unstable. Essentially, under appropriate conditions explained later, the heavier water near 4°C sinks and the lighter water at 0°C rises setting up convection currents in the soil. These convection currents ultimately fix the size and shape of the stone polygons as explained in steps (iii) and (iv). We are able to apply a mathematical analysis to this natural

convection phenomenon. This and the next two chapters are concerned with stability analyses for the layer and predictions for the size of the stone polygons. Previous mathematical analyses show that convection can only occur in the layer provided permeability is equal to or greater than a critical value often larger than the usual permeability for the type of silty soils in which patterned ground occurs. Hence the need for the permeability enhancement step (i). It would also appear that the density difference for water between 0°C and 4°C is too small to produce natural convection. However laboratory experiments confirm that the density difference *can* induce natural convection in porous materials whenever the porous media is heated from above, the lower surface is at 0°C and the permeabilty is above the critical value.

(iii) *Formation of patterned surface in the permafrost.* Viewed from the horizontal plane the circulation of water sets up a field of hexagonal convection cells. Water flows up the centre and down the edges. The downflow carries warmer water from near the surface towards the frozen soil barrier and causes accelerated melting along the edges of the hexagon. The cell centre upflow carries cold water to the surface and retards melting. This results in a number of isolated frozen soil peaks surrounded by an interconnected trough in the permafrost (or frozen barrier) surface.

(iv) *Genesis of patterned ground through frost heaving.* In regions which are subject to vigorous frost action, rocks buried deep with the soil gradually work their way to the surface. This process is known as frost heaving and can be observed both in the laboratory and on a cleared farmer's field, especially in silty soils. The direction of the movement of the stones is perpendicular to the freezing front and may not always be vertical (Washburn 1973). In patterned ground sites, rocks in the thawed active layer move at right angles to the undulant frozen barrier. In so doing they thrust upward and horizontally away from the isolated frozen soil peaks and over the troughs of the hexagonal circulation cells, forming polygonal stone nets, i.e. the patterned ground mimics the underlying pattern in the permafrost interface. However a stationary frozen surface cannot produce

frost heaving; the permafrost interface must move upward during the fall and winter (and during the night in the diurnal case). Because water overlies the frozen barrier this freezing action must come from below. For this to happen the permafrost must be much colder than the freezing point of water at that depth. This allows heat to be conducted away from the water-ice interface causing the interface to slowly freeze in the upward direction. Since the temperature of permafrost at depths of 5-10m is approximately equal to the average air temperature for the region, polygon nets are not expected to occur in areas with annual mean temperature greater than $-5°C$. Field observations and laboratory tests seem to verify this observation (see George *et al.* 1979, Goldthwaite 1976).

(v) *Perpetuation of the hexagonal pattern.* Once the stones have begun to concentrate over the trough in the permafrost, the higher conductivity of rocks compared with soil accelerates the melting of the troughs in the frozen soil barrier; the troughs have become self perpetuating. At this time the natural convection of water in the active layer may actually be choked off due to the removal of stones by frost heaving from the centres of the cells, with a corresponding decrease in permeability. Despite this the stones will still segregate because of the continuing presence of the undulating permafrost surface allied with the higher conductivity of the rocks concentrated over the cell borders.

These steps are explained in detail in Ray *et al.* (1983) and George *et al.* (1989), where previous work is reviewed.

Previous mathematical analyses of patterned ground in Ray *et al.* (1983) predict a width-to-depth ratio (polygon width/active layer depth) of 3.81 compared with 3.57 for field studies. However these theoretical predictions apply to square rather than hexagonal convection cells. Furthermore, the theory also employs a temperature profile which is valid for the very short time when the profile is perturbed only infinitesimally by natural convection. Palm (1960) and Gleason (1984) use a weakly nonlinear stability analysis to study natural convection. In particular Gleason (1984) undertakes the analysis for water near its freezing point in a porous medium heated from above. The analysis showed that for these

conditions water flowed up the centres of cells and down the outer periphery, consistent with steps (i)-(v). Gleason (1984) employed a hexagonal geometry for the weakly nonlinear analysis and predicted a width-to-depth ratio of 3.60 measured point-to-point, or 3.12 from side-to-side, in good agreement with field studies. Gleason *et al.* (1988) also investigate the effects of variable viscosity, thermal conductivity, permeability and expansion coefficient on polygon size.

The model we consider is based upon step (ii), the onset of natural convection in the soil. Analysis of patterned ground in George *et al.* (1989) employed the quadratic equation of state proposed by Veronis (1963). In this chapter we use the cubic density advocated by Merker *et al.* (1979) and described in chapter 4. The weakly nonlinear analyses of Ray *et al.* (1983) and Gleason (1984) are limited to the onset of convection before the initial temperature distribution has changed substantially. Here, as in George *et al.* (1989), we perform both a linear instability and *nonlinear stability* analysis. The later is achieved using an energy method, as employed in chapter 4, which may be applied to the temperature gradients once they have reached their steady state; but the introduction of the cubic dependence of density on temperature makes the energy analysis more complicated than that in George *et al.* (1989). The linear results and predictions are still valuable as the analysis is simpler and they provide a qualitative study of the geological phenomenon.

In the analysis we allow for compaction within the thawed soil layer. We achieve this by assuming that the permeability of the soil decreases linearly with depth. Furthermore, the boundary conditions we choose allow for heating of the upper soil surface via conduction/convection and radiation. Conduction heating occurs during very cloudy or foggy weather with high winds which decrease the resistance to heat transfer from the air to the soil interface. Alternatively radiation heating from the sun is known to be the main contributor to ground heating (Andersland & Anderson 1978), and field data in Ray *et al.* (1983) and Gleason (1984) support adoption of boundary conditions appropriate to solar heating.

At the lower boundary we neglect the moving effect of the water-ice interface

and the phase change occuring there since the timescale of convection is much faster than that of the interface movement. We believe this simpler stationary boundary condition is justified because of the good agreement of our results with field data and the further excessive numerical computation a moving boundary would entail (although in George *et al.* (1989) the writers indicate that they intend to include this effect in future work).

6.2 Convection in a porous medium with a cubic density law

We shall suppose the porous material is occupying the infinite layer between $z = 0$ and $z = d$. The lower plane is kept at constant temperature 0°C (the temperature at which the water in the soil freezes), while the upper plane temperature is allowed to vary. The equations of motion we adopt are based upon Darcy's law and the Boussinesq approximation (see e.g. Joseph 1976). However, since the porous material is saturated with water we employ the equation of state advocated by Merker *et al.* (1979):

$$\rho = \rho_0(1 + AT - BT^2 + CT^3),$$

where ρ is the liquid density, ρ_0 is the density at 0°C, T is temperature in °C and, to recap, A, B, C have values

$$A = 6.85650 \times 10^{-5}(^\circ\mathrm{C})^{-1},$$

$$B = 8.82063 \times 10^{-6}(^\circ\mathrm{C})^{-2},$$

$$C = 4.16668 \times 10^{-8}(^\circ\mathrm{C})^{-3}.$$

Thus in this model we have a gravitationally unstable layer lying below a stably stratified one. Convective motion which occurs in the lower layer will penetrate into the upper layer.

Following the notation of Joseph (1976), the equations of motion are:

$$\rho_0\hat{\phi}^{-1}\frac{\partial \mathbf{u}}{\partial t'} = -\nabla p - \rho_0 g\mathbf{k}[1 + AT - BT^2 + CT^3] - \frac{\mu}{k'}\mathbf{u}, \tag{6.1}$$

$$\nabla \cdot \mathbf{u} = 0, \tag{6.2}$$

$$(\rho_0 C_0)_m \frac{\partial T}{\partial t'} + (\rho_0 C_0)_f \mathbf{u} \cdot \nabla T = \nabla \cdot (k_m \nabla T), \tag{6.3}$$

where $\hat{\phi}$, $\mathbf{u}$, p, g, μ, k', C_0, k_m, t' are, respectively, porosity, fluid velocity, pressure, gravity constant, dynamic viscosity, permeability, specific heat, thermal diffusivity, time and $\mathbf{k} = (0, 0, 1)$. Subscript m denotes the matrix whereas subscript f denotes the fluid. The pore average velocity $\mathbf{u}_{pa}$ is defined by

$$\mathbf{u}_{pa} = \hat{\phi}^{-1}\mathbf{u}.$$

In general μ and k' are functions of temperature, although it is possible for permeability to vary with depth because of soil compaction. Here we restrict attention to the cases where $\mu = \mu_0$ (constant) and k' is a linearly increasing function of z. We also assume that k_m and C_0 are constant.

If we introduce the variable

$$t = t' \frac{(\rho_0 C_0)_f}{(\rho_0 C_0)_m},$$

we may rewrite (6.3) as

$$\frac{\partial T}{\partial t} + \mathbf{u} \cdot \nabla T = \kappa \nabla^2 T, \tag{6.4}$$

where thermal diffusivity, κ, is given by

$$\kappa = k_m/(\rho_0 C_0)_f.$$

The boundary conditions we choose are those of George *et al.* (1989) which allow for a combination of prescribed temperature and radiation heating at the upper surface. So,

$$\begin{gathered} \mathbf{u} \cdot \mathbf{k} = 0 \qquad \text{at} \qquad z = 0, d; \\ T = 0°\text{C} \quad \text{at} \quad z = 0; \qquad \delta_1 \frac{\partial T}{\partial z} + \delta_2 T = c \quad \text{at} \quad z = d; \end{gathered} \tag{6.5}$$

where c is a prescribed constant and δ_1, δ_2 are constants given in terms of the "radiation parameter" $a(\geq 0)$ by

$$\delta_1 = 1/(1+a), \qquad \delta_2 = a/(1+a).$$

Equations (6.1)–(6.5) admit the conduction only solution

$$\bar{\mathbf{u}} \equiv \mathbf{0}, \qquad \bar{T} = \beta z, \tag{6.6}$$

where $\beta = T_1/d$, with the upper surface temperature T_1 being given in terms of d, c and a by

$$T_1 = dc(1+a)/(1+ad).$$

The hydrostatic pressure $\bar{p}$ corresponding to (6.5) is easily found from (6.1) as a fourth order polynomial in z.

The onset of instability criterion is now investigated by performing a linear *instability* - nonlinear energy *stability* analysis of the steady state (6.6). Details of nonlinear energy methods as employed here may be found in the previous chapters and the article of Lindsay & Straughan (1990). Perturbations p, $\mathbf{u}$, θ to the steady solution $(\bar{p}, \bar{\mathbf{u}}, \bar{T})$ are introduced and then non-dimensionalised according to the scales:

$$t = T^+ t^*, \qquad T^+ = \frac{k_0' \rho_0}{\mu}, \qquad \mathbf{u} = U\mathbf{u}^*, \qquad U = \frac{d\mu}{k_0' \rho_0},$$

$$\mathbf{x} = d\mathbf{x}^*, \qquad p = Pp^*, \qquad P = \frac{dU\mu}{k_0'}, \qquad \theta = T^\sharp \theta^*,$$

$$Pr = \frac{d^2\mu}{k_0' \rho_0 \kappa}, \qquad T^\sharp = U\sqrt{\frac{PrT_1}{dgA}}, \qquad R = \sqrt{\frac{dgAT_1 k_0' \rho_0}{\kappa\mu}},$$

$$a_1 = \frac{B}{A}T_1, \qquad a_2 = \frac{C}{A}T_1^2, \qquad L = \frac{(\rho_0 C_0)_f}{(\rho_0 C_0)_m \hat{\phi}},$$

where starred quantities are non-dimensional; to take into account compaction we have selected $k'(z^*) = k_0'(1+\gamma z^*)$ where γ is a constant and k_0' is the permeability at the lower plane. Pr is the Prandtl number, R^2 is associated with the Rayleigh number and L is an inertia coefficient.

With this scaling and the further definition

$$f(z^*) = \frac{k_0'}{k'} = (1+\gamma z^*)^{-1},$$

the non-dimensional perturbation equations are (where for convenience we shall omit all stars):

$$Lu_{i,t} = -p_{,i} - fu_i - R\theta k_i F(z) + k_i \theta^2 G(z) - k_i \theta^3 \frac{a_2 Pr^2}{R}, \tag{6.7}$$

$$u_{i,i} = 0, \tag{6.8}$$

$$Pr(\theta_{,t} + u_i \theta_{,i}) = -Rw + \Delta\theta, \tag{6.9}$$

where (6.7)–(6.9) hold on the spatial region $\mathbf{R}^2 \times (0,1)$, $w = u_3$, and where $F(z)$, $G(z)$ are given by

$$F(z) = 1 - 2a_1 z + 3a_2 z^2, \qquad G(z) = Pr(a_1 - 3a_2 z).$$

The perturbation boundary conditions become:

$$\theta = w = 0 \quad \text{on} \quad z = 0; \qquad w = 0, \quad \theta_{,z} + a\theta = 0 \quad \text{on} \quad z = 1. \tag{6.10}$$

The constant temperature condition $a =$'∞' corresponds to heating of the ground surface by conduction from the air. The constant flux condition $a = 0$ simulates the situation where the soil is heated only by radiation from the sun which falls with the same intensity over the entire polygon surface.

We shall assume the perturbations have an x, y form which forms a pattern which tiles the plane: field work sees hexagonal patterns and this is our motivation. Finally, because the fluid acceleration in the soil is small compared with the final term in (6.2), we neglect the fluid inertia term, $Lu_{i,t}$, in the Darcy momentum equation (6.7). On physical grounds this is expected, although in George *et al.* (1989) it was necessary to retain inertia to perform the mathematical analysis. We overcome this by employing a different nonlinear energy analysis.

6.2.1 Linear instability

To find the linear instability threshold we neglect the nonlinear terms in (6.7), (6.9), and we shall also neglect the $\theta_{,t}$ term in (6.9). This is tantamount to assuming any instability is caused by stationary convection. We can prove this for $\gamma = 0$ and our numerical results for the linear and nonlinear stability problems are very close which demonstrate we are justified in this procedure. The question of exchange of stabilities, which deals with when stationary convection is dominant, is discussed in general in Lindsay & Straughan (1990) where a fuller explanation of the linearization procedure is also given.

The stationary convection boundary is then found by finding the first eigen-

value R^2 to the system:

$$R\theta \mathbf{k}F + f\mathbf{u} + \nabla p = 0,$$
$$\nabla \cdot \mathbf{u} = 0, \tag{6.11}$$
$$\Delta\theta - Rw = 0,$$

together with boundary conditions (6.10), and minimizing R^2 with respect to the wavenumber k which arises due to a normal mode representation in x, y in system (6.11). Due to $z-$dependent coefficients the calculation of finding R^2 and minimizing in k^2 is performed numerically and the results are discussed in the section 6.3.

The above linear analysis gives an *instability* threshold. We now use an energy integral technique to obtain a rigorous *stability* bound. In the section 6.3 it is seen that the two bounds are very close thereby showing that the linearized approach has captured the essential physics of the onset of pattern formation in the ground.

6.2.2 Nonlinear stability

Let V be a cell for the perturbation and let Γ be that part of the boundary of V which lies in the plane $z = 1$. We form energy identities by multiplying (6.7) by u_i and integrating over V, and by multiplying (6.9) by θ and integrating over V to obtain, after some integrations by parts and use of (6.10):

$$\frac{Pr}{2}\frac{d}{dt}\|\theta\|^2 = -R < w\theta > -\|\nabla\theta\|^2 - a\int_\Gamma \theta^2 dA, \tag{6.12}$$

$$< f|\mathbf{u}|^2 >= -R < F\theta w > + < Gw\theta^2 > -\frac{a_2 Pr^2}{R} < \theta^3 w >, \tag{6.13}$$

where $\|.\|$ denotes the norm on $L^2(V)$ and $< . >$ indicates integration over V. If we attempt to repeat the analysis of George *et al.* (1989) by forming $\eta(6.12) + (6.13)$ then the energy procedure breaks down. Partly because there is not sufficient stabilization to control the $< \theta^3 w >$ term but also due to lack of the fluid inertia term. We proceed instead to define $\phi = \theta^2$ and then form an energy identity for ϕ by multiplying (6.9) by θ^3 and integrating over V to obtain:

$$\frac{Pr}{4}\frac{d}{dt}\|\phi\|^2 = -R < w\theta\phi > -\frac{3}{4}\|\nabla\phi\|^2 - a\int_\Gamma \phi^2 dA. \tag{6.14}$$

(It is of interest to observe that a controlling term like $\|\phi\|^2$ was also necessary in Galdi *et al.* (1987), although there due to the need to control boundary nonlinearities.)

Now, for $\eta, \xi > 0$ to be chosen we form $\eta(6.12) + (6.13) + \xi(6.14)$, to find

$$\begin{aligned} \frac{dE}{dt} = -RI - D - \frac{3}{4}\xi\|\nabla\phi\|^2 - a\xi\int_\Gamma \phi^2 dA + < Gw\phi > \\ - \Big(\frac{a_2 Pr^2}{R} + R\xi\Big) < \phi\theta w >, \end{aligned} \tag{6.15}$$

where

$$E = \frac{1}{2}Pr\eta\|\theta\|^2 + \frac{1}{4}Pr\xi\|\phi\|^2,$$

$$I = < (\eta + F)w\theta >,$$

$$D = \eta\|\nabla\theta\|^2 + a\eta\int_\Gamma \theta^2 dA + < f|\mathbf{u}|^2 > .$$

The quantities η, ξ are "coupling parameters" which we select for entirely different reasons. The parameter η is selected to optimize the critical Rayleigh number of energy theory whereas ξ is selected in such a way as to control the cubic nonlinearity in (6.15).

To see how η is utilized we define R_E by

$$R_E^{-1} = \max_{\mathcal{H}} \frac{-I}{D},$$

where $\mathcal{H}$ is the space of admissible solutions, and then define the fourth to sixth terms on the right of (6.15) by $-J$, I_1, I_2, respectively. From (6.15) we then deduce, provided $R < R_E$,

$$\frac{dE}{dt} \leq -\alpha D - \frac{3\xi}{4}\|\nabla\phi\|^2 - J + I_1 + I_2, \tag{6.16}$$

where $\alpha = (R_E - R)/R_E$. We proceed to estimate I_i; J is easily seen to be non-negative.

From the arithmetic-geometric mean inequality, for $\zeta(> 0)$ to be chosen,

$$< Gw\phi > \quad \leq \quad G_m < w\phi > \quad \leq \quad \frac{G_m}{2\zeta}\|w\|^2 + G_m\frac{\zeta}{2}\|\phi\|^2, \tag{6.17}$$

where

$$G_m = \max_{z\in[0,1]} |G(z)| \leq Pr(a_1 + 3a_2) = G^*.$$

Choose now $\zeta = G^*(1+\gamma)/\alpha$ and further observe

$$D \geq < f|\mathbf{u}|^2 > \geq \frac{1}{1+\gamma}\|\mathbf{u}\|^2.$$

From (6.17) in (6.16) we then find

$$\begin{aligned}\frac{dE}{dt} \leq & -\alpha\Big(\eta\|\nabla\theta\|^2 + a\eta\int_\Gamma \theta^2 dA + \frac{1}{2(1+\gamma)}\|\mathbf{u}\|^2\Big) \\ & - \frac{3\xi}{4}\|\nabla\phi\|^2 + \frac{(G^*)^2(1+\gamma)}{2\alpha}\|\phi\|^2 + I_2.\end{aligned} \tag{6.18}$$

To bound I_2 we use the Cauchy-Schwarz inequality and then the Sobolev inequality

$$< \phi^4 > \leq c_1^4\|\nabla\phi\|^4,$$

for a positive constant c_1, in the following manner:

$$< \theta\phi w > \leq \|w\| < \phi^2\theta^2 >^{1/2} \leq c_1\|w\|\|\phi\|^{1/2}\|\nabla\phi\|. \tag{6.19}$$

From the definition of E we may show that

$$\|\phi\|^{1/2} \leq \Big(\frac{4}{Pr\xi}E(t)\Big)^{1/4}.$$

We now put this and (6.19) in (6.18), and use Poincaré's inequality $\|\phi\|^2 \leq \lambda_1^{-1}\|\nabla\phi\|^2$. Then defining

$$H = \frac{a_2 Pr^2}{R} + R\xi,$$

we may obtain

$$\begin{aligned}\frac{dE}{dt} \leq & -\alpha\Big(\eta\|\nabla\theta\|^2 + \frac{1}{2(1+\gamma)}\|\mathbf{u}\|^2\Big) \\ & - \Big[\frac{3\xi}{4} - \frac{(G^*)^2(1+\gamma)}{2\lambda_1\alpha}\Big]\|\nabla\phi\|^2 \\ & + \frac{2Hc_1\sqrt{1+\gamma}}{(Pr\xi)^{1/4}}E^{1/4}\|\nabla\phi\|\frac{\|\mathbf{u}\|}{\sqrt{2(1+\gamma)}}.\end{aligned} \tag{6.20}$$

Next, choose ξ so large that

$$\xi > \frac{2(G^*)^2(1+\gamma)}{3\lambda_1\alpha}$$

and let

$$M = \frac{3\xi}{4} - \frac{(G^*)^2(1+\gamma)}{2\lambda_1\alpha} \quad (>0).$$

If we define $\mathcal{D}$ and the constant K by

$$\mathcal{D} = \alpha\eta\|\nabla\theta\|^2 + \frac{\alpha}{2(1+\gamma)}\|\mathbf{u}\|^2 + M\|\nabla\phi\|^2,$$

$$K = \frac{2Hc_1\sqrt{1+\gamma}}{(Pr\xi)^{1/4}\sqrt{\alpha M}},$$

and utilize the inequalities

$$\|\mathbf{u}\| \le \Big(\frac{2(1+\gamma)}{\alpha}\mathcal{D}\Big)^{1/2}, \qquad \|\nabla\phi\| \le \Big(\frac{1}{M}\mathcal{D}\Big)^{1/2},$$

the energy inequality (6.20) may then be rearranged as

$$\frac{dE}{dt} \le -\mathcal{D}(1 - KE^{1/4}). \tag{6.21}$$

From (6.21) it is now easy to show $E(t) \to 0$ (at least exponentially) provided

$$E(0) < 1/K^4 \qquad (\sim \mathrm{O}(\alpha^2, \xi)), \tag{6.22}$$

and

$$R < R_E. \tag{6.23}$$

Inequalities (6.22), (6.23) define our nonlinear stability threshold. Before investigating the energy critical Rayleigh number R_E^2 we observe that (6.22), (6.23) guarantee E decays and so $\|\phi\|^2, \|\theta\|^2$ decay rapidly. However, under the same conditions (6.21) allows us to conclude $\mathcal{D} \in L^1(0,\infty)$ and, in particular, $\|\mathbf{u}\|^2 \in L^1(0,\infty)$. This shows $\|\mathbf{u}\| \to 0$ also except perhaps on sets of vanishingly small measure. From a practical point of view we believe our nonlinear stability result is strong.

We rearrange the maximum problem by setting $\psi = \eta^{1/2}\theta$ then

$$R_E^{-1} = \max_{\mathcal{H}} \frac{-2 < \mathcal{F} w\psi >}{\|\nabla\psi\|^2 + < f|\mathbf{u}|^2 > + a\int_\Gamma \psi^2 dA},$$

where $\mathcal{F} = (\eta + F)/2\sqrt{\eta}$.

The Euler-Lagrange equations for this maximum problem are

$$\begin{aligned} \nabla\pi &= f\mathbf{u} + R_E\psi\mathbf{k}\mathcal{F}, \\ 0 &= -R_E\mathcal{F}w + \Delta\psi, \end{aligned} \tag{6.24}$$

where π is a Lagrange multiplier. The solution of this system for the lowest eigenvalue R_E^2 was performed numerically by the compound matrix method. We determine

$$\max_{\eta} \min_{k^2} R_E^2(k^2; \eta),$$

where k is again a wavenumber.

An analysis of the linear instability/nonlinear stability results and their implication for patterned ground formation is given in the next section.

6.3 Numerical results and conclusions

We now compare our numerical results with those of George *et al.* (1989) who employ the quadratic density model of Veronis (1963). In particular, we compare the critical wavenumber, k, and the critical Rayleigh numbers.

In George *et al.* (1989) the writers choose a Rayleigh number which reflects the layer depth which is destabilizing, namely

$$Ra = \chi^3 \Big(\frac{g\alpha\rho_0 k_0' d T_1^2}{\kappa\mu_0} \Big), \tag{6.25}$$

where $\alpha = 7.68 \times 10^{-6}\,(^\circ\mathrm{C}^{-2})$ and $\chi = 4/T_1$. In order that we may directly compare our results with those of George *et al.* (1989), we choose an analogous Rayleigh number. In terms of the non-dimensional number R defined in section 6.2, the Rayleigh number we adopt is:

$$Ra = \frac{4\alpha}{A}\chi^2 R^2 \approx 0.448\chi^2 R^2.$$

6.3.1 Tables and results

In the tables that follow we present the critical wavenumbers, k_L, k_E, critical Rayleigh numbers Ra_L, Ra_E, of linear and energy theory, and the best coupling parameter value, $\bar{\eta}$, for the cubic density model. Tables 6.1–6.3 concentrate on a fixed upper surface temperature ($a \to \infty$) and variable permeability with γ changing from $0 \to 1$. Unlike George *et al.* (1989), detailed results are included when the upper temperature T_1 is less than 4°C; this is likely to be valuable in the field. Table 6.4 investigates varying the radiation parameter a for a fixed permeability.

T_1	Ra_L	k_L	Ra_E	k_E	$\bar{\eta}$
0.5	1209.546	3.142	1209.441	3.142	0.936
1.0	324.427	3.143	324.298	3.143	0.874
1.5	155.419	3.145	155.259	3.145	0.812
2.0	94.727	3.148	94.526	3.149	0.752
2.5	66.083	3.153	65.827	3.156	0.694
3.0	50.363	3.162	50.031	3.166	0.638
3.5	40.922	3.176	40.486	3.181	0.585
4.0	34.957	3.197	34.374	3.204	0.535
4.5	31.120	3.230	30.331	3.238	0.489
5.0	28.705	3.283	27.628	3.287	0.448

Table 6.1 Critical Rayleigh numbers of linear theory, Ra_L, and energy theory, Ra_E, together with the respective critical wavenumbers k_L, k_E, and the best value of η, $\bar{\eta}$. T_1 is the upper surface temperature, $Ra = 0.448\chi^2 R^2$, $\gamma = 0.0$ and $a = \infty$.

T_1	Ra_L	k_L	Ra_E	k_E	$\bar{\eta}$
0.5	975.188	3.152	975.103	3.152	0.934
1.0	262.195	3.151	262.090	3.151	0.869
1.5	125.953	3.151	125.822	3.151	0.806
2.0	77.013	3.151	76.847	3.153	0.744
2.5	53.927	3.153	53.713	3.156	0.684
3.0	41.281	3.158	40.999	3.162	0.627
3.5	33.720	3.167	33.344	3.174	0.572
4.0	28.988	3.184	28.476	3.192	0.521
4.5	26.005	3.212	25.298	3.222	0.474
5.0	24.210	3.260	23.223	3.267	0.432

Table 6.2 Critical Rayleigh numbers of linear theory, Ra_L, and energy theory, Ra_E, together with the respective critical wavenumbers k_L, k_E, and the best value of η, $\bar{\eta}$. $\gamma = 0.5$ and $a = \infty$.

T_1	Ra_L	k_L	Ra_E	k_E	$\bar{\eta}$
0.5	822.162	3.174	822.091	3.174	0.933
1.0	221.423	3.172	221.334	3.171	0.867
1.5	106.573	3.169	106.462	3.170	0.802
2.0	65.311	3.167	65.168	3.169	0.739
2.5	45.854	3.167	45.669	3.170	0.678
3.0	35.212	3.170	34.967	3.174	0.619
3.5	28.872	3.176	28.541	3.183	0.563
4.0	24.934	3.189	24.478	3.198	0.511
4.5	22.494	3.213	21.855	3.225	0.463
5.0	21.085	3.259	20.178	3.268	0.421

Table 6.3 Critical Rayleigh numbers of linear theory, Ra_L, and energy theory, Ra_E, together with the respective critical wavenumbers k_L, k_E, and the best value of η, $\bar{\eta}$. $\gamma = 1.0$ and $a = \infty$.

a	Ra_L	k_L	Ra_E	k_E	$\bar{\eta}$
1000	34.938	3.195	34.354	3.202	0.535
100	34.773	3.182	34.183	3.189	0.534
10	33.505	3.072	32.874	3.079	0.521
5	32.592	2.983	31.937	2.991	0.511
2	31.116	2.826	30.436	2.833	0.496
1	30.068	2.704	29.377	2.710	0.486
0.5	29.267	2.604	28.572	2.612	0.478
0.0	28.097	2.450	27.403	2.458	0.467

Table 6.4 Critical Rayleigh numbers of linear theory, Ra_L, and energy theory, Ra_E, together with the respective critical wavenumbers k_L, k_E, and the best value of η, $\bar{\eta}$. The upper surface temperature is fixed at 4°C, $Ra = 0.448\chi^2 R^2$, and $\gamma = 0.0$.

6.3.2 Discussion

The critical Rayleigh number defines the conditions necessary for the onset of natural convection in the soil. Most of the parameters which appear in the Rayleigh number are either fixed or vary over a narrow range. However, permeability depends on the location and may vary greatly. Because of the difficulty in obtaining accurate measurements of permeability in active stone polygons, it is difficult to compare our Rayleigh number predictions with field studies. The critical wavenumber is, however, of direct use. The wavenumber fixes the width-to-depth ratio of stone polygons via the relation

$$k = 7.644\frac{d}{L} \tag{6.26}$$

where L is the diameter of a single circular convection cell and d is the depth of the polygon as described in section 6.2. (An explanation of why circular results are appropriate for hexagons is given in George *et al.* (1989).)

A direct comparison between tables 6.1–6.4 and the corresponding data in George *et al.* (1989) suggests that the predictions made by Merker *et al.* (1979) regarding their cubic density model are indeed accurate. On comparing our results for both linear and energy theory with those in George *et al.* (1989), we find that, in general, the critical Rayleigh numbers predicted using the cubic model are 5–10% lower than those for the quadratic one. This is good physically because it means the convection process commences more easily and hence the start of patterned ground formation is more likely to occur. The critical wavenumbers for both models differ by no more than 0.5%.

Tables 6.1–6.4 show that the energy method yields predictions very close to those of the linear theory, which gives confidence in using linear results since the closeness to the nonlinear results means that linear theory has indeed captured the physics of the onset of convection. For upper surface temperatures of less than 4°C both models produce almost the same results. For top temperatures of more than 4°C the difference between the methods is less than 15% for the Rayleigh number and less than 10% for the wave number, even if we allow top

temperatures as high as 7°C.

Our results exhibit the same overall behaviour as those in George *et al.* (1989). Tables 6.1–6.3 show that a linear increase in permeability as the upper surface is approached produces a decrease in the Rayleigh number. This decrease corresponds to lowering the threshold for the onset of convection in the soil. However, the increase in vertically varying permeability has very little effect on the critical wavenumber. The presence of vertically stratified permeability in the soil should, therefore, produce very little change in the width-to-depth ratio for stone polygons, as is borne out by field studies, see Ray *et al.* (1983).

Tables 6.1–6.3 also show that the Rayleigh number decreases with increasing upper surface temperature. The decrease is in fact a result of the χ^3 factor in definition (6.25). Temperatures greater than 4°C will actually have a stabilizing effect on the fluid motion. The increase in critical wavenumber with increasing temperature implies a decrease in the width-to-depth ratio of the stone polygons.

The radiation parameter a provides for a smooth transition from a constant upper boundary temperature (a large) to a constant flux condition ($a = 0$). Our data shows that the constant flux boundary condition is associated with more unstable fluid layers and smaller critical wave numbers in agreement with previous analyses.

6.3.3 Conclusion

The numerical results presented herein justify our choice of density model, despite the extra analysis this model entails. The critical Rayleigh numbers are indeed lower than those in George *et al.* (1989) in both linear and energy theory. However, the critical wavenumbers which ultimately fix the width-to-depth ratio of the stone polygons, are virtually the same in both studies. Certainly, our results exhibit behaviour which agrees very well with the observations made previously in George *et al.* (1989) regarding the agreement between theory and field data, except that the cubic density model *does* allow for a lower convection onset threshold. Given the short time during the summer when many of the Rocky

mountain sites are sufficiently thawed to allow patterned ground formation (see Ray *et al.* 1983, George *et al.* 1989), we believe the lower threshold is physically correct.

Chapter 7

Patterned ground formation and solar radiation ground heating

7.1 Introduction: Time–periodic heating

When a saturated porous layer is subject to a time–periodic thermal boundary condition, the base flow within the layer is also time–periodic (i.e. a time–dependent temperature gradient). A number of authors discuss the linear stability of time–periodic flows in both fluid and porous layers, e.g. Gresho & Sani (1970), Rosenblat & Tanaka (1971), Yih & Li (1972), Chhuon & Caltagirone (1979). Similarly Homsy (1974) and Caltagirone (1980) utilize the method of energy in order to obtain nonlinear stability bounds. Barenghi & Jones (1989) and Riley & Laurence (1976) also discuss the stability of Taylor–Couette flow subject to time–dependent boundary conditions. However the presence of such time–dependency in the problem makes any mathematical analysis complicated. The solution of the equations of motion must involve techniques and methods very different from those in the time–independent case.

In this chapter we again consider the onset of natural cellular convection in patterned ground formation. Previous mathematical analyses of patterned ground in chapter 6 and George *et al.* (1989) consider only the situation where the upper soil surface is subject to *constant* boundary conditions, e.g. constant heat flux or fixed surface temperature. However, as mentioned earlier the soil is subject to *alternate* freeze–thaw cycles (annual or diurnal), with periodic heating when the layer is thawed. This suggests that any upper surface boundary condition should take into account the time–periodic nature of these cycles.

With this in mind we apply our analysis to the situation where the upper soil

surface is subject to a time–periodic heat flux. Physically, an upper surface heat flux implies heating of the soil exclusively by radiation from the sun, which falls with the same intensity over the entire polygon surface at any moment in time. It is well known (Andersland & Anderson 1978) that heating of the ground occurs predominantly in this manner. Since we are only interested in the time when the active layer is thawed, one cycle of the flux will correspond to the brighest hours of daylight in diurnal heating and the sunnier months of the year in the annual cycle. In the latter example the results produced for one summer cycle will still be valid for successive years since the permafrost often melts to nearly the same depth each summer (Ives 1973).

Initially we consider the linear theory. On account of the time–periodic nature of the system we must obtain our numerical predictions via the Galerkin method and Floquet theory. In the nonlinear system we employ the stability criteria developed by Homsy (1974) for a large class of modulated Bénard problems. Both criteria produce stability limits which hold for disturbances of arbitrary amplitude.

7.2 The time–periodic model

We shall suppose the porous material is occupying the infinite layer between $z = 0$ and $z = d$. The lower plane is kept at constant temperature 0°C , while the upper plane is subject to a time–varying heat flux. In this chapter we choose the quadratic equation of state for water proposed by Veronis (1963),

$$\rho = \rho_0(1 - \alpha(T - 4)^2), \tag{7.1}$$

where we recall ρ is density, ρ_0 is the density at 4°C, T is temperature in °C, and $\alpha \simeq 7.68 \times 10^{-6}(^\circ\mathrm{C}^{-2})$.

The equations of motion we adopt are equivalent to (6.1)–(6.3) with the appropriate modification of (6.1) for the introduction of the quadratic density, i.e. replace $(1 + AT - BT^2 + CT^3)$ in (6.1) with $\left(1 - \alpha(T - 4)^2\right)$.

The boundary conditions we choose are:

$$\begin{aligned} \mathbf{k} \cdot \mathbf{u} &= 0 && \text{at } z = 0, d, \\ T &= 0^\circ\mathrm{C} && \text{at } z = 0, \\ \frac{\partial T}{\partial z} &= \delta(1 + \epsilon \cos \omega' t) && \text{at } z = d, \end{aligned} \tag{7.2}$$

where δ is the flux in the unmodulated case, ω' is the frequency of the time–varying heat flux and ϵ is a constant.

Equations (6.1)–(6.3), (7.2) admit the time–periodic base solution

$$\overline{\mathbf{u}} \equiv \mathbf{0}, \qquad \overline{T} = \delta z + \delta\epsilon \,\mathrm{Re}\left\{ e^{i\omega' t} \frac{\sinh \beta z}{\beta \cosh \beta d} \right\}, \tag{7.3}$$

where

$$\beta = \left(\frac{i\omega'}{\kappa} \right)^{1/2}.$$

The hydrostatic pressure $\overline{p}$ is obtained from (6.1).

Perturbations p, $\mathbf{u}$, θ to the base solution $(\overline{p}, \overline{\mathbf{u}}, \overline{T})$ are now introduced and equations (6.1)–(6.3) are non–dimensionalized via:

$$\mathbf{x} = d\mathbf{x}^*, \qquad \mathbf{u} = U\mathbf{u}^*, \qquad t = T^+ t^*, \qquad \theta = T^\# \theta^*,$$

$$p = Pp^*, \qquad T^+ = \frac{d^2}{\kappa}, \qquad P = \frac{d\mu_0 U}{k_0'}, \qquad U = \frac{\kappa}{d},$$

$$A = \frac{(\rho_0 C_0)_f \rho_0 k_0' \kappa}{(\rho_0 C_0)_m \hat{\phi} d^2 \mu_0}, \qquad T^\# = \left(\frac{\kappa \mu_0}{k_0' \rho_0 d g \alpha}\right)^{1/2},$$

$$R = \left(\frac{k_0' \rho_0 \alpha g d^3 \delta^2}{\mu_0 \kappa}\right)^{1/2},$$

where A is an inertia coefficient, R is associated with the Rayleigh number, and starred quantities are non–dimensional. We choose $k'(z) = k_0'(1 + \gamma z)$ in non–dimensional units, and define

$$f(z) = \frac{k_0'}{k'} = (1 + \gamma z)^{-1}.$$

The non–dimensional perturbation equations are then (omitting all stars):

$$A\frac{\partial u_i}{\partial t} = -p_{,i} + 2\theta R k_i \left\{ z - \xi + \epsilon \,\mathrm{Re}\left(e^{i\omega t} \frac{\sinh \beta d z}{\beta d \cosh \beta d} \right) \right\} + \theta^2 k_i - f u_i \,, \tag{7.4}$$

$$u_{i,i} = 0 \,, \tag{7.5}$$

$$\frac{\partial \theta}{\partial t} + u_i \theta_{,i} = -Rw \left\{ 1 + \epsilon \,\mathrm{Re}\left(e^{i\omega t} \frac{\cosh \beta d z}{\cosh \beta d} \right) \right\} + \Delta\theta \,, \tag{7.6}$$

where

$$w = u_3, \qquad \omega = \frac{\omega' d^2}{\kappa}, \qquad \xi = \frac{4}{T_1}, \qquad T_1 = \delta d,$$

and βd may be rewritten as

$$\beta d = (i\omega)^{1/2} = (1 + i)\left(\frac{\omega}{2}\right)^{1/2}.$$

T_1 is the average upper surface temperature. This non-dimensionalization is different to that in George *et al.* (1989) and is chosen in order to take into account the small frequencies of our cycles, e.g., in the *diurnal* cycle a period of 12 hours corresponds to a frequency $\omega' = 1.5 \times 10^{-5}\mathrm{sec}^{-1}$. However, for patterned ground formation the depth of sorting $d \sim O(10^2)$cm (Ray *et al.* 1983), the thermal diffusivity of water $\kappa \sim O(10^{-3})\mathrm{cm}^2\mathrm{s}^{-1}$ (Weast 1988), frequency

$\omega' \sim O(10^{-5} - 10^{-7})$, while $(\rho_0 C_0)_f/(\rho_0 C_0)_m$ is approximately 1. Thus ω, our non-dimensional frequency, is given by

$$\omega = \frac{d^2}{\kappa}\omega' \sim O(1 - 10^2).$$

In our calculations in section 7.5 we consider ω in the range $\omega = 1$ (annual cycle) to $\omega = 200$ (diurnal cycle).

In order to reflect the depth of the destabilizing layer, we choose the Rayleigh number, Ra, as

$$Ra = \xi^3 R^2. \tag{7.7}$$

The perturbation boundary equations become

$$\begin{aligned} w &= 0 \qquad \text{at } z = 0, 1, \\ \theta &= 0 \qquad \text{at } z = 0, \\ \frac{\partial \theta}{\partial z} &= 0 \qquad \text{at } z = 1. \end{aligned} \tag{7.8}$$

It is reasonable to assume $\mathbf{u}$, θ and p are periodic in x and y since we expect periodic boundary convection cells. Finally, for the sandstone soils in which patterned ground occurs, typically $k_0' \sim O(10^{-5})\text{cm}^2$ (Freeze & Cherry 1979) and $d^2 \sim O(10^4)\text{cm}^2$. So the inertia coefficient, A, is small and is set equal to zero in the linear theory. However, as in George *et al.* (1989), we retain the coefficient in the nonlinear system. This allows us to employ the inertia term in the energy analysis.

7.3 Linear instability

To find the linear instability boundary we neglect the nonlinear terms in (7.4), (7.6). We must therefore solve the system of equations:

$$p_{,i} = -2\theta R k_i\big(\xi - z - \epsilon F_1(z,t)\big) - f u_i\,, \tag{7.9}$$

$$u_{i,i} = 0\,, \tag{7.10}$$

$$\theta_{,t} = -Rw\big(1 + \epsilon F_2(z,t)\big) + \Delta\theta\,, \tag{7.11}$$

where

$$F_1(z,t) = \mathrm{Re}\left(e^{i\omega t}\frac{\sinh\beta dz}{\beta d\cosh\beta d}\right), \tag{7.12}$$

$$F_2(z,t) = \mathrm{Re}\left(e^{i\omega t}\frac{\cosh\beta dz}{\cosh\beta d}\right). \tag{7.13}$$

We first take (curl curl) of (7.9) and consider the third component of the resulting equation. A normal mode form

$$\theta = \Theta(z,t)H(x,y)\,, \qquad w = W(z,t)H(x,y)$$

is next assumed, where

$$\Delta^* = \frac{\partial^2}{\partial x^2} + \frac{\partial^2}{\partial y^2}\,, \qquad \Delta^* H(x,y) = -k^2 H(x,y)$$

and k is the wavenumber. The linear system now reduces to

$$(D^2 - k^2)W = \frac{-f'}{f}DW + 2Rk^2 f^{-1}\big(\xi - z - \epsilon F_1(z,t)\big)\Theta\,, \tag{7.14}$$

$$\frac{\partial\Theta}{\partial t} = -RW\big(1 + \epsilon F_2(z,t)\big) + (D^2 - k^2)\Theta\,, \tag{7.15}$$

where $D = \frac{\partial}{\partial z}$ and $f' = \frac{df}{dz}$. This system is solved subject to boundary conditions

$$\begin{aligned} W(0,t) &= W(1,t) = 0\,, \\ \Theta(0,t) &= D\Theta(1,t) = 0\,. \end{aligned} \tag{7.16}$$

The solution to equations (7.14)–(7.16) is approximated using the Galerkin method (see e.g. Finlayson 1972). The perturbations Θ, W are represented by linearly independent functions satisfying the boundary conditions, i.e.

$$\begin{aligned} \Theta(z,t) &= \sum_{j=1}^{N} a_j(t)\Theta_j(z)\,, \\ W(z,t) &= \sum_{j=1}^{N} b_j(t)W_j(z)\,, \end{aligned} \tag{7.17}$$

where $\Theta_j = \sin(j-\frac{1}{2})\pi z$, $W_j = \sin j\pi z$ and N is the order of the approximation. We replace Θ, W in (7.14), (7.15) by their expansions in (7.17). Equation (7.14) is now multiplied by W_l, while (7.15) is multiplied by Θ_l. Integrating each equation over the height of the layer we obtain:

$$\begin{aligned} \sum_{j=1}^{N} b_j \int_0^1 (D^2-k^2)W_jW_l\,dz = \sum_{j=1}^{N} b_j \int_0^1 \left(-\frac{f'}{f}\right) DW_jW_l\,dz \\ + 2Rk^2 \sum_{j=1}^{N} a_j \int_0^1 \left(\frac{1}{f}\right)\big(\xi - z - \epsilon F_1(z,t)\big)\Theta_jW_l\,dz, \end{aligned} \tag{7.18}$$

$$\begin{aligned} \sum_{j=1}^{N} \frac{da_j}{dt} \int_0^1 \Theta_j\Theta_l\,dz = -R\sum_{j=1}^{N} b_j \int_0^1 \big(1+\epsilon F_2(z,t)\big)W_j\Theta_l\,dz \\ + \sum_{j=1}^{N} a_j \int_0^1 (D^2-k^2)\Theta_j\Theta_l\,dz\,. \end{aligned} \tag{7.19}$$

This system of ordinary differential equations (7.18), (7.19) can be written in matrix form

$$\begin{aligned} A\mathbf{b} &= B\mathbf{a}\,, \\ C\frac{d\mathbf{a}}{dt} &= D\mathbf{b} + E\mathbf{a}\,, \end{aligned} \tag{7.20}$$

where $\mathbf{a} = \mathrm{col}\,(a_1,\ldots,a_N)$, $\mathbf{b} = \mathrm{col}\,(b_1,\ldots,b_N)$, and A–E are $N \times N$ matrices

defined for $j, l = 1, \ldots, N$ by

$$
\begin{aligned}
A_{lj} &= \int_0^1 (D^2 - k^2) W_j W_l + \frac{f'}{f} D W_j W_l \, dz \,, \\
B_{lj} &= \int_0^1 \frac{2Rk^2}{f} \big(\xi - z - \epsilon F_1(z,t)\big) \Theta_j W_l \, dz \,, \\
C_{lj} &= \int_0^1 \Theta_j \Theta_l \, dz \,, \\
D_{lj} &= \int_0^1 R\big(1 + \epsilon F_2(z,t)\big) W_j \Theta_l \, dz \,, \\
E_{lj} &= \int_0^1 (D^2 - k^2) \Theta_j \Theta_l \, dz \,.
\end{aligned}
\tag{7.21}
$$

B and D are time–periodic matrices with period $\tau = \frac{2\pi}{\omega}$. Equations (7.20) may now be rewritten

$$
\begin{aligned}
\frac{d\mathbf{a}}{dt} &= C^{-1}(DA^{-1}B + E)\mathbf{a} \\
&= G(t)\mathbf{a} \,,
\end{aligned}
\tag{7.22}
$$

where $G(\tau) = G(0)$.

Since $G(t)$ is periodic in t with period τ, we may discuss the stability of the solutions to (7.22) on the basis of Floquet theory (see e.g. Ince 1944, Coddington & Levinson 1955). Let

$$
x_i^n(t) = \mathrm{col}[x_1^n(t), \ldots, x_N^n(t)] \tag{7.23}
$$

be a solution to (7.22) which satisfies the initial conditions

$$
x_i^n(0) = \delta_{in} \,,
$$

where δ_{in} is the Kronecker Delta. Taking $n = 1, \ldots, N$ we see that (7.22) has N linearly independent solutions of the form (7.23). Once these solutions have been found, we can form the $N \times N$ matrix

$$
Q = [Q_{in}] = [x_i^n(\frac{2\pi}{\omega})] \,.
$$

The eigenvalues $\lambda_1, \ldots, \lambda_N$ of Q are the *characteristic multipliers* for the system (7.22). The numbers μ_r defined by the relations

$$\lambda_r = \exp\left(\frac{2\pi}{\omega}\mu_r\right), \qquad r = 1, \ldots, N,$$

are the *characteristic exponents*. Assume μ_r are ordered so that

$$\mathrm{Re}(\mu_1) \geq \mathrm{Re}(\mu_2) \geq \ldots \geq \mathrm{Re}(\mu_N).$$

From the linear theory the system is stable, to infinitesimal disturbances only, provided $\mathrm{Re}(\mu_1) < 0$. For more general disturbances, the system will be unstable once $\mathrm{Re}(\mu_1) > 0$. In order to find a linear instability threshold we require to find critical values of R and the wavenumber k which satisfy $\mathrm{Re}(\mu_1) = 0$. If $\mathrm{Im}(\mu_1) = 0$ at this critical point the disturbance is synchronous with the unsteady part of the base temperature solution. Otherwise $\mathrm{Im}(\mu_1) = \pm\pi/\tau$ and the disturbance has frequency half that of the base solution. For these critical values of R and k (for given ϵ, ω, γ and N), the critical Rayleigh number for linear instability, Ra_L, is now given by $Ra_L = \xi^3 R_L^2$ where

$$R_L = \min_{k^2} R.$$

The results and discussion for this linear instability analysis are given in section 7.5. The results were produced on the University of Glasgow's I.B.M. 3090 computer. A number of subroutines in the program were vectorized in order to reduce the processor time required to solve the system. Without vectorization the computer time needed to carry out the numerous integrations and matrix operations for large values of N was excessive and impractical.

7.4 Nonlinear energy analysis

The method of energy is now used to develop two nonlinear stability criteria as proposed by Homsy (1974). The first, global stability, requires the energy of disturbance to decay monotonically and exponentially with time. Homsy (1974) argues that the stability thresholds produced in such a manner might be conservative. As an alternative he proposes a second criterion, asymptotic stability, which requires only that disturbances decay asymptotically to zero over many cycles of modulation, although disturbances are allowed to increase within a cycle.

7.4.1 Global stability

We form energy identities by multiplying (7.4) by u_i, multiplying (7.6) by θ and integrating both equations over the period cell V to give, after use of integration by parts,

$$\frac{A}{2}\frac{d}{dt}\|\mathbf{u}\|^2 = < -f|\mathbf{u}|^2 > + < \theta^2 w > \\ - 2R < \theta w\big(\xi - z - \epsilon F_1(z,t)\big) > , \tag{7.24}$$

$$\frac{1}{2}\frac{d}{dt}\|\theta\|^2 = -R < \theta w\big(1 + \epsilon F_2(z,t)\big) > - \|\nabla\theta\|^2 , \tag{7.25}$$

where $\|.\|$ denotes the norm on $L^2(V)$ and $<.>$ denotes integration over V.

For $\eta > 0$ to be chosen we define an "energy" $E_\eta(t)$ by

$$E_\eta(t) = \frac{1}{2}A\|\mathbf{u}\|^2 + \frac{1}{2}\eta\|\theta\|^2 . \tag{7.26}$$

Although this energy appears to be similar to that chosen in George *et al.* (1989), the analysis and calculations which follow are made more complicated with the introduction of the parameter t explicitly in identities (7.24), (7.25). From (7.24), (7.25) we may show that

$$\frac{dE_\eta}{dt} = -D_\eta + RI_\eta + < \theta^2 w > , \tag{7.27}$$

where

$$D_\eta = \eta\|\nabla\theta\|^2 + < f|\mathbf{u}|^2 > ,$$

$$I_\eta(t) = - < \theta w\big[2\xi - 2z - 2\epsilon F_1(z,t) + \eta\big(1 + \epsilon F_2(z,t)\big)\big] > .$$

Let

$$\frac{1}{R_E(t,\eta)} = \max_{\mathcal{H}} \frac{I_\eta(t)}{D_\eta}\,, \tag{7.28}$$

where $\mathcal{H}$ is the space of admissible functions, and define

$$\hat{R}_E = \min_{t\in\left[0,\frac{2\pi}{\omega}\right)} R_E(t;\eta)\,.$$

Then from (7.27),

$$\begin{aligned}\frac{dE_\eta}{dt} &\le -D_\eta\left(1-\frac{R}{R_E(t;\eta)}\right)+<\theta^2 w>\\ &\le -D_\eta R\left(\frac{1}{R}-\frac{1}{\hat{R}_E}\right)+<\theta^2 w>\,.\end{aligned} \tag{7.29}$$

Utilizing Hölder's inequality and the Sobolev inequality

$$\|\phi^2\| \le c\|\nabla\phi\|^2$$

for some constant $c>0$, we may obtain

$$\begin{aligned}<\theta^2 w> &\le \|\theta^2\|\|w\| \le c\|w\|\|\nabla\theta\|^2\\ &\le \frac{c}{\eta}\left(\frac{2E_\eta(t)}{A}\right)^{1/2} D_\eta\,.\end{aligned} \tag{7.30}$$

Suppose now $R<\hat{R}_E$, and let $\alpha' = R\left(\frac{1}{R}-\frac{1}{\hat{R}_E}\right)$ (>0). Using (7.30) we may rearrange (7.29) as

$$\frac{dE_\eta}{dt} \le -\alpha' D_\eta\left(1-\frac{c}{\eta\alpha'}\left(\frac{2}{A}\right)^{1/2} E_\eta^{1/2}(t)\right)\,. \tag{7.31}$$

From (7.31) it is now easy to show $E(t)\to 0$ (at least exponentially) as $t\to\infty$, provided

$$(i)\quad R<\hat{R}_E \qquad \text{and} \qquad (ii)\quad E_\eta^{1/2}(0) < \frac{\eta\alpha'}{c}\left(\frac{A}{2}\right)^{1/2}\,. \tag{7.32}$$

This establishes our (conditional) nonlinear global stability. The conditional stability threshold is determined from (7.28).

The Euler–Lagrange equations for the maximum problem (7.28) are (for fixed parameter t),

$$\begin{aligned} 2\Delta\phi - R_E M(z,t,\eta)w &= 0\,, \\ 2fu_i + R_E M(z,t,\eta)\phi k_i &= \pi_{,i}\,, \end{aligned} \tag{7.33}$$

where $\phi = \eta^{1/2}\theta$, π is a Lagrange multiplier and

$$M(z,t,\eta) = \frac{1}{\eta^{1/2}}\Big[2\xi - 2z - 2\epsilon F_1(z,t) + \eta\big(1+\epsilon F_2(z,t)\big)\Big]\,.$$

We take the third component of (curl curl) $(7.33)_2$ and decompose into normal modes

$$\phi = \Phi(z,t)H(x,y)\,, \qquad w = W(z,t)H(x,y)\,,$$

where

$$\left(\frac{\partial^2}{\partial x^2} + \frac{\partial^2}{\partial y^2}\right)H(x,y) = -k^2 H(x,y)$$

and k is the wavenumber. Equations (7.33) now become

$$\begin{aligned} \frac{2f'}{f}DW + 2(D^2-k^2)W - \frac{k^2 R_E}{f}M(z,t,\eta)\Phi &= 0\,, \\ 2(D^2-k^2)\Phi - R_E M(z,t,\eta)W &= 0\,. \end{aligned} \tag{7.34}$$

System (7.34) is solved subject to the boundary conditions

$$\begin{aligned} W(0,t) = W(1,t) &= 0\,, \\ \Phi(0,t) = D\Phi(1,t) &= 0\,. \end{aligned}$$

This eigenvalue problem is solved numerically by the compound matrix method, with the optimal Rayleigh number of global stability, Ra_E, found by choosing η such that

$$\begin{aligned} Ra_E &= \min_{t\in\left[0,\frac{2\pi}{\omega}\right)} \max_{\eta} \min_{k} \xi^3 R_E^2(k;t,\eta) \\ &= \max_{\eta} \min_{k} \xi^3 \hat{R}_E^2(k;\eta)\,. \end{aligned}$$

Conditional global stability is now guaranteed provided $Ra < Ra_E$ and (7.32) is true. The max/min calculations were carried out using the Golden Section Search algorithm. The numerical results and discussion, with values for Ra_E and critical values of k, ωt and η, are given in section 7.5.

Calculating the minimum R_E^2 over all possible values of the parameter t in a period provides sufficient conditions for the exponential decay of *all* disturbances satisfying $(7.32)_{(ii)}$. Therefore in energy theory it is unimportant whether a disturbance is synchronous or subharmonic (half frequency). Because of this minimization we don't necessarily expect the energy method to give sharp stability bounds. However our results show that, in general, the critical Rayleigh numbers of linear and energy theory are very close.

Our max/min calculations may be simplified if we employ parametric differentation. At the critical values of t and η we may show that

$$\int_0^1 \frac{\partial M}{\partial a}(z,t,\eta)\Phi(z)W(z)\,dz = 0,$$

where $a = \eta$ or t. This *suggests* that the critical values occur when

$$\int_0^1 \frac{\partial M}{\partial t}(z,t,\eta)\,dz = \int_0^1 \frac{\partial M}{\partial \eta}(z,t,\eta)\,dz = 0\,.$$

The relations which follow provide a useful estimation of the critical values of the parameters, but they do not take into account permeability (since $M(z,t,\eta)$ is independent of γ). We therefore omit any results obtained using this technique.

7.4.2 A heuristic approach to unconditional stability

In order to establish global asymptotic stability we define a new *weighted* energy

$$E_A(t) = \frac{A}{2}\|\mathbf{u}\|^2 + \frac{1}{2} < (\lambda - 2z)\theta^2 > ,$$

where $\lambda(> 2)$ is a constant. In the following discussion we shall assume $f(z) \equiv 1$.

From equations (7.4), (7.6) we may derive

$$\frac{dE_A}{dt} = -\|\mathbf{u}\|^2 + R < \theta w N(z,t,\lambda) > - < \hat{\lambda}|\nabla\theta|^2 > + \int_{\partial V} \theta^2 \, dA \,, \tag{7.35}$$

where

$$\hat{\lambda} = \lambda - 2z \,,$$

$$N(z,t,\lambda) = z - \xi + \epsilon F_1(z,t) - \hat{\lambda}\big(1 + \epsilon F_2(z,t)\big) \,,$$

and $\int_{\partial V} . \, dA$ denotes integration over that part of the boundary of V which lies in the plane $z = 1$. By Hölder's inequality and boundary conditions (7.8),

$$\theta^2(x,y,1) \leq \int_0^1 (\theta_{,z})^2 \, dz \,.$$

Thus

$$\begin{aligned} \int_{\partial V} \theta^2(x,y,z) \, dA &\leq \int_{\partial V} \left(\int_0^1 (\theta_{,z})^2 \, dz \right) dA \\ &\leq \int_V |\nabla\theta|^2 \, dV \\ &\leq \frac{1}{\lambda - 2} < \hat{\lambda}|\nabla\theta|^2 > \,. \end{aligned}$$

Hence (7.35) now gives

$$\frac{dE_A}{dt} \leq -\|\mathbf{u}\|^2 + R < \theta w N(z,t,\lambda) > - \left(\frac{\lambda - 3}{\lambda - 2} \right) < \hat{\lambda}|\nabla\theta|^2 > \,. \tag{7.36}$$

Define

$$\sigma = \frac{\lambda - 3}{\lambda - 2} \,,$$

$$\mathcal{D} = \|\mathbf{u}\|^2 + \sigma < \hat{\lambda}|\nabla\theta|^2 > ,$$

and

$$I = < \theta w N(z,t,\lambda) > ,$$

and further restrict $\lambda > 3$ to ensure $\mathcal{D}$ is positive definite. Then from (7.36) we may show that

$$\begin{aligned} \frac{dE_A}{dt} &\leq RI - \mathcal{D} \\ &\leq \nu(t) E_A \,, \end{aligned}$$

where

$$\nu(t) = \max_{\mathcal{H}'} \frac{RI - \mathcal{D}}{E_A} \,, \tag{7.37}$$

and $\mathcal{H}'$ is the space of all admissible functions. Thus

$$E_A(t) \leq E_A(0) \exp\left\{ \int_0^t \nu(\tau)\, d\tau \right\}.$$

So following the definition given by Homsy (1974), the base state is asymptotically stable if

$$\int_0^{2\pi/\omega} \nu(\tau)\, d\tau < 0 \,. \tag{7.38}$$

The parameter λ is chosen to ensure that (7.38) holds for the largest possible value of R, denoted by R_A. Asymptotic stability is then guaranteed provided $Ra < \xi^3 R_A^2$.

The Euler–Lagrange equations for (7.37) are

$$\begin{aligned} RwN(z,t,\lambda) + 2\sigma\hat{\lambda}\Delta\theta - 4\sigma\theta_{,z} - \nu(t)\hat{\lambda}\theta = 0 \,, \\ R\theta N(z,t,\lambda)k_i - 2u_i - A\nu(t)u_i = \pi_{,i} \,, \end{aligned} \tag{7.39}$$

where π is a Lagrange multiplier.

As mentioned earlier, our numerical results show that the critical Rayleigh numbers of global *conditional* stability and linear instability are very close. So in this situation we deem it inessential to evaluate the critical numbers of system (7.39). The results from (7.39) are likely to be weak because of the provision $\lambda > 3$ and the presence of the very small inertia coefficient term A in $(7.39)_2$.

7.5 Numerical results and discussion

We now compare the behaviour of our numerical results with those of George *et al.* (1989). In particular, we compare the critical wavenumbers and the critical Rayleigh numbers.

7.5.1 Tables and figures

In the following tables we denote the critical values of the parameters η and t in the energy method as η_c, t_c respectively. In order to achieve acceptable accuracy in linear theory we choose N, the order of the approximation in the Galerkin method, to be 16.

Figure 7.1 is a plot of the critical Rayleigh numbers Ra_L and Ra_E versus the average upper surface temperature T_1. In tables 7.1 to 7.4 we present the critical wavenumbers k_L, k_E and critical Rayleigh numbers Ra_L, Ra_E of linear and energy theory. Table 7.1 shows the effect of varying the frequency, ω, when the soil permeability is constant and the average upper surface temperature, T_1, is fixed. Table 7.2 assumes a fixed permeability and frequency but investigates varying the average surface temperature. Table 7.3 concentrates on a constant frequency and average surface temperature, but allows the permeability of the soil to vary as γ changes from $0 \rightarrow 1$. In table 7.4 we vary the parameter ϵ, defined in (7.2) as a fraction of the heat flux modulation amplitude, while all other variables are fixed. $\epsilon = 0$ corresponds to the case when the upper surface heat flux is time–independent (i.e. constant).

ω	Ra_L	k_L^2	k_L	Ra_E	k_E^2	k_E	η_c	ωt_c
1	50.122	9.726	3.119	27.376	5.703	2.388	1.076	4.990
2	44.042	8.316	2.884	25.752	5.617	2.370	1.054	5.429
5	35.009	6.457	2.541	24.596	5.622	2.371	0.932	5.684
10	32.307	6.114	2.473	24.969	5.723	2.392	0.815	6.114
20	31.427	6.029	2.455	25.960	5.813	2.411	0.771	0.394
35	31.136	6.008	2.451	27.060	5.842	2.417	0.796	0.830
50	31.040	6.001	2.450	27.776	5.851	2.419	0.825	1.040
100	30.961	5.996	2.449	28.871	5.885	2.426	0.876	1.285
150	30.945	5.995	2.449	29.285	5.916	2.432	0.898	1.357
200	30.940	5.994	2.448	29.498	5.937	2.437	0.909	1.391

Table 7.1 Variation of the critical Rayleigh and wavenumbers Ra_L, Ra_E, k_L, k_E with frequency ω.

$\gamma = 0, \quad \epsilon = 1, \quad T_1 = 4°\mathrm{C}.$

η_c denotes the optimal value of the coupling parameter η.

T_1	Ra_L	k_L^2	k_L	Ra_E	k_E^2	k_E	η_c	ωt_c
2.5	53.927	5.581	2.362	48.117	5.471	2.339	1.812	1.135
3.0	42.022	5.666	2.380	37.605	5.546	2.355	1.362	1.110
3.5	35.102	5.794	2.407	31.459	5.663	2.380	1.049	1.079
4.0	31.040	6.001	2.450	27.776	5.851	2.419	0.825	1.040
4.5	28.845	6.362	2.522	25.637	6.156	2.481	0.663	0.997
5.0	28.006	7.037	2.653	24.536	6.649	2.578	0.547	0.960
5.5	28.146	8.363	2.892	24.132	7.423	2.725	0.467	0.951
6.0	28.721	10.664	3.266	24.147	8.573	2.928	0.415	0.996
6.5	29.201	13.604	3.688	24.346	10.123	3.182	0.381	1.104

Table 7.2 Variation of the critical Rayleigh and wavenumbers Ra_L, Ra_E, k_L, k_E with T_1.

$\gamma = 0, \quad \epsilon = 1, \quad \omega = 50.$

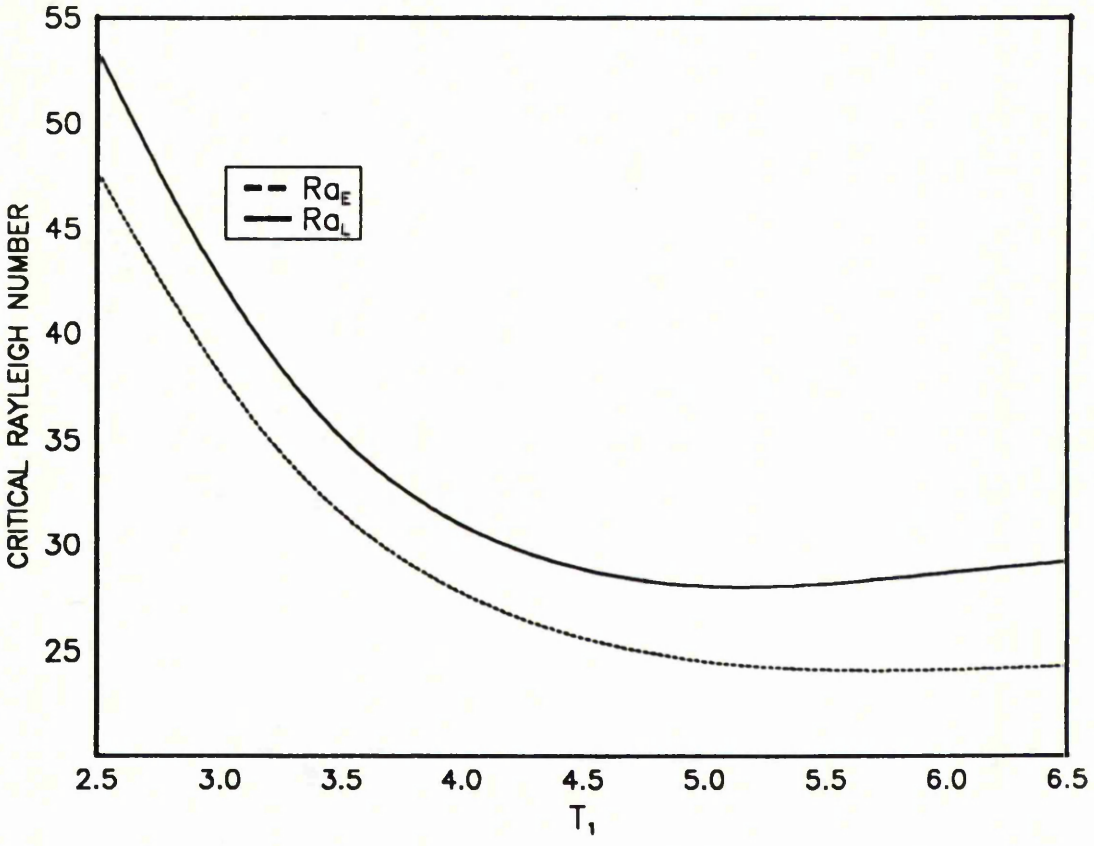

Figure 7.1 Critical Rayleigh numbers Ra_L and Ra_E versus the average surface temperature T_1.

$\gamma = 0, \quad \epsilon = 1, \quad \omega = 50.$

γ	ω	Ra_L	k_L^2	k_L	Ra_E	k_E^2	k_E	η_c	ωt_c
0	10	32.307	6.114	2.473	24.969	5.723	2.392	0.815	6.114
0.5	10	25.217	5.881	2.425	19.989	5.647	2.376	0.798	6.050
1.0	10	21.426	5.860	2.421	16.812	5.649	2.377	0.786	6.011
0	20	31.427	6.029	2.455	25.960	5.813	2.411	0.771	0.394
0.5	20	25.569	5.906	2.430	20.877	5.731	2.394	0.742	0.326
1.0	20	21.748	5.883	2.426	17.617	5.730	2.394	0.724	0.282
0	50	31.040	6.001	2.450	27.776	5.851	2.419	0.825	1.040
0.5	50	26.348	5.987	2.447	22.378	5.762	2.400	0.789	0.976
1.0	50	22.447	5.962	2.442	18.907	5.758	2.399	0.766	0.935

Table 7.3 Variation of the critical Rayleigh and wavenumbers Ra_L, Ra_E, k_L, k_E with ω and γ.

$\epsilon = 1, \quad T_1 = 4°\text{C}.$

ϵ	Ra_L	k_L^2	k_L	Ra_E	k_E^2	k_E	η_c	ωt_c
0	30.933	5.993	2.448	30.185	6.031	2.456	0.945	–
10^{-2}	30.933	5.994	2.448	30.159	6.029	2.455	0.944	1.124
10^{-1}	30.934	5.995	2.448	29.927	6.010	2.451	0.932	1.116
0.5	30.960	5.996	2.449	28.935	5.931	2.435	0.882	1.082
1	31.040	6.001	2.450	27.776	5.851	2.419	0.825	1.040
2	31.361	6.025	2.454	25.713	5.732	2.394	0.728	0.960
5	33.661	6.250	2.500	21.063	5.542	2.354	0.543	0.768

Table 7.4 Variation of the critical Rayleigh and wavenumbers Ra_L, Ra_E, k_L, k_E with ϵ.

$T_1 = 4°\text{C}, \quad \omega = 50, \quad \gamma = 0.$

7.5.2 Discussion

The data in tables 7.1–7.4 show that the linear theory yields predictions reasonably close to those of the energy method. In general the difference between methods is less than 20% for the Rayleigh numbers, and less than 5% for the wavenumber (except at low frequency). The closeness of the results suggests that the linear theory, even with the time–dependent analysis, has again captured the physics of the onset of convection in the soil. Following the discussion in section 7.3, linear theory also predicts that, for the examples considered, all disturbances are synchronous with the base temperature.

In table 7.1, as the frequency of the time modulation is increased (i.e. the period of disturbance is decreased), the linear Rayleigh numbers decrease to a constant limiting value, while the energy Rayleigh numbers increase to a similar limit. The critical wavenumbers k_L and k_E also approach constant values as frequency is increased. This suggests that any small variations of a large frequency have virtually no effect on the stability of the layer or the size of the stone polygons. Indeed, as the frequency is increased the critical numbers approach the values given in table 7.4 which correspond to a time *independent* upper surface heat flux, i.e., $\epsilon = 0$. As $\omega \to 0$ the difference between critical Rayleigh numbers increases. However, as mentioned in Homsy (1974) and Finucane & Kelly (1976), the increase in linear Rayleigh number as $\omega \to 0$ (the quasi–static limit) is a consequence of the stability criterion chosen; it is possible that during a cycle a disturbance may grow to an amplitude which invalidates the use of linear theory. In this situation the energy method enables us to predict the region over which possible subcritical instabilities may occur. For a layer of fluid which is subject to a lower surface temperature modulation, Homsy (1974) predicts that in the quasi–static limit

$$Ra_E = \frac{R_c}{1+a},$$

where a is the temperature modulation and R_c is the critical linear Rayleigh number in the *unmodulated* problem. The analagous limit in our analysis will be very similar to that above, but such quasi–static results are relatively unimpor-

tant in the predictions for patterned ground formation. Although the difference between critical Rayleigh numbers varies, the critical wavenumbers remain close (within approximately 20 %). We may still, therefore, accurately predict the size of the stone polygons via relation (6.26) in the previous chapter.

The data presented in figure 7.1 and tables 7.2 and 7.3 exhibit the same overall behaviour as those in George *et al.* (1989) and chapter 6. Table 7.2 and figure 7.1 show that average surface temperatures greater than 4°C will have a stabilizing effect on the fluid motion, although the Rayleigh numbers actually decrease as T_1 approaches 5.5°C. This decrease is due to the ξ^3 factor in definition (7.7). Furthermore, the increase of critical wavenumbers as T_1 increases implies a decrease in the width–to–depth ratio of the stone nets.

Table 7.3 indicates that a vertically varying permeability has very little effect on the critical wavenumber, i.e. the presence of vertically stratified permeability in the soil produces very little change in the width–to–depth ratio for the stone polygons. As in chapter 6, a linear increase in permeability as the upper surface is approached produces a decrease in critical Rayleigh number, corresponding to a lowering of the threshold for natural convection in the soil.

Table 7.4 shows that as ϵ is increased the critical Rayleigh numbers of linear theory increase, while those of the energy method decrease. Consequently the difference between the Rayleigh numbers of the linear and energy theory also increases as ϵ increases, making it more difficult to predict the onset of convection. When $\epsilon = 0$ the results are almost identical to those in George *et al.* (1989) for the constant heat flux problem, while for small ϵ the critical wavenumber of linear theory is within 0.5% of the energy wavenumber. However, as ϵ increases the difference between wavenumbers grows until there is a 5% disparity. This suggests that when the flux modulation amplitude is small we can accurately predict the size of the stone nets. When the amplitude is larger we may still make valuable predictions, but with less precision than before. Physically, $\epsilon > 1$ corresponds to a negative heat flux during at least part of the cycle. Since our model is based on a thawed active layer in the soil which only occurs in the

sunniest months (or daylight in the diurnal case), we have calculated results for $\epsilon > 1$ only as a test of our mathematical techniques; they are not predictions for patterned ground formation.

7.5.3 Conclusion

Despite the time–periodic nature of our original model and the different mathematical techniques required, the numerical results presented herein exhibit behaviour which agrees very well with the observations made previously in George *et al.* (1989). The time–periodicity of our base flow lowers the critical Rayleigh numbers of the energy method, especially at low frequencies, indicating that the time–periodic heat flux may reduce the threshold for the onset of convection in the porous layer. But in spite of this, the critical wavenumbers of linear and energy theory, which ultimately fix the width–to–depth ratio of the stone polygons, remain close to each other even when the frequency and modulation amplitude are allowed to vary. We may therefore determine the value and accuracy of our original porous layer model by comparing our wavenumber predictions with those produced from field data.

Chapter 8

Patterned ground formation under water

8.1 Introduction

In this chapter we study a mathematical model for the curious formation of patterned ground *under water*. Compared to the theoretical studies on land little has been done for the equivalent problem under water. Nevertheless, the basic mechanisms would still seem to apply and this is an equally interesting phenomenon.

Ray *et al.* (1983) briefly mention the formation of stone polygons in shallow alpine lakes and produce an ad hoc model for its study. Gleason (1984) reports field studies for eight underwater polygons found in California and Wyoming: the field investigators reported by Gleason were Krantz, Caine and Gunn. Krantz *et al.* (1988) contains some beautiful photographs of underwater patterns in lakes in Alaska: Ray *et al.* (1983) p.336 also contains a photograph which clearly demonstrates the existence of underwater sorted polygons in the Snowy Mountain range of Wyoming. Krantz *et al.* (1988) p.74 contains a striking aerial photograph which reveals the stone patterns are confined to the shallow perimeter of the lake where freezing extends into the lake bed.

The model of Ray *et al.* (1983) for patterned ground formation under water simply alters the boundary condition at the upper surface of the porous layer (lake bed). However, Krantz *et al.* (1988) p.75 write ..., *the convection cells that generate underwater polygons circulate into the lake itself...* . Thus, in this analysis we present a *mathematical model* we believe capable of accurately describing the formation of patterned ground on the bed of a shallow lake. We analyse our model numerically and assess our quantitative findings with the fundamental

field work and physical descriptions of the groups' of Professors R. D. Gunn and W. B. Krantz. Fortunately we have found that Nield (1977) has previously developed a model for convection in a fluid layer which overlies a porous medium. He writes that such a system is of geophysical interest, but does not give any examples. Hence, we here adapt his model by allowing the permeability to depend on the depth coordinate and by incorporating penetrative convection via the Veronis (1963) model. Nield (1977) did not have any specific application and hence studied only the critical Rayleigh number for constant heat flux boundary conditions and thereby was able to develop an asymptotic solution. Such boundary conditions are not necessarily the correct ones in patterned ground formation, and also due to the penetrative effect and the fact that the permeability depends on the vertical coordinate we necessarily have to analyse the system numerically.

8.2 A model for patterned ground formation under water

The physical situation is as shown in figure 8.1. Due to the water density maximum at approximately 4°C, under suitable conditions convection currents will be set up in both the fluid and porous medium; it is these convection cells which ultimately fix the size and shape of the patterned ground cells, as explained in chapter 6.

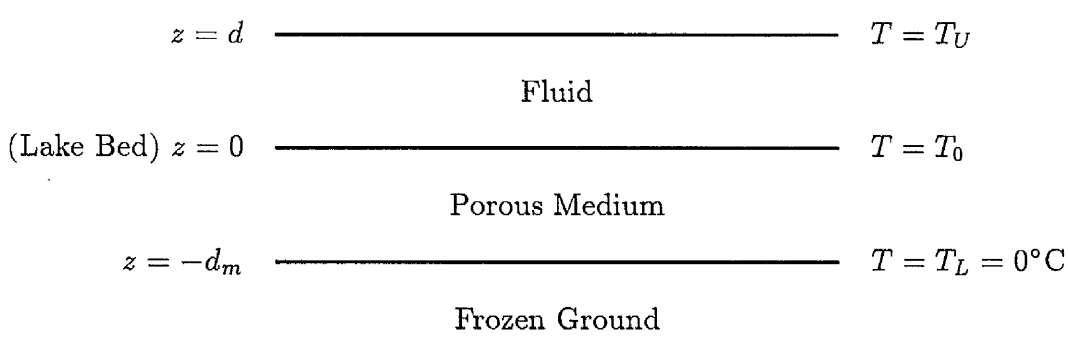

Figure 8.1 Geometry of layer.

We consider, therefore, a fluid layer $z \in (0, d)$ overlying a layer of porous medium $z \in (-d_m, 0)$ under which is a bed of frozen material. The temperature T_U of the free fluid surface is fixed and $T_U > T_L = 0°C$. We now write the equations governing non-isothermal flow in the fluid and in the porous medium, c.f. Nield (1977). Throughout, a superscript m denotes the porous layer.

In the fluid layer $z \in (0, d)$, we have a linear viscous, incompressible fluid with the quadratic buoyancy law of Veronis (1963). The equations of motion are

$$v_{i,t} + v_j v_{i,j} = -\frac{1}{\rho_0} p_{,i} + \nu \Delta v_i - g k_i \left[1 - \alpha_V (T-4)^2\right], \tag{8.1}$$

$$v_{i,i} = 0, \tag{8.2}$$

$$T_{,t} + v_i T_{,i} = \kappa \Delta T, \tag{8.3}$$

where v_i, p , T are velocity, pressure, temperature, ν, ρ_0, g, κ are kinematic viscosity, (constant) density, gravity, thermal diffusivity, α_V is an expansion coefficient, $\mathbf{k} = (0, 0, 1)$ and standard indicial notation has been employed. In the porous medium $z \in (-d_m, 0)$, Darcy's law is assumed although the buoyancy law is again that of Veronis (1963) and the fluid inertia is ignored (c.f. equations (6.1), (6.4) in chapter 6),

$$0 = -p^m_{,i} - \frac{\mu}{k} v^m_i - \rho_0 g k_i \left[1 - \alpha_V (T^m - 4)^2\right], \tag{8.4}$$

$$v^m_{i,i} = 0, \tag{8.5}$$

$$T^m_{,t^m} + v^m_i T^m_{,i} = \kappa^m \Delta T^m, \tag{8.6}$$

where μ is the dynamic viscosity of water and k is the (variable) permeability.

For the boundary conditions we assume on the fluid surface

$$T = T_U, \quad w = \frac{\partial u}{\partial z} = \frac{\partial v}{\partial z} = 0 \quad \text{on } z = d, \tag{8.7}$$

i.e. the surface is free. On the frozen ground - active patterned ground cell boundary we have

$$T^m = T_L = 0^\circ\text{C}, \quad w^m = 0 \quad \text{on } z = -d_m. \tag{8.8}$$

The boundary conditions on the interface $z = 0$ are interesting. Here we follow Nield (1977) who uses the empirical relation suggested by Beavers & Joseph (1967) which relates the slip velocity to the flow in the fluid by

$$\frac{\partial u}{\partial z} = \frac{\alpha}{\sqrt{k}}(u - u^m), \quad \frac{\partial v}{\partial z} = \frac{\alpha}{\sqrt{k}}(v - v^m), \tag{8.9}$$

where $\frac{\partial u}{\partial z}$ denotes the derivative as $z \to 0^+$ and α is a dimensionless quantity depending on the material parameters which characterize the structure of permeable material within the boundary region. Beavers & Joseph (1967) based their law on experimental evidence using three types of Foametal and two types of Aloxite for the porous media. For these materials k and α have values ranging from $k = 9.7 \times 10^{-9}$ (m^2) to 8.2×10^{-8} and $\alpha = 0.78$ to 4 for Foametal, and

$k = 6.5 \times 10^{-10}$ (m^2) to 1.6×10^{-9} and $\alpha = 0.1$ for Aloxite. Jones (1973) offers an alternative boundary condition involving shear stress rather than just velocity shear:

$$\frac{\partial u}{\partial z} + \frac{\partial w}{\partial x} = \frac{\alpha}{\sqrt{k}}(u - u^m), \quad \frac{\partial v}{\partial z} + \frac{\partial w}{\partial y} = \frac{\alpha}{\sqrt{k}}(v - v^m). \tag{8.10}$$

Although this condition is objective it would appear from our numerical results that the contribution of the differentials with respect to x and y is minimal. Ignoring these terms we derive the condition (8.9) suggested by Beavers & Joseph (1967). (We are grateful to Professor K. Hutter for pointing out the relevance of viscous sliding law (8.10) to us.) As far as we are aware this is the first study of this type in patterned ground formation and so we limit attention to the simpler model (8.9), although the alternative condition (8.10) is briefly examined in section 8.3.

From Darcy's law, Beavers & Joseph (1967) replace (u^m, v^m) by $-\frac{k}{\mu}(\frac{\partial p}{\partial x}, \frac{\partial p}{\partial y})$. The boundary conditions at the interface $z = 0$ may then be written (c.f. Nield 1977)

$$\begin{aligned}
&\frac{\partial u}{\partial z} = \frac{\alpha}{\sqrt{k}}\left(u + \frac{k}{\mu}\frac{\partial p^m}{\partial x}\right),\\
&\frac{\partial v}{\partial z} = \frac{\alpha}{\sqrt{k}}\left(v + \frac{k}{\mu}\frac{\partial p^m}{\partial y}\right),\\
&w = w^m,\\
&-p + 2\mu\frac{\partial w}{\partial z} = -p^m,\\
&T = T^m = T_0,\\
&\kappa\frac{\partial T}{\partial z} = \kappa_m\frac{\partial T^m}{\partial z}.
\end{aligned} \tag{8.11}$$

N.B. $(8.11)_4$ expresses continuity of the normal stress. The condition on the heat flux is arguable since solar radiation may well heat the lake bed directly and thus lead to an appreciable change in the critical Rayleigh number for radiation heating in a fluid, c.f. chapter 5 and Straughan (1991, 1992a). Alternatively, radiation may enter the equations of motion in the porous layer as a heat source, c.f. Matthews & Heaney (1987) and Matthews (1988). Nevertheless, at this stage we wish to keep our model simple as it is a first analysis of underwater patterned

ground, so such heating effects are ignored.

To investigate conditions for the onset of convection we use a linearized instability analysis. The conduction solution to (8.1)–(8.6) which satisfies the boundary conditions is

$$\begin{aligned}
&\bar{v}_i = 0, \qquad \bar{T} = T_0 - (T_0 - T_U)\frac{z}{d}, \\
&\bar{p} = p_0 - g\rho_0\Big[\big(1 - \alpha_V(T_0 - 4)^2\big)z + (T_0 - 4)(T_0 - T_U)\alpha_V\frac{z^2}{d} \\
&\qquad\qquad - \left(\frac{T_0 - T_U}{d}\right)^2\frac{\alpha_V}{3}z^3\Big], \\
&\bar{v}_i^m = 0, \qquad \bar{T}^m = T_0\big(\frac{z}{d_m} + 1\big), \\
&\bar{p}^m = p_0 - g\rho_0\Big[\big(1 - \alpha_V(T_0 - 4)^2\big)z - (T_0 - 4)T_0\alpha_V\frac{z^2}{d_m} \\
&\qquad\qquad - \frac{T_0^2}{d_m^2}\frac{\alpha_V}{3}z^3\Big],
\end{aligned} \tag{8.12}$$

where p_0, T_0 are the pressure and temperature at $z = 0$. The interface temperature, T_0, is made determinate by requiring continuity of heat flux at the lake bed so

$$\kappa^m\frac{d\bar{T}^m}{dz} = \kappa\frac{d\bar{T}}{dz}, \qquad \text{on } z = 0, \tag{8.13}$$

from which we find

$$T_0 = \frac{T_U\kappa d_m}{\kappa^m d + d_m\kappa}.$$

In terms of the pressure p_d at the lake surface, $z = d$,

$$p_0 = p_d + \rho_0 g d\big[1 - \alpha_V(T_0 - 4)(T_U - 4) - \frac{\alpha_V}{3}(T_0 - T_U)^2\big].$$

Perturbations are introduced via

$$\begin{aligned}
&T = \bar{T} + \theta, \quad v_i = \bar{v}_i + u_i, \quad p = \bar{p} + \pi, \\
&T^m = \bar{T}^m + \theta^m, \quad v_i^m = \bar{v}_i^m + u_i^m, \quad p^m = \bar{p}^m + \pi^m,
\end{aligned} \tag{8.14}$$

and the perturbation equations are non-dimensionalized with the scalings (stars denoting dimensionless quantities):

Fluid layer:

$$t = \frac{d^2}{\nu}t^*, \quad \pi = \frac{\nu\rho_0}{d}\pi^*, \quad u_i = Uu_i^*, \quad \theta = T^\sharp\theta^*,$$
$$x_i = dx_i^*, \quad U = \frac{\nu}{d}, \quad Pr = \frac{\nu}{\kappa}, \quad T^\sharp = U\sqrt{\frac{\nu}{d\kappa\alpha_V g}}, \quad R^2 = \frac{d^5\beta^2 g\alpha_V}{\kappa\nu}; \tag{8.15}$$

Porous layer:

$$t^m = \frac{\rho_0 k_0}{\mu}t^{m*}, \quad u_i^m = U^m u_i^{m*}, \quad \theta^m = T^{m\sharp}\theta^{m*}, \quad x_i = d_m x_i^*$$
$$\pi^m = \frac{\mu d_m U^m}{k_0}\pi^{m*}, \quad U^m = \frac{d_m\mu}{k_0\rho_0}, \quad Pr^m = \frac{d_m^2\mu}{k_0\rho_0\kappa},$$
$$T^{m\sharp} = U^m\sqrt{\frac{Pr^m}{d_m g\alpha_V}}, \quad R^{m2} = \frac{d_m^3\beta_m^2 g\alpha_V k_0\rho_0}{\kappa\mu}; \tag{8.16}$$

To take into account compaction in the porous layer the permeability k has been chosen to be, in nondimensional units,

$$k = k_0\big(1+\gamma(1+z)\big), \quad z \in (-1,0),$$

for constants k_0 and γ. We further define the function $f(z)$ by

$$f(z) = \frac{1}{1+\gamma(1+z)}, \qquad z \in (-1,0).$$

In (8.15), (8.16) and in the following we also make use of the quantities

$$\beta = \frac{T_U - T_0}{d}, \quad \beta_m = \frac{T_0}{d_m}, \quad \xi = \frac{4-T_0}{T_U - T_0}, \quad \xi_m = \frac{4-T_0}{T_0}.$$

Even though the timescales are non-dimensionalized differently this will not affect the instability analysis since attention is restricted to stationary convection.

The non-dimensional perturbation equations are then (stars omitted)

$$u_{i,t} + u_j u_{i,j} = -\pi_{,i} + \Delta u_i + 2R(z-\xi)\theta k_i + Pr\theta^2 k_i, \tag{8.17}$$

$$u_{i,i} = 0, \tag{8.18}$$

$$Pr(\theta_{,t} + u_i\theta_{,i}) = \Delta\theta - Rw, \tag{8.19}$$

in $z \in (0,1)$, and

$$\pi^m_{,i} = -fu^m_i + 2R^m(z-\xi_m)\theta^m k_i + Pr^m\theta^{m2}k_i, \quad (8.20)$$

$$u^m_{i,i} = 0, \quad (8.21)$$

$$Pr^m(\theta^m_{,t^m} + u^m_i\theta^m_{,i}) = \Delta\theta^m - R^m w^m, \quad (8.22)$$

for $z \in (-1,0)$, where $w = u_3$ and $w^m = u^m_3$.

The boundary conditions on the perturbation variables become

$$\begin{aligned} w = w_{,zz} = \theta = 0, \qquad z = 1, \\ w^m = \theta^m = 0, \qquad z = -1, \end{aligned} \quad (8.23)$$

where the condition for $w_{,zz}$ on $z = 1$ may be derived from equation (8.17) and boundary condition (8.7). The interface boundary conditions (8.11) may be reduced as in Nield (1977) to here yield

$$\begin{aligned} w^m &= \frac{\lambda}{\hat{d}}w, \\ \theta^m &= \left(\frac{T_U - T_0}{T_0}\right)^{\frac{1}{2}} \frac{\lambda^{3/2}}{\hat{d}}\theta, \\ \frac{\partial\theta^m}{\partial z} &= \left(\frac{T_U - T_0}{T_0}\right)^{-\frac{1}{2}} \frac{\lambda^{3/2}}{\hat{d}}\frac{\partial\theta}{\partial z}, \\ \frac{\partial w^m}{\partial z} &= \lambda\left(\frac{\partial w}{\partial z} - \frac{\zeta\hat{d}}{\alpha}\frac{\partial^2 w}{\partial z^2}\right), \\ -\frac{\partial w^m}{\partial z} &= \zeta^2\hat{d}^2\lambda\left(\frac{\partial^2}{\partial z^2} + 3\Delta^*\right)\frac{\partial w}{\partial z}, \end{aligned} \quad (8.24)$$

on $z = 0$, where $\Delta^* = \frac{\partial^2}{\partial x^2} + \frac{\partial^2}{\partial y^2}$ and the dimensionless parameters ζ, λ and $\hat{d}$ are defined by

$$\zeta = \frac{\sqrt{k}}{d_m}, \quad \lambda = \frac{k_0}{d^2}, \quad \hat{d} = \frac{d_m}{d}.$$

Due to this nature of this problem and the hexagonal geometry of the stone nets we may also assume that the fields u_i, θ, π and u^m_i, θ^m, π^m are periodic in x and y.

N.B. The reduction of (8.11) to (8.24) is as in Nield (1977), only $(8.24)_{4,5}$ need comment. To arrive at $(8.24)_4$ one uses the continuity equation on $(8.11)_{1,2}$ and the equation of motion in the porous medium, whereas to deduce $(8.24)_5$ one eliminates π, π^m from $(8.11)_4$ with the aid of the continuity equation and equations of motion in the respective layer. We point out that Nield (1977) considers mixed heat transfer boundary conditions at $z = \pm 1$. We could do this, but this introduces other parameters and we have no physical reason to do so in the patterned ground context.

We now perform a linearized instability analysis and consider only stationary convection. Certainly, it may be true that oscillatory convection is not negligible in this problem. However, our results do agree well with the field study measurements reported by Gleason (1984). From (8.17)–(8.22) the linearized equations for stationary convection are

$$\pi_{,i} = \Delta u_i + 2R(z - \xi)\theta k_i \,, \tag{8.25}$$

$$0 = \Delta\theta - Rw \tag{8.26}$$

in $z \in (0, 1)$, and

$$\pi^m_{,i} = -f u^m_i + 2R^m(z - \xi_m)\theta^m k_i \,, \tag{8.27}$$

$$0 = \Delta\theta^m - R^m w^m \tag{8.28}$$

in $z \in (-1, 0)$. We now take the third component of curl curl (8.25) and then expand w, θ in normal mode form

$$w = W(z)h(x, y), \qquad \theta = \Theta(z)h(x, y).$$

$W(z)$, $\Theta(z)$ are the $z-$dependent parts of w, θ, and for hexagonal cells the planform $h(x, y)$ is given by (see Drazin & Reid 1981),

$$h(x, y) = \cos\frac{1}{2}a(\sqrt{3}x + y) + \cos\frac{1}{2}a(\sqrt{x} - y) + \cos ay. \tag{8.29}$$

We can verify that

$$\Delta^* h \equiv \left(\frac{\partial^2}{\partial x^2} + \frac{\partial^2}{\partial y^2}\right)h = -a^2 h,$$

where a is the wavenumber.

Similarly, we take the third component of curl curl (8.27) before expanding w^m and θ^m. The normal mode expansion for w^m, θ^m is similar to above with the planform, $h_m(x,y)$, equivalent to (8.29) with a replaced by the wavenumber for the porous region, a_m;

$$\text{i.e.} \qquad \left(\frac{\partial^2}{\partial x^2}+\frac{\partial^2}{\partial y^2}\right)h_m = -a_m^{\,2}h_m.$$

Thus, employing normal modes the linearized equations (8.25)–(8.28) become

$$\begin{aligned}(D^2-a^2)^2W - 2R(z-\xi)a^2\Theta = 0,\\ (D^2-a^2)\Theta - RW = 0,\end{aligned} \tag{8.30}$$

for $z\in(0,1)$, and

$$\begin{aligned}(D^2-a_m^{\,2})W^m + \frac{f'}{f}DW^m + 2\frac{R^m}{f}(z-\xi_m)a_m^{\,2}\Theta^m = 0,\\ (D^2-a_m^{\,2})\Theta^m - R^mW^m = 0,\end{aligned} \tag{8.31}$$

for $z\in(-1,0)$, where $D=d/dz$ and $f'=df/dz$. In terms of the $z-$dependent parts, the boundary conditions are

$$\begin{aligned}W = W'' = \Theta = 0 \quad \text{on } z=1,\\ W^m = \Theta^m = 0 \quad \text{on } z=-1,\end{aligned} \tag{8.32}$$

while on the $z=0$ interface,

$$W^m = \frac{\lambda}{\hat{d}}W, \qquad \Theta^m = \left(\frac{T_U-T_0}{T_0}\right)^{\frac{1}{2}}\frac{\lambda^{3/2}}{\hat{d}}\Theta, \qquad \Theta^{m\prime} = \left(\frac{T_U-T_0}{T_0}\right)^{-\frac{1}{2}}\frac{\lambda^{3/2}}{\hat{d}}\Theta',$$

$$W^{m\prime} = \lambda(W' - \frac{\zeta\hat{d}}{\alpha}W''), \qquad -W^{m\prime} = \zeta^2\hat{d}^{\,2}\lambda(W''' - 3a^2W'). \tag{8.33}$$

To solve (8.30)–(8.33) numerically we observe that the eigenvalues R, R^m are not unrelated. In fact from the definitions in (8.15), (8.16)

$$R^{m\,2} = \left(\frac{T_0}{T_U-T_0}\right)\hat{d}^{\,2}\lambda R^2. \tag{8.34}$$

It must also follow from (8.15), (8.16) that the wavenumbers are related via

$$\hat{d} = \frac{d_m}{d} = \frac{a_m}{a}.$$

Thus by replacing R^m and a_m in (8.31), we may regard (8.30), (8.31) as a single system with a single eigenvalue R and wavenumber a.

To find our critical numbers we first rewrite (8.30) and (8.31) as systems of first order differential equations in the variables $(W, W', W'', W''', \Theta, \Theta')$ and $(W^m, W^{m\prime}, \Theta^m, \Theta^{m\prime})$, respectively. We shall denote

$$\mathbf{Y_i} = (W_i, W_i', W_i'', W_i''', \Theta_i, \Theta_i') \qquad \text{and} \qquad \mathbf{Y_i^m} = (W_i^m, W_i^{m\prime}, \Theta_i^m, \Theta_i^{m\prime}).$$

For *fixed* R, let $\mathbf{Y_1}$ be the solution to the initial value problem given by (8.30), $(8.32)_1$ where integration is from $z = 1$ to $z = 0$ and the initial conditions are

$$\mathbf{Y_1} = (0, 1, 0, 0, 0, 0) \qquad \text{on } z = 1.$$

Similarly let $\mathbf{Y_2}$, $\mathbf{Y_3}$ be solutions to (8.30), $(8.32)_1$ with initial conditions

$$\mathbf{Y_2} = (0, 0, 0, 1, 0, 0) \qquad \text{on } z = 1$$

and

$$\mathbf{Y_3} = (0, 0, 0, 0, 0, 1) \qquad \text{on } z = 1.$$

Then since $\mathbf{Y_1}$, $\mathbf{Y_2}$ and $\mathbf{Y_3}$ are linearly independent, the general solution to the sixth order problem (8.30) in $z \in (0, 1)$, with the conditions on $z = 1$ given by $(8.32)_1$, is

$$\mathbf{Y} = a_1\mathbf{Y_1} + a_2\mathbf{Y_2} + a_3\mathbf{Y_3},$$

for constants a_1, a_2 and a_3.

Correspondingly, we can also produce a general solution for (8.31), $(8.32)_2$ in $z \in (-1, 0)$,

$$\mathbf{Y^m} = b_1\mathbf{Y_1^m} + b_2\mathbf{Y_2^m},$$

where b_1, b_2 are constants. $\mathbf{Y_1^m}$, $\mathbf{Y_2^m}$ are solutions to the initial value problem given by (8.31), $(8.32)_2$ along with the additional conditions

$$\mathbf{Y_1^m} = (0, 1, 0, 0) \quad \text{on } z = -1,$$

and

$$\mathbf{Y_2^m} = (0, 0, 0, 1) \quad \text{on } z = -1,$$

respectively. Here integration is from $z = -1$ to $z = 0$.

The critical Rayleigh number of our system (8.30)–(8.33), including the conditions at the interface, is now the critical value of R^2 such that $\mathbf{Y}$ and $\mathbf{Y^m}$ satisfy the boundary conditions (8.33) at $z = 0$,

$$\text{i.e.} \qquad a_1 W_1 + a_2 W_2 + a_3 W_3 = \frac{\lambda}{\hat{d}}(b_1 W_1^m + b_2 W_2^m) \quad \text{at } z = 0, \text{ etc.}$$

Thus we can find R by interpolation on the determinant relation

$$\begin{vmatrix} W_1^m & W_2^m & AW_1 & AW_2 & AW_3 \\ W_1^{m\prime} & W_2^{m\prime} & BW_1'' - \lambda W_1' & BW_2'' - \lambda W_2' & BW_3'' - \lambda W_3' \\ W_1^{m\prime} & W_2^{m\prime} & C(W_1''' - 3a^2 W_1') & C(W_2''' - 3a^2 W_2') & C(W_3''' - 3a^2 W_3') \\ \Theta_1^m & \Theta_2^m & D\Theta_1 & D\Theta_2 & D\Theta_3 \\ \Theta_1^{m\prime} & \Theta_2^{m\prime} & E\Theta_1' & E\Theta_2' & E\Theta_3' \end{vmatrix} = 0, \tag{8.35}$$

evaluated at $z = 0$, where

$$A = -\frac{\lambda}{\hat{d}}, \quad B = \frac{\lambda \zeta \hat{d}}{\alpha}, \quad C = \zeta^2 \hat{d}^2 \lambda,$$

$$D = -\left(\frac{T_U - T_0}{T_0}\right)^{1/2} \frac{\lambda^{3/2}}{\hat{d}}, \quad E = -\left(\frac{T_U - T_0}{T_0}\right)^{-1/2} \frac{\lambda^{3/2}}{\hat{d}}.$$

The minimum over a^2 is then found by golden section search with the critical values of R^2 and $R^{m\,2}$ for this minimum a denoted by Ra and Ra^m, respectively. All computations were performed on the University of Glasgow's IBM 3090 computer.

N.B. We have deliberately chosen what amounts to a standard shooting method despite the notorious error build up sometimes found with this technique. By careful computation we believe we have avoided such errors. The reason we chose a shooting method is that we wish to also compute the eigenfunctions to observe the effect of the interface $z = 0$. It is not difficult to implement a more accurate method such as the compound matrix technique to find R, but the calculation of the eigenfunction is then not so obvious.

8.3 Numerical results and conclusions

8.3.1 Tables and figures

In tables 8.1–8.3 and 8.5 we assume α and the ratio of diffusivities, κ_m/κ, are unity. In table 8.1 we investigate the effect of the parameter λ on our numerical results when all other variables are fixed. Table 8.2 concentrates on variables γ and $\hat{d}$ for λ and T_U constant, whereas table 8.3 allows upper surface temperature to vary. Table 8.4 contains a number of results for specific values of $\hat{d}$, α, κ_m/κ and λ not considered in the previous tables. Finally, table 8.5 contains numerical predictions obtained using the fluid/porous layer interface boundary condition suggested by Jones (1973): this condition is further discussed below. In figures 8.2 and 8.3 we plot two-dimensional streamlines for a roll cell and normalized perturbation eigenfunctions (W, Θ) for the whole region at the onset of convection.

Ra	Ra^m	a^2	a_m^2	w/d	λ
982.626	1.2×10^{-3}	6.010	1.502	6.74	10^{-5}
941.943	1.2×10^{-2}	5.921	1.480	6.79	10^{-4}
782.371	9.8×10^{-2}	5.589	1.397	6.99	0.001
499.097	0.312	5.084	1.271	7.32	0.005
355.830	0.445	4.799	1.200	7.54	0.01
134.501	0.841	3.748	0.937	8.53	0.05
89.931	1.124	3.175	0.794	9.27	0.1

Table 8.1 Critical Rayleigh numbers, wavenumbers squared and width-to-depth ratios, Ra, Ra^m, a^2, a_m^2, w/d. $\hat{d} = 0.5$, $\gamma = 0.0$, $T_U = 4°\text{C}$, $T_0 = 1.33°\text{C}$.

Ra	Ra^m	a^2	a_m^2	w/d	γ	$\hat{d}$	T_0
432.990	0.186	5.526	0.677	10.04	0	0.35	1.037
380.182	0.163	5.467	0.670	10.09	0.5	0.35	1.037
342.765	0.147	5.397	0.661	10.16	1.0	0.35	1.037
355.830	0.445	4.799	1.200	7.54	0	0.5	1.333
306.040	0.383	4.770	1.192	7.56	0.5	0.5	1.333
271.912	0.340	4.716	1.179	7.60	1.0	0.5	1.333
300.770	0.826	4.060	1.715	6.30	0	0.65	1.576
254.062	0.698	4.063	1.716	6.30	0.5	0.65	1.576
222.889	0.612	4.033	1.704	6.32	1.0	0.65	1.576

Table 8.2 Critical Rayleigh numbers, wavenumbers squared and width-to-depth ratios. $\lambda = 0.01$, $T_U = 4°C$.

Ra	Ra^m	a^2	a_m^2	w/d	T_0	T_U
105.956	0.132	4.785	1.196	7.55	0.667	2.0
199.634	0.250	4.784	1.196	7.55	1.0	3.0
355.830	0.445	4.799	1.200	7.54	1.333	4.0
657.112	0.821	4.894	1.223	7.47	1.667	5.0
1346.228	1.683	5.435	1.359	7.08	2.0	6.0
2772.631	3.466	7.084	1.771	6.20	2.333	7.0
4870.030	6.088	8.484	2.121	5.67	2.667	8.0

Table 8.3 Critical Rayleigh numbers, wavenumbers squared and width-to-depth ratios. $\lambda = 0.01$, $\gamma = 0$, $\hat{d} = 0.5$.

Ra	Ra^m	a^2	a_m^2	w/d	$\hat{d}$	λ	T_0	κ_m/κ	α
921.736	0.092	5.575	5.575	3.50	1.0	10^{-4}	2	1	1
721.981	0.722	4.606	4.606	3.85	1.0	0.001	2	1	1
213.278	2.133	2.585	2.585	5.14	1.0	0.01	2	1	1
36.048	3.605	1.825	1.825	6.11	1.0	0.1	2	1	1
661.383	5.291	1.415	5.659	3.47	2.0	10^{-3}	2.667	1	1
375.481	10.138	0.436	3.919	4.17	3.0	10^{-3}	3	1	1
912.811	0.023	6.420	1.605	6.52	0.5	10^{-3}	0.364	5	1
836.754	0.105	5.739	1.435	6.89	0.5	10^{-3}	1.333	1	3
725.274	0.091	5.397	1.349	7.11	0.5	10^{-3}	1.333	1	0.5

Table 8.4 Critical Rayleigh numbers, wavenumbers squared and width-to-depth ratios for selected values of $\hat{d}$, λ, κ_m/κ and α. $\gamma = 0$, $T_U = 4.0°\mathrm{C}$.

Ra	Ra^m	a^2	a_m^2	w/d	γ	$\hat{d}$	λ	T_0	T_U
780.894	0.098	5.600	1.400	6.98	0	0.5	0.001	1.333	4
349.740	0.437	4.900	1.225	7.46	0	0.5	0.01	1.333	4
130.462	0.815	3.891	0.973	8.37	0	0.5	0.05	1.333	4
87.522	1.094	3.317	0.829	9.07	0	0.5	0.1	1.333	4
59.380	2.969	2.102	2.102	5.70	0	1.0	0.05	2	4
36.066	3.607	1.870	1.870	6.04	0	1.0	0.1	2	4
104.210	0.130	4.872	1.218	7.48	0	0.5	0.01	0.667	2
1315.515	1.644	5.574	1.394	6.99	0	0.5	0.01	2	6
299.159	0.374	4.891	1.223	7.47	0.5	0.5	0.01	1.333	4
264.996	0.331	4.851	1.213	7.50	1.0	0.5	0.01	1.333	4
425.214	0.182	5.639	0.691	9.93	0	0.35	0.01	1.037	4
295.674	0.812	4.146	1.752	6.24	0	0.65	0.01	1.576	4

Table 8.5 Critical Rayleigh numbers, wavenumbers squared and width-to-depth ratios calculated using boundary condition (8.10).

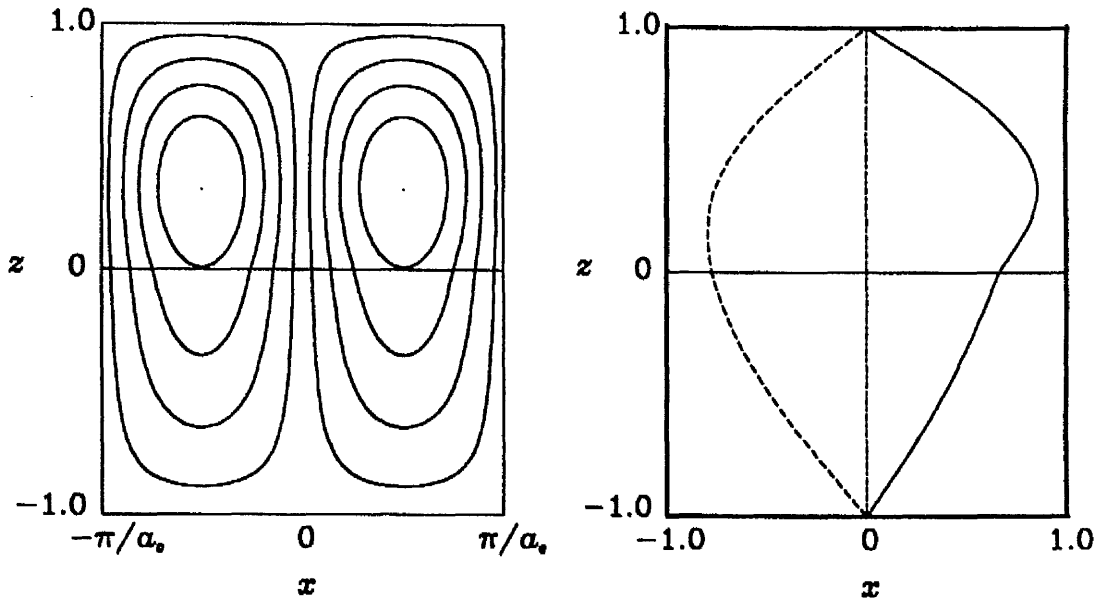

Figure 8.2 Two dimensional streamlines and normalized eigenfunctions $W(z)$, $\Theta(z)$ at the onset of convection.

$\hat{d} = 1.0, \qquad \lambda = 0.01, \qquad T_U = 4°\mathrm{C},$

$Ra = 213.278, \qquad a^2 = 2.583.$

$W(z)$:——, $\Theta(z)$: ----.

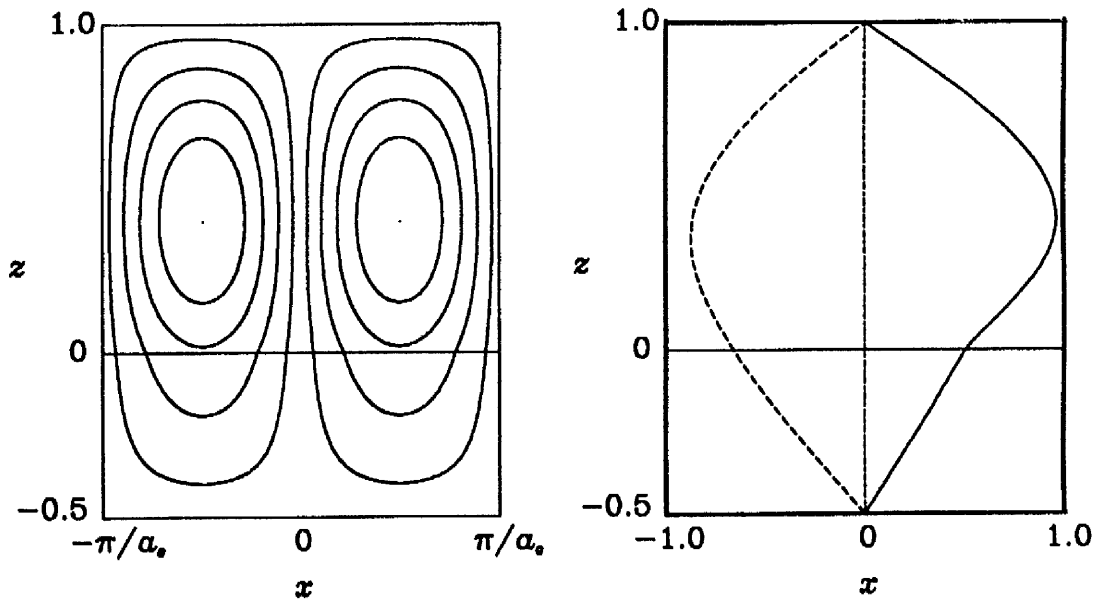

Figure 8.3 Two dimensional streamlines and normalized eigenfunctions $W(z)$, $\Theta(z)$ at the onset of convection.

$\hat{d} = 0.5, \qquad \lambda = 0.01, \qquad T_U = 4°\mathrm{C},$

$Ra = 355.830, \qquad a^2 = 4.799.$

$W(z)$:——, $\qquad \Theta(z)$: ----.

8.3.2 Discussion

In the discussion which follows we shall in particular consider the critical wavenumber for the porous layer, a_m. As mentioned earlier, this critical number is of direct use in the analysis as it fixes the width-to-depth ratio of the stone polygons via the relation

$$w/d = \frac{W}{d_m} = \frac{7.664}{a_m}, \tag{8.36}$$

where W is the width of a polygon from side to side (see Ray *et al.* 1983). We wish to compare our wavenumber predictions with field studies in Gleason (1984). However the widths given by Gleason (1984) for each polygon are averaged; the polygon widths he describes are actually 1.0774 times the width from side-to-side. Thus, to compare *directly* our predictions with those measured in Gleason (1984), we define our width-to-depth ratio, as calculated in tables 8.1–8.4, as

$$w/d = \frac{8.257}{a_m}. \tag{8.37}$$

Table 8.1 shows the effect on the Rayleigh number and wavenumber as λ increases (or effectively as permeability increases). The decrease in wavenumber as λ increases corresponds to an increase in width-to-depth ratio. The fluid layer Rayleigh number also decreases indicating that natural convection is now more likely to occur in the layer. From table 8.2 we observe that if permeability increases linearly from $z = -1$ to $z = 0$, the critical Rayleigh number in the soil decreases while the wavenumber is practically unaffected, in agreement with previous analyses of patterned ground formation (George *et al.* (1989) and chapter 6). The models for polygon formation suggested by Ray *et al.* (1983) and George *et al.* (1989) require permeability enhancement in the soil due to needle ice and frost heaving. Once the required permeability has been achieved natural convection may occur in the soil. The linear increase in permeability with z demonstrated in table 8.2 lowers the threshold for the onset of convection, thereby resulting in lower critical Rayleigh numbers. However the width-to-depth ratio for the polygons would appear to be unaffected by this linear increase. Furthermore, table 8.2 indicates that as $\hat{d}$ increases and the fluid layer becomes smaller

with respect to the porous layer, the critical Rayleigh number for the fluid layer decreases while the critical number for the porous layer increases.

From tables 8.2 and 8.4, as $\hat{d}$ increases the width-to-depth ratio decreases from approximately 10.0 when $\hat{d} = 0.35$, to 5.1 when $\hat{d} = 1.0$. This compares with field observations in Gleason (1984) which range from $w/d = 3.5$ to 6.05. In fact, a least squares fit of the eight data points of Gleason (1984) taken from sites in California and Wyoming shows

$$W = 5.043D - 0.0446,$$

W and D denoting, respectively, (averaged) width and depth. The numerical results would heuristically suggest that our model is most accurate when $\hat{d} \simeq 1.0$ (and from table 8.1, when λ is small).

Finally, our choice of boundary conditions must be examined. The boundary condition which we employ on the free surface is for a fixed water upper surface temperature – such a condition typically occurs in very cloudy or foggy weather with high winds (George *et al.* 1989). As this upper temperature increases, both the critical Rayleigh numbers and wavenumbers increase. The increase in Rayleigh number is due to the increased upper temperature stabilizing the fluid motions. The increase in critical wavenumber is equivalent to a decrease in width-to-depth ratio approaching the values predicted by field studies. As pointed out earlier the Beavers-Joseph condition itself is also the subject for discussion. Adopting the condition (8.10) of Jones (1973) involving shear stress, boundary conditions $(8.11)_{1,2}$ become

$$\begin{aligned} \frac{\partial u}{\partial z} + \frac{\partial w}{\partial x} &= \frac{\alpha}{\sqrt{k}}(u + \frac{k}{\mu}\frac{\partial p^m}{\partial x}), \\ \frac{\partial v}{\partial z} + \frac{\partial w}{\partial y} &= \frac{\alpha}{\sqrt{k}}(v + \frac{k}{\mu}\frac{\partial p^m}{\partial y}). \end{aligned} \tag{8.38}$$

Differentiating $(8.38)_1$ with respect to x and $(8.38)_2$ with respect to y then using (8.18) and (8.21), we may show that the dimensionless boundary condition $(8.24)_4$ becomes

$$\frac{\partial w^m}{\partial z} = \lambda\left(\frac{\partial w}{\partial z} - \frac{\zeta\hat{d}}{\alpha}\left(\frac{\partial^2 w}{\partial z^2} - \nabla_2^2 w\right)\right). \tag{8.39}$$

We have solved system (8.30)–(8.33) subject to this alternative boundary condition and some results are given in table 8.5. Comparing these results with those in tables 8.1–8.4 we can see that the difference between predictions for each condition is very small, while the *behaviour* of the critical numbers is the same in both cases.

We believe that the analysis and results presented here provide a useful insight into the process involved in underwater pattern formation, and suggest appropriate values for $\hat{d}$ and λ; the model also presents a valuable numerical analysis of convective motions when a fluid layer overlies a porous layer. To demonstrate this behaviour, in figures 8.2 and 8.3 we plot two dimensional streamlines for the fluid motion and the eigenfunctions of the z-dependent parts of (w, θ) at the onset of convection.

The model we have described for patterned ground formation and the planforms chosen in the normal mode expansion assume that a convection cell for the motion must be three dimensional. It is very difficult, however, to reproduce three dimensional streamlines graphically. Instead we simplify the problem and instead concentrate on a two dimensional roll cell. Although the stone nets are obviously not the result of a roll cell, this analysis will allow us to observe the penetration of fluid motion into the porous region. These two dimensional streamlines are very similar to those obtained by considering a vertical plane in the hexagonal cell (either from point to point or side to side). For geometrical reasons the two are not identical, but the fluid motions in each case are very similar.

To produce the figures we first dimensionalize the eigenfunctions found via the shooting method (8.35). This dimensionalization will allow us to show graphically the effect of variable fluid/matrix depth on the fluid motions, and also ensures continuity of the eigenfunctions at $z = 0$. Since we do not know the values d and d_m explicitly, we dimensionalize according to the size of their ratio $\hat{d}$. In the following discussion all non-dimensional terms will be denoted by a superscript *.

Case 1: $\hat{d} \geq 1$

Fix $d_m = 1$, $U^m = 1$ and $T^{m\sharp} = 1$, where U^m, $T^{m\sharp}$ are the dimensional terms used in the non-dimensionalization (8.16). Thus from (8.15) and (8.16),

$$\begin{aligned} \mathbf{u} &= \frac{\hat{d}}{\lambda}\mathbf{u}^*, \qquad \theta = \frac{1}{\chi}\theta^*, \\ \mathbf{u^m} &= 1.\mathbf{u^{m*}}, \quad \theta^m = 1.\theta^{m*}, \end{aligned} \tag{8.40}$$

where

$$\chi = \frac{T^\sharp}{T^{m\sharp}} = \frac{\hat{d}}{\lambda^{3/2}}\left(\frac{T_0}{T_U - T_0}\right)^{1/2}.$$

Case 2: $\hat{d} < 1$

Fix $d = 1$, $U = 1$ and $T^\sharp = 1$, to give

$$\begin{aligned} \mathbf{u} &= 1.\mathbf{u}^*, \qquad \theta = 1.\theta^*, \\ \mathbf{u^m} &= \frac{\lambda}{\hat{d}}\mathbf{u^{m*}}, \quad \theta^m = \chi\theta^{m*}. \end{aligned} \tag{8.41}$$

The eigenfunctions for the whole region are now

$$W_c(z) = \begin{cases} W^m(z), & -d_m \leq z < 0, \\ W(z), & 0 \leq z \leq d. \end{cases} \qquad \Theta_c(z) = \begin{cases} \Theta^m(z), & -d_m \leq z < 0, \\ \Theta(z), & 0 \leq z \leq d. \end{cases}$$

In figures 8.2 and 8.3 we normalize these eigenfunctions before plotting.

For the two dimensional streamlines the planform we have chosen for the roll cell is

$$g_c(x) = \cos a_c x, \qquad x \in \left[-\frac{\pi}{a_c}, \frac{\pi}{a_c}\right].$$

We have defined

$$a_c = \frac{a}{d} \equiv \frac{a_m}{d_m}$$

to take into account that although the fluid and porous regions have different length scales, once we redimensionalize the systems via (8.40), (8.41) above we may represent both regions by a single planform (e.g. *before* dimensionalization the roll cell planform would have been given by

$$g(x) = \cos ax \qquad \text{for fluid layer } z \in (0, 1),$$

and

$$g_m(x) = \cos a_m x \qquad \text{for porous layer } z \in (-1, 0)).$$

We now require a streamfunction $\Psi(x, z)$ satisfying

$$-\Psi_{,x} = w, \qquad \Psi_{,z} = u \qquad \text{for } z \in [0, d],$$

and

$$-\Psi_{,x} = w^m, \qquad \Psi_{,z} = u^m \qquad \text{for } z \in [-d_m, 0),$$

where $x \in [-\frac{\pi}{a_c}, \frac{\pi}{a_c}]$ and

$$u(\pm\frac{\pi}{a_c}, z) = u^m(\pm\frac{\pi}{a_c}, z) = u(0, z) = u^m(0, z) = 0,$$
$$w(x, d) = w^m(x, -d_m) = 0.$$

From the normal mode expansion we know that

$$w = W(z)\cos a_c x, \quad z \in [0, d]; \qquad w^m = W^m(z)\cos a_c x, \quad z \in [-d_m, 0].$$

It follows that we may choose our streamfunction to be

$$\Psi(x, z) = \begin{cases} -\frac{1}{a_c} W(z)\sin a_c x, & z \in [0, d], \\ -\frac{1}{a_c} W^m(z)\sin a_c x, & z \in [-d_m, 0). \end{cases} \tag{8.42}$$

Streamlines are now given by lines in the (x, z) plane where $\Psi(x, z) \equiv$ constant.

Figures 8.2 and 8.3 demonstrate the effect of variable porous layer depth on the fluid motions and the resulting cellular convection in the soil. The velocity and temperature perturbation fields attain their maximum in approximately the centre of the fluid layer. The resulting convection cell is also centred in the fluid layer with fluid motions penetrating into the porous matrix. This penetration increases as the depth ratio $\hat{d}$ is increased.

Chapter 9

The stabilizing influence of rotation on a plane layer subject to internal heating

9.1 Introduction

In this concluding chapter we consider a problem which, although related to those in the preceding chapters, is not specifically the result of penetrative convection. However, the model we describe *does* allow for internal heat generation effects; and we also employ a generalized energy, examples of which have been utilized throughout this thesis.

To be precise, in this chapter we shall discuss the stabilizing effect of rotation on convection in a fluid layer subject to internal heating. The important influence of rotation on Bénard convection has been the subject of many articles dealing with both the theoretical and experimental analyses. Chandrasekhar (1981) demonstrates stabilization of the linear system as angular velocity increases. Galdi & Straughan (1985) and Galdi & Padula (1990) also produce stability boundaries which increase as rotation increases in the *nonlinear* system using generalized energies, while Rossby (1969) describes the stabilization obtained experimentally. (See Galdi & Straughan (1985) and Galdi & Padula (1990) for a complete list of references.) Convection in a fluid layer which is subject to (possibly non-uniform) internal heating has also been discussed in chapter 5. Hamabata & Takashima (1983) consider the combination of rotation and internal heating in the *linear* system, while Namikawa *et al.* (1970) study the effect of rotation when instability is induced by surface tension as well as buoyancy.

Our aim is to obtain critical Rayleigh numbers which define the conditions for stability/instability in the layer. For the nonlinear system standard

energy methods, as employed in previous chapters, produce critical Rayleigh numbers which are independent of the rate of rotation. To overcome this Galdi & Straughan (1985) and Galdi & Padula (1990) utilize generalized energies which have no simple physical justification. Similar generalized energies are employed by Galdi (1985) and Rionero & Mulone (1988) for nonlinear stability analyses of the magnetic Bénard problem. Using generalized functionals Galdi & Straughan (1985) and Galdi & Padula (1990) are able to show that the critical energy Rayleigh number, which defines sufficient conditions for a disturbance to decay to zero, is also an increasing function of rotation so demonstrating the stabilizing effect of rotation on a fluid body. Unfortunately when the heat source is present we have not been able to employ the method of Galdi & Straughan (1985) due to the presence of a function of the vertical ordinate in the perturbation heat equation (c.f. chapter 5). Thus in this analysis we employ the method of Galdi & Padula (1990). Although the new approach of Galdi & Padula (1990) will allow us to obtain an energy Rayleigh number which is an increasing function of rotation, the stability bounds obtained are not the best possible (e.g. in the rotation only case the generalized function results of Galdi & Straughan (1985) indicate a region of possible subcritical instabilities much smaller than that of Galdi & Padula (1990)). However the method advocated in Galdi & Padula (1990) is more general and can be applied to a more varied range of systems (e.g. magnetic Bénard problem with or without Hall current).

In section 9.2 we present the model we shall use and define the energy appropriate to the system. In section 9.3 we prove monotonic stability of the base solution in the fluid, while in section 9.4 we derive our condition on the Rayleigh number which guarantees stability. We reproduce critical Rayleigh numbers and discuss the differential equations obtained from the linear and nonlinear systems.

9.2 Model for a rotating fluid layer

We shall consider a horizontal layer of heat conducting, linear, viscous fluid occupying the region $z \in (0, d)$ with the temperature fixed at $T = T_0$ when $z = 0$ and $T = T_1$ when $z = d$, where $T_0 > T_1$. The equations of motion for a layer rotating at angular velocity $\Omega > 0$ about an axis parallel to $\mathbf{k} = (0, 0, 1)$, subject to internal heating, are (c.f. Chandrasekhar 1981)

$$u_{i,t} + u_j u_{i,j} = -\frac{1}{\rho_0} p_{,i} - g k_i [1 - \alpha_V (T - T_0)] + \nu \Delta u_i + 2\Omega (\mathbf{u} \times \mathbf{k})_i, \quad (9.1)$$

$$u_{i,i} = 0, \quad (9.2)$$

$$T_{,t} + u_i T_{,i} = \kappa \Delta T + q, \quad (9.3)$$

where $\mathbf{u}$, T, p, ρ_0, g, α_V, ν, κ and q are, respectively, velocity, temperature, pressure, (constant) density, gravity, thermal expansion coefficient, kinematic viscosity, thermal diffusivity and constant heat source. We have assumed a linear equation of state for the fluid. Equations (9.1)–(9.3) are defined on $\mathbf{R}^2 \times (0, d)$ and we have employed standard indicial notation.

Equations (9.1)–(9.3) possess the motionless solution $(\bar{\mathbf{u}}, \bar{p}, \bar{T})$ given by

$$\bar{u_i} \equiv 0, \qquad \bar{T}(z) = \frac{qz}{2\kappa}(d - z) + \left(\frac{T_1 - T_0}{d}\right) z + T_0,$$

with pressure $\bar{p}$ determined from $\frac{d\bar{p}}{dz} = -g\rho(\bar{T})$.

Suppose $(\mathbf{u}, \pi, \theta)$ are perturbations to steady solution $(\bar{\mathbf{u}}, \bar{p}, \bar{T})$. Then if we introduce the non-dimensionalization

$$\begin{gathered} x_i = d x_i^*, \quad u_i = U u_i^*, \quad \pi = P\pi^*, \quad t = T^+ t^*, \quad \theta = T^\sharp \theta^*, \\ T^+ = \frac{d^2}{\nu}, \quad U = \frac{\nu}{d}, \quad P = \frac{U\nu\rho_0}{d}, \quad Pr = \frac{\nu}{\kappa}, \quad \beta = \frac{T_0 - T_1}{d}, \\ Ta = \frac{2d^2\Omega}{\nu}, \quad T^{\sharp 2} = \frac{U^2 \beta Pr}{g\alpha}, \quad R^2 = \frac{\beta d^4 g\alpha}{\nu\kappa}, \end{gathered} \quad (9.4)$$

and define

$$Q = \frac{dq}{\beta\kappa}, \quad f(z) = 1 + Q(z - \frac{1}{2}),$$

the equations governing the non-dimensional perturbation variables can be written (after dropping all stars):

$$u_{i,t} + u_j u_{i,j} = -\pi_{,i} + R\theta k_i + \Delta u_i + Ta\big(\mathbf{u} \times \mathbf{k}\big)_i, \tag{9.5}$$

$$u_{i,i} = 0, \tag{9.6}$$

$$Pr(\theta_{,t} + u_i\theta_{,i}) = Rf(z)w + \Delta\theta. \tag{9.7}$$

R^2, Ta^2 and Pr are the Rayleigh number, Taylor number and Prandtl number, respectively. We suppose the surfaces $z = 0, 1$ are free so the boundary conditions are

$$\theta = u_{,z} = v_{,z} = w = 0 \qquad \text{on} \qquad z = 0, 1, \tag{9.8}$$

while from equation (9.7),

$$\theta_{,zz} = 0 \qquad \text{on} \qquad z = 0, 1. \tag{9.9}$$

We also assume the $(\mathbf{u}, \pi, \theta)$ fields are periodic in the x, y directions with periods $2a_1$, $2a_2$, respectively. Finally, to exclude rigid motions, we assume

$$\int_C u \, d\mathbf{x} = \int_C v \, d\mathbf{x} = 0, \tag{9.10}$$

where $C = \big\{(x, y, z) \in (0, \frac{\pi}{a_1}] \times (0, \frac{\pi}{a_2}] \times (0, 1)\big\}$.

A simple energy analysis will not show any stabilizing effect of rotation on the fluid motion. However, we can use this technique to prove that rotation is *never destabilizing*. Consider the energy functional

$$E^* = \frac{1}{2}\int_C \big(|\mathbf{u}|^2 + Pr|\theta|^2\big) \, d\mathbf{x}.$$

From (9.5)–(9.7) and boundary conditions (9.8), (9.9) we may show that

$$\frac{dE^*}{dt} = I^* - D^*,$$

where

$$I^* = \int_C \big(1 + f(z)\big)\theta w \, d\mathbf{x}, \qquad D^* = \int_C \big(|\nabla\mathbf{u}|^2 + |\nabla\theta|^2\big) \, d\mathbf{x}.$$

Notice that rotation no longer enters the problem because

$$Ta \int_C \mathbf{u} \cdot (\mathbf{u} \times \mathbf{k})\, d\mathbf{x} = 0.$$

Defining

$$\frac{1}{R_E} = \max_{\mathcal{H}} \frac{I^*}{D^*},$$

where $\mathcal{H}$ is the space of admissible solutions, we may show that $E(t) \to 0$, at least exponentially, provided $R < R_E$. Since R_E is independent of Taylor number Ta^2, it follows that rotation cannot have a destabilizing influence.

To prove any stabilizing effect we first rewrite (9.5)–(9.7) in the form

$$\begin{aligned} Bu_{,t} &= Au + RSu + TaMu + Nu \\ &= Au + R'\Sigma u + TaMu + Nu \\ &= Lu + Nu, \end{aligned} \tag{9.11}$$

where u is the component vector $(\mathbf{u}, \theta)$ such that

$$u \in C^1\big(0, \infty; Y(L) \cap \{J(C) \times L^2(C)\}\big),$$

$Y(L)$ is the domain of L, $J(C)$ is the subspace of $L^2(C)$ consisting of solenoidal vectors $\mathbf{u}$ with $w = 0$ at $z = 0, 1$, and we define

$$\begin{gathered} Bu = \begin{pmatrix} \mathbf{u} \\ Pr\theta \end{pmatrix}, \quad Au = \begin{pmatrix} -\operatorname{curl}\operatorname{curl}\mathbf{u} \\ \Delta\theta \end{pmatrix}, \quad Su = \begin{pmatrix} \Pi(\theta\mathbf{k}) \\ f(z)w \end{pmatrix}, \\ Mu = \begin{pmatrix} \Pi(\mathbf{u} \times \mathbf{k}) \\ 0 \end{pmatrix}, \quad Nu = \begin{pmatrix} -\Pi(\mathbf{u} \cdot \nabla\mathbf{u}) \\ -Pr\mathbf{u} \cdot \nabla\theta \end{pmatrix}, \\ s = \frac{1}{2} \sup_{z \in [0,1]} |1 + f(z)| = 1 + \frac{Q}{4}, \quad R' = sR, \quad \Sigma u = \frac{1}{s} Su. \end{gathered} \tag{9.12}$$

Π is the projection from $L^2(C)$ to $J(C)$. In the following analysis $(\cdot, \cdot)$ and $\|\cdot\|$ will denote the scalar product and norm on $J(C) \times L^2(C)$. Since when $\|\mathbf{u}\| = 1$,

$$\begin{aligned} (Su, u) &= \int_C \big[1 + f(z)\big]\theta w\, d\mathbf{x} \\ &\le \sup_{z \in [0,1]} |1 + f(z)| \int_C \theta^2 w^2\, d\mathbf{x} \\ &\le s, \end{aligned}$$

this definition guarantees that $\|\Sigma\| = 1$.

The method employed by Galdi & Padula (1990) requires commutivity of the operators A and M. Before we demonstrate this we must first verify that Au lies in the domain of M for all $u \in Y(A)$ and vice versa. We do this by proving that the components of Au and Mu satisfy the same boundary conditions as u, e.g. the components $-(\text{curl curl})\,\mathbf{u}$ and $\Delta\theta$ of Au satisfy (9.8)–(9.10) since for $i = 1, 2$:

$$-(\text{curl curl}\,\mathbf{u})_{i,z} = u_{i,jjz} = 0 \quad \text{on} \quad z = 0, 1;$$

$$-(\text{curl curl}\,\mathbf{u})_3 = w_{,jj} = 0 \quad \text{on} \quad z = 0, 1;$$

$$\Delta\theta = \theta_{,zz} = 0 \quad \text{on} \quad z = 0, 1;$$

$$\int_C -(\text{curl curl}\,\mathbf{u})_i \, d\mathbf{x} = 0.$$

Thus $Au \in Y(M)$ for all $u \in Y(A) \cap C^4(\bar{C})$ where

$$Y(A) = \Big\{ u \in J(C) \times L^2(C) : \mathbf{u}, \theta \text{ satisfy (9.8)–(9.10)}; \int_C \left(|\text{curl curl}\,\mathbf{u}|^2 + |\Delta\theta|^2 \right) d\mathbf{x} < \infty \Big\}.$$

Similarly, $Mu \in Y(A)$ for all $u \in Y(M) \cap C^4(\bar{C})$. We now observe that

$$MAu = \begin{pmatrix} -\Pi\big(\text{curl curl}(\mathbf{u} \times \mathbf{k})\big) \\ 0 \end{pmatrix} = \begin{pmatrix} -\nabla\big(\nabla \cdot (\mathbf{u} \times \mathbf{k})\big) + \Delta(\mathbf{u} \times \mathbf{k}) - \nabla\zeta \\ 0 \end{pmatrix}$$

where

$$\Delta\zeta = -\Delta\big(\nabla \cdot (\mathbf{u} \times \mathbf{k})\big) + \nabla \cdot \big(\Delta(\mathbf{u} \times \mathbf{k})\big) = 0$$

and

$$\zeta_{,z} = -[\nabla \cdot (\mathbf{u} \times \mathbf{k})]_{,3} + \Delta(\mathbf{u} \times \mathbf{k})_3 = 0 \quad \text{on } z = 0, 1;$$

i.e. $\zeta = \text{constant}$.

Thus A and M are commutative since

$$MAu = \begin{pmatrix} -\nabla\big(\nabla \cdot (\mathbf{u} \times \mathbf{k})\big) + \Delta(\mathbf{u} \times \mathbf{k}) \\ 0 \end{pmatrix} = \begin{pmatrix} \Delta\Pi(\mathbf{u} \times \mathbf{k}) \\ 0 \end{pmatrix} = AMu.$$

Using the commutivity of the operators, and since A is symmetric and M is skew-symmetric, it follows that

$$(Au, Mu) = (u, AMu) = (u, MAu) = -(Mu, Au),$$

i.e. $(Au, Mu) = 0$. In a similar manner we may show $\Sigma u \in Y(A)$ for all $u \in J(C) \times L^2(C)$ and $(\Sigma Mu, Mu) = 0$. From boundary conditions (9.8) and the solenoidal nature of $\mathbf{u}$, it also follows that (Nu, u)=0.

In the absence of rotation we expect the destabilizing part of S to be dominated by the dissipative term $-(Au, u)$; when rotation is present we wish M to have a stabilizing influence. To this end we define

$$D(u) = -(Au, u)$$

and now we can show using Poincaré's inequality,

$$\begin{aligned}
(\Sigma u, u) &= \frac{1}{s}\int_C \left(\Pi(\theta\mathbf{k})\cdot\mathbf{u} + f(z)w\theta\right) d\mathbf{x} \\
&= \frac{1}{s}\int_C (1+f(z))\theta w \, d\mathbf{x} \\
&\leq \frac{2}{\pi^2}\left(\int_C (\theta_{,z})^2 \, d\mathbf{x}\right)^{1/2}\left(\int_C (w_{,z})^2 \, d\mathbf{x}\right)^{1/2} \\
&\leq \frac{2}{\pi^2} D(u)^{1/2} D(Mu)^{1/2} \\
&= k_1 D(u)^{1/2} D(Mu)^{1/2}, \qquad (9.13)
\end{aligned}$$

where $D(u) \equiv \int_C |\nabla\mathbf{u}|^2 + |\nabla\theta|^2 \, d\mathbf{x}$ and

$$\begin{aligned}
D(Mu) &= \int_C \operatorname{curl}\operatorname{curl}\Pi(\mathbf{u}\times\mathbf{k})\cdot\Pi(\mathbf{u}\times\mathbf{k})\, d\mathbf{x} \\
&= -\int_C \Delta\Pi(\mathbf{u}\times\mathbf{k})\cdot\Pi(\mathbf{u}\times\mathbf{k})\, d\mathbf{x} \\
&= \int_C |\mathbf{u}_{,z}|^2 \, d\mathbf{x}. \qquad (9.14)
\end{aligned}$$

If we set

$$w = B^{1/2}u = \begin{pmatrix} \mathbf{u} \\ Pr^{1/2}\theta \end{pmatrix}, \qquad (9.15)$$

our system (9.11) becomes

$$w_{,t} = B^{-1/2}Au + R'B^{-1/2}\Sigma u + TaB^{-1/2}Mu + B^{-1/2}Nu. \tag{9.16}$$

We have already shown the non-destabilizing influence of rotation. The equivalent result using system (9.11) and the above operators may be obtained by defining

$$E_1 = \frac{1}{2}\|w\|^2.$$

From (9.8), (9.9) and (9.16) we may prove the exponential decay of E_1 provided $R' < R'_E$, where

$$\frac{1}{R'_E} = \max_{u \in Y(A)} \left\{ -\frac{(\Sigma u, u)}{(Au, u)} \right\}. \tag{9.17}$$

(Note that from the definition of Σu and Au, $sR'_E = R_E$.)

We now have to choose an energy functional which will allow for stabilization due to rotation. Galdi & Padula (1990) prove that *no such stabilization* will occur if

$$\left(B^{-1}(Au + R'\Sigma u), Mu\right) \equiv 0.$$

Since we have already proved that $(Au, Mu) = 0$, stabilization is only possible provided

$$(\Sigma w, Mw) \not\equiv 0.$$

To study the possible stabilizing effect of M on the base solution we choose the energy functional E_1 to which we add the coupling $(\Sigma w, Mw)$ term. To this we must also add a constant multiple of $\|Mw\|^2$ to guarantee that our energy is positive definite. Thus the energy functional we choose is (c.f. Galdi & Padula 1990):

$$\begin{aligned} E &= \frac{1}{2}\left(\|w\|^2 + \lambda_2\|Mw\|^2\right) + \lambda(\Sigma w, Mw) \\ &= \frac{1}{2}\left(\|w\|^2 + Pr\|\theta\|^2 + \lambda_2\|\Pi(\mathbf{u}\times\mathbf{k})\|^2\right) \\ &\qquad + \frac{1}{s}\lambda Pr^{1/2}\int_C \Pi(\mathbf{u}\times\mathbf{k})\cdot\theta\mathbf{k}\,d\mathbf{x}, \end{aligned} \tag{9.18}$$

where $\lambda_2 > |\lambda|^2$ in order to guarantee that E is positive definite. From (9.16) we derive the differential equation

$$\begin{aligned}\frac{dE}{dt} = &-D(u) - \lambda_2 D(Mu) + R'(u, \Sigma u) + \left(R'\lambda_2 - Ta\lambda Pr^{1/2}\right)(Mu, M\Sigma u) \\ &+ \lambda Pr^{-1/2}(Mu, \Sigma Au) + R'\lambda Pr^{-1/2}(Mu, \Sigma\Sigma u) \\ &+ \lambda Pr^{1/2}(\Sigma u, MAu) + \lambda Pr^{1/2}(\Sigma u, MNu) \\ &+ \lambda Pr^{-1/2}(Mu, \Sigma Nu) + \lambda_2(Mu, MNu).\end{aligned} \tag{9.19}$$

The $(M\Sigma u, Mu)$ term is not always one signed and may be destabilizing, so to remove it we choose $\lambda > 0$ and fix

$$\lambda_2 = \frac{\lambda Ta Pr^{1/2}}{R'}.$$

Thus

$$\frac{dE}{dt} = \mathcal{I} - \mathcal{D} + \mathcal{N}, \tag{9.20}$$

where

$$\begin{aligned}\mathcal{I} &= R'\Big\{(u, \Sigma u) + \frac{\lambda}{Pr^{1/2}R'}(Mu, \Sigma Au) + \frac{\lambda Pr^{1/2}}{R'}(\Sigma u, MAu) \\ &\qquad + \lambda Pr^{-1/2}(Mu, \Sigma\Sigma u)\Big\}, \\ \mathcal{D} &= D(u) + \lambda_2 D(Mu), \\ \mathcal{N} &= \lambda_2(Mu, MNu) + \lambda Pr^{-1/2}(Mu, \Sigma Nu) \\ &\qquad + \lambda Pr^{1/2}(\Sigma u, MNu).\end{aligned} \tag{9.21}$$

Since we require

$$\lambda_2 = \frac{\lambda Ta Pr^{1/2}}{R'} > |\lambda|^2, \tag{9.22}$$

we now assume $\lambda = \xi Pr^{1/2}\frac{Ta}{R'}$ for constant $\xi \in (0, 1)$ to be chosen later.

9.3 Monotonic stability

In this section we will prove monotonic stability of the base solution $(\bar{\mathbf{u}}, \bar{p}, \bar{T})$. We do this by defining the energy parameter

$$m = \sup_{\mathcal{H}} \left\{ \frac{\mathcal{I}}{\mathcal{D}} \right\} < \infty, \tag{9.23}$$

where $\mathcal{H}$ is the class of solutions in $C^4(\bar{C}) \cap Y(A)$, and attempting to show that perturbations to the base solution conditionally decay provided $m < 1$.

We begin by assuming $m < 1$. From (9.20) and (9.23) we have

$$\frac{dE}{dt} \leq (m-1)\mathcal{D} + \mathcal{N}.$$

In order to obtain decay of E we require to show that the nonlinear terms in $\mathcal{N}$ may be dominated by dissipative terms. This is achieved by first obtaining upper bounds for a number of norms.

Let $\mathbf{v} \in L^2(C)$ be any vector, periodic in the x, y directions, which satisfies

$$v_3 = 0 \qquad \text{on } z = 0, 1.$$

By the definition of the projection Π, there exists φ such that

$$\Pi(\mathbf{v}) = \mathbf{v} - \nabla\varphi,$$
$$\Delta\varphi = \nabla \cdot \mathbf{v},$$

with

$$\varphi_{,z} = v_3 = 0 \qquad \text{on } z = 0, 1.$$

Since $\Pi(\mathbf{v})$ is divergence free, from the divergence theorem and the above we can show that

$$\begin{aligned} \int_C |\Pi(\mathbf{v})|^2 \, d\mathbf{x} &= \int_C \Pi(\mathbf{v}) \cdot \mathbf{v} \, d\mathbf{x} \\ &= \int_C \left(|\mathbf{v}|^2 - \nabla\varphi \cdot \mathbf{v} \right) d\mathbf{x} \\ &= \int_C \left(|\mathbf{v}|^2 + \varphi \nabla \cdot \mathbf{v} \right) d\mathbf{x} \end{aligned}$$

$$
\begin{aligned}
&= \int_C \left(|\mathbf{v}|^2 + \varphi\Delta\varphi\right) d\mathbf{x} \\
&= \int_C \left(|\mathbf{v}|^2 - |\nabla\varphi|^2\right) d\mathbf{x} \\
&\leq \int_C |\mathbf{v}|^2 \, d\mathbf{x}.
\end{aligned}
$$

Using this result and boundary conditions (9.8), the norm of Nu may be bounded as follows:

$$
\begin{aligned}
\|Nu\|^2 &= \int_C \left(|\Pi(\mathbf{u}\cdot\nabla\mathbf{u})|^2 + Pr^2|\mathbf{u}\cdot\nabla\theta|^2\right) d\mathbf{x} \\
&\leq \int_C \left(|\mathbf{u}\cdot\nabla\mathbf{u}|^2 + Pr^2|\mathbf{u}\cdot\nabla\theta|^2\right) d\mathbf{x} \\
&\leq (1+Pr^2) \sup_C |\mathbf{u}|^2 \int_C \left(|\nabla\mathbf{u}|^2 + |\nabla\theta|^2\right) d\mathbf{x} \\
&\leq c_1^2 D_1^2, \qquad (9.24)
\end{aligned}
$$

where

$$
D_1 = \|Au\|^2 + D(u), \qquad c_1^2 = (1+Pr^2)K^2,
$$

and from Galdi & Straughan (1985) we have used

$$
\sup_C |\mathbf{u}| \leq K\left(\int_C |\text{curl curl}\,\mathbf{u}|^2 \, d\mathbf{x}\right)^{1/2},
$$

$$
K = \left[\frac{3}{\sqrt{2}}(\sqrt{2}-1)\pi h^3\right]^{1/2} + \frac{40h^{3/5}}{3}, \qquad h = \min\{a_1, a_2, 1\}.
$$

Similarly,

$$
\|MNu\|^2 \leq K^2 {D_1}^2. \qquad (9.25)
$$

Bounds may be obtained for $\|u\|$ and $\|Mu\|$ if we first consider the definition of the energy functional E. From (9.18) we can show that

$$
E \geq \frac{1}{2}(\|w\| - |\lambda|\|Mw\|)^2 + \frac{1}{2}(\lambda_2 - \lambda^2)\|Mw\|^2
$$

or (9.26)

$$
E \geq \frac{\lambda_2}{2}(\|Mw\| - \frac{|\lambda|}{\lambda_2}\|w\|)^2 + \frac{1}{2}(1 - \frac{\lambda^2}{\lambda_2})\|w\|^2.
$$

If we define b_1 to be the minimum eigenvalue of B and observe that $w = B^{1/2}u$, we now have

$$\begin{aligned} \|u\|^2 &\leq \frac{2}{b_1}\left(\frac{\lambda_2}{\lambda_2 - \lambda^2}\right)E = \frac{2l_1^2}{b_1}E, \\ \|Mu\|^2 &\leq \frac{2}{b_1}\left(\frac{1}{\lambda_2 - \lambda^2}\right)E = \frac{2l_2^2}{b_1}E \end{aligned} \tag{9.27}$$

where

$$l_1^2 = \frac{1}{1-\xi}, \qquad l_2^2 = \frac{R'^2}{Ta^2 Pr\xi(1-\xi)}.$$

Inequalities (9.24), (9.25) and (9.27) are now employed to control the terms in $\mathcal{N}$ as follows:

$$\begin{aligned} (Mu, MNu) &\leq \|Mu\|\|MNu\| \leq \sqrt{\frac{2}{b_1}}l_2 K D_1 E^{1/2}, \\ (Mu, \Sigma Nu) &\leq \|Mu\|\|Nu\| \leq \sqrt{\frac{2}{b_1}}l_2 c_1 D_1 E^{1/2}, \\ (\Sigma u, MNu) &\leq \|u\|\|MNu\| \leq \sqrt{\frac{2}{b_1}}l_1 K D_1 E^{1/2}. \end{aligned} \tag{9.28}$$

We now utilize inequalities (9.28) to give

$$\frac{dE}{dt} \leq (m-1)\mathcal{D} + \alpha D_1 E^{1/2}$$

where

$$\alpha = \sqrt{\frac{2}{b_1(1-\xi)}}\left[c_1\sqrt{\frac{\xi}{Pr}} + \frac{KTa}{R'}(Pr\xi + \sqrt{\xi Pr})\right].$$

In order to dominate the increasing nonlinear terms occuring in $D_1 E^{1/2}$ we add another piece to the energy functional (c.f. Galdi & Straughan 1985):

$$\begin{aligned} E_2 &= \frac{1}{2}[\|w\|^2 + D(w)] \\ &\equiv \frac{1}{2}[\|\mathbf{u}\|^2 + Pr\|\theta\|^2 - (\mathbf{u}, \text{curl curl}\,\mathbf{u}) + Pr\|\nabla\theta\|^2]. \end{aligned}$$

The above functional is used to dominate the nonlinearities; it will not affect the stability bounds. Differentiating E_2 we have

$$\begin{aligned} \frac{dE_2}{dt} = (u, Au) + R'(u, \Sigma u) - \|Au\|^2 \\ - R'(Au, \Sigma u) - (Au, Nu). \end{aligned} \tag{9.29}$$

The final term in (9.29) may be bounded using (9.24) as follows

$$(Au, Nu) \leq c_1 \|Au\| D(u)^{1/2} \|Au\| \leq \sqrt{\frac{2}{b_1}} c_1 D_1 {E_2}^{1/2}.$$

Thus, introducing $\eta(> 0)$ a coupling parameter to be chosen later, we now obtain

$$\begin{aligned} \frac{d}{dt}(E + \eta E_2) \leq (m-1)\mathcal{D} - \eta D_1 + R'\eta(u - Au, \Sigma u) \\ + \alpha D_1 E^{1/2} + \sqrt{\frac{2}{b_1}} \eta c_1 D_1 {E_2}^{1/2}. \end{aligned} \tag{9.30}$$

We must now find bounds for the $(-Au, \Sigma u)$ term which occurs on the right hand side of (9.30): using Poincaré's inequality and Hölder's inequality,

$$\begin{aligned} |(Au, \Sigma u)| &\leq \frac{1}{s} \sup_C |1 + f(z)| \left| \int_C w \Delta\theta \, d\mathbf{x} \right| \\ &\leq \frac{2}{\pi} \left(\int_C (w_{,z})^2 \, d\mathbf{x} \right)^{1/2} \left(\int_C (\Delta\theta)^2 \, d\mathbf{x} \right)^{1/2} \\ &\leq \frac{2}{\pi} [D(Mu) D_1(u)]^{1/2}, \end{aligned} \tag{9.31}$$

or

$$|(Au, \Sigma u)| \leq \frac{2}{\pi} [D(u) D_1(u)]^{1/2}, \tag{9.32}$$

where $D(u)$ and $D(Mu)$ were expanded earlier and $D_1(u)$ may be rewritten as

$$D_1(u) = \int_C \left(|\nabla \mathbf{u}|^2 + |\nabla\theta|^2 + |\Delta\theta|^2 + |\text{curl curl } \mathbf{u}|^2 \right) d\mathbf{x}.$$

We now show that E decays exponentially provided $E(0)$ does not exceed a certain limit. In order to guarantee the stabilizing effect of rotation on the solution we require that this bound does not tend to zero as Ta increases. We can demonstrate stability once we produce upper limits for the $(u - Au, \Sigma u)$ term which occurs in (9.30).

We first consider the case $Ta > 1$. By (9.13), (9.31) and the Cauchy-Schwarz inequality,

$$R'\eta(\Sigma u, u - Au) \leq \frac{\eta}{2} D_1(u) + {R'}^3 \eta \frac{(k_1^2 \pi^2 + 4)}{\pi^2 \lambda Ta \sqrt{Pr}} \mathcal{D}.$$

Thus (9.30) now becomes

$$\frac{d}{dt}(E+\eta E_2) \le \left[(m-1)+R'^3\eta\frac{(k_1^2\pi^2+4)}{\pi^2\lambda Ta\sqrt{Pr}}\right]\mathcal{D} + \left[\alpha E^{1/2}+\eta c_1\sqrt{\frac{2}{b_1}}{E_2}^{1/2}-\frac{1}{2}\eta\right]D_1. \tag{9.33}$$

If we set

$$\eta = \frac{(1-m)\xi\pi^2 Ta^2 Pr}{2R'^4(k_1^2\pi^2+4)}$$

which is positive since $m<1$, we now have

$$\frac{d\mathcal{E}}{dt} \le \left\{-1+\frac{2}{(\eta b_1)^{1/2}}\left(\left(\frac{b_1}{\eta}\right)^{1/2}\alpha+c_1\sqrt{2}\right)\mathcal{E}^{1/2}\right\}\mathcal{D}^* \tag{9.34}$$

where

$$\mathcal{E}=E+\eta E_2, \qquad \mathcal{D}^*=\frac{1}{2}[(1-m)\mathcal{D}+\eta D_1]. \tag{9.35}$$

Thus exponential decay of the energy (stability of the base solution) is guaranteed provided

$$\mathcal{E}^{1/2}(0) \le \frac{(\eta b_1)^{1/2}}{2\left(\left(\frac{b_1}{\eta}\right)^{1/2}\alpha+c_1\sqrt{2}\right)}, \tag{9.36}$$

which is an increasing function of Ta.

If $Ta \le 1$ from (9.17) we have

$$(\Sigma u, u) \le \frac{D(u)}{R'_E}.$$

Thus using (9.17),

$$\frac{d}{dt}(E+\eta E_2) \le \left[(m-1)+\frac{\eta}{2R'_E}\left(2R'+\frac{4}{\pi^2}R'^2R'_E\right)\right]\mathcal{D} + \left[\tilde{\alpha}E^{1/2}+\eta c_1\sqrt{\frac{2}{b_1}}{E_2}^{1/2}-\frac{1}{2}\eta\right]D_1, \tag{9.37}$$

where

$$\tilde{\alpha}=\alpha\big|_{Ta=1}.$$

Choosing

$$\eta=\frac{(1-m)R'_E\pi^2}{2R'\pi^2+4R'^2R'_E}$$

will give a result equivalent to (9.34) with α replaced by $\tilde{\alpha}$.

9.4 Conditional stability condition

Having proved the conditional stability of solution $(\bar{\mathbf{u}}, \bar{p}, \bar{T})$, we now require to find sufficient conditions to guarantee that

$$m = \sup_{C}\{\frac{\mathcal{I}}{\mathcal{D}}\} < 1.$$

To do this we obtain a curve $R_c(Ta)$ which satisfies the following:

(i) $m < 1$ if $R^2 < R_c(Ta)$,

(ii) $R_c(0) = R_E^2$,

(iii) $R_c(Ta)$ is increasing with Ta,

(iv) $R_c(Ta)$ is strictly increasing for $Ta \geq Ta^*$ where Ta^* is the maximum Ta such that $R_c(Ta^*) = R_E^2$.

Once again, before producing the estimate for the curve, we obtain using Poincaré's inequality a number of bounds for terms in $\mathcal{I}$ and $\mathcal{D}$ which are useful in our calculations :

$$\begin{aligned}(Mu, \Sigma\Sigma u) &= \frac{1}{s^2}\int_V \Pi(\mathbf{u}\times\mathbf{k})\cdot f(z) w\mathbf{k}\, d\mathbf{x} \\ &\leq \frac{f_m}{s^2\pi^2} D(Mu) \\ &= k_2 D(Mu) \end{aligned} \tag{9.38}$$

where $f_m = \sup_{z\in[0,1]}|f(z)| = 1 + \frac{Q}{2}$, and

$$\begin{aligned}(\Sigma Au, Mu) = (A\Sigma u, Mu) &= \frac{1}{s}\int_V \Pi(\mathbf{u}\times\mathbf{k})\cdot\Delta(\theta\mathbf{k})\, d\mathbf{x} \\ &\leq k_3[D(Mu)D(u)]^{1/2}, \end{aligned} \tag{9.39}$$

where $k_3 = 1/s$. From (9.21), (9.38) and (9.39) we now have

$$\begin{aligned}\mathcal{I} - \mathcal{D} \leq -X^2 &- \lambda Pr^{1/2}\Big(\frac{Ta}{R'} - k_2 Pr^{-1}R'\Big)Y^2 \\ &+ \big(R'k_1 + \lambda Pr^{1/2}k_3(1+Pr^{-1})\big)XY,\end{aligned}$$

where $X^2 = D(u)$ and $Y^2 = D(Mu)$. In order to have $m < 1$ we require $\mathcal{I} - \mathcal{D}$ to be negative definite, i.e.

$$\frac{4\lambda}{Pr^{1/2}}\left(\frac{Ta}{R'} - \frac{k_2 R'}{Pr}\right) > \left(\frac{k_1 R'}{Pr^{1/2}} + \lambda(1 + Pr^{-1}k_3)\right)^2 \tag{9.40}$$

for $\lambda \in (0, \frac{Ta}{R'} Pr^{1/2})$. Let $\tau^2 = k_3^2(1 + Pr^{-1})^2$. Then for

$$C = \frac{Ta}{R'^2} - k_1\tau - \frac{k_2}{Pr}, \tag{9.41}$$

(9.40) is equivalent to

$$\tau^2\lambda^2 - 2\lambda Pr^{-1/2}\left[\frac{Ta}{R'} + R'C - \frac{k_2}{Pr}\right] + \frac{k_1^2 R'^2}{Pr} < 0.$$

So provided $C > 0$ we require

$$\left[\left(\frac{Ta}{R'} - \frac{k_2 R'}{Pr}\right)^{1/2} - (R'C)^{1/2}\right]^2 < \tau^2\lambda Pr^{1/2} < \left[\left(\frac{Ta}{R'} - \frac{k_2 R'}{Pr}\right)^{1/2} + (R'C)^{1/2}\right]^2. \tag{9.42}$$

Choose

$$\tau^2\lambda Pr^{1/2} = \frac{2\delta Ta}{R'}, \qquad \text{i.e.} \quad \xi = \frac{2\delta}{k_3^2 Pr(1 + Pr^{-1})^2}$$

where $\xi \in (0,1)$ is the constant defined in (9.22) and $\delta \in (0,1)$ is a constant which ensures that (9.42) is indeed satisfied. Then $C > 0$ provided

$$R'^2 < \frac{s^2\pi^2 TaPr}{Pr + 1 + f_m(Pr + 2)}.$$

Bearing in mind that our Rayleigh number $R^2 = R'^2/s^2$, our stability condition is

$$R^2 < R_c(Ta),$$

where

$$\begin{aligned} R_c(Ta) &= \max\left\{R_E^2, \frac{\pi^2 TaPr}{Pr + 1 + f_m(Pr + 2)}\right\} \\ &= \max\left\{R_E^2, \frac{2\pi^2 TaPr}{4Pr + 6 + Q(Pr + 2)}\right\}, \\ &= \max\left\{R_E^2, c(Q, Pr)Ta\right\}. \end{aligned} \tag{9.43}$$

In table 9.1 we list values for R_E^2 and Ta^{*2} for a range of Q and Pr. Recall that Ta^{*2} is defined to be the critical Taylor number for which

$$R_c(Ta^*) = R_E^2.$$

We shall also include values for a_E^2, the critical wavenumber corresponding to R_E^2. To demonstrate the rate at which $R_c(Ta)$ increases with Ta for $Ta > Ta^*$, we also include in the table values for $c(Q, Pr)$, the coefficient of Ta in (9.43).

Q	Pr	R_E^2	a_E^2	Ta^{*2}	$c(Q, Pr)$
0	0.5	657.512	4.935	2.84×10^5	1.234
0	5.0			3.0×10^4	3.796
1	0.5	657.309	4.936	4.89×10^5	0.940
1	5.0			4.83×10^4	2.991
10	0.5	638.015	5.088	4.55×10^6	0.299
10	5.0			3.85×10^5	1.028
100	0.5	267.669	7.796	4.90×10^7	0.038
100	5.0			3.88×10^6	0.136

Table 9.1 Variation of R_E^2, Ta^{*2} and $c(Q, Pr)$ with heat source Q and Prandtl number Pr.

Ideally we would produce conditions which guarantee $m < 1$ by considering the Euler-Lagrange equations of (9.23). From these Euler-Lagrange equations we can derive the system of equations:

$$\begin{aligned}
&\frac{2m}{R'}\Delta^2 w + \left(\frac{1+f(z)}{s}\right)\Delta^*\theta + \frac{\lambda}{Pr^{1/2}s^2}f(z)\Delta^*\zeta = 0,\\
&\left(\frac{1+f(z)}{s}\right)w + \frac{2m}{R'}\Delta\theta + \frac{\lambda}{sR'Pr^{1/2}}(Pr+1)\Delta\zeta = 0,\\
&\frac{\lambda}{Pr^{1/2}s^2}f(z)\Delta^* w + \frac{\lambda}{sR'Pr^{1/2}}(Pr+1)\Delta^*\Delta\theta + \frac{2m\lambda\,\mathrm{Pr}^{1/2}}{R'^2}\Delta^2\zeta = 0,
\end{aligned} \tag{9.44}$$

where $\zeta = \Pi(\mathbf{u}\times\mathbf{k})_3$ and $\Delta^* = \frac{\partial^2}{\partial x^2} + \frac{\partial^2}{\partial y^2}$. By setting $m = 1$ we could obtain the critical value of the Rayleigh number which guarantees stability from this set of equations. However the system is difficult to solve because it is of tenth order and because of the presence of the $f(z)$ due to the heat source.

We may also compare our energy Rayleigh numbers with those obtained from linear theory. From equations (9.5)–(9.7) the linear system of equations (assuming exchange of stabilities) is

$$\begin{aligned}
\pi_{,i} &= R\theta k_i + \Delta u_i + Ta(\mathbf{u}\times\mathbf{k})_i,\\
0 &= Rf(z)w + \Delta\theta,\\
0 &= \Delta\varpi + Taw_{,z}
\end{aligned} \tag{9.45}$$

where ϖ is the third component of vorticity and $(9.45)_3$ is obtained by taking the third component of the curl of (9.5). Although exchange of stabilities is assumed it is possible that motions at the onset of convection are not the result of stationary convection. However in the case when there is no heat source (i.e. $Q \equiv 0$) it can be shown that instability occurs as stationary convection provided $Pr \geq 1$ (c.f. Chandrasekhar 1981). In our problem, by continuity it follows that exchange of stabilities is also guaranteed for Q in some neighbourhood of 0. It is the energy results and their relationship with the Taylor number which we are concerned

with here, so the assumption that exchange of stabilities exists is adequate in this analysis.

Decomposing (9.45) into normal modes we may rewrite the system as a solitary sixth order differential equation:

$$D^6W = 3a^2D^4W - (3a^4 + Ta^2)D^2W + (a^6 - a^2R^2f(z))W, \tag{9.46}$$

where $W(z)$ is the z-dependent part of w, a is the wave number and $D = \frac{\partial}{\partial z}$.

From boundary conditions (9.8) and (9.9) we also have

$$W = D^2W = D^4W = 0 \qquad \text{at} \qquad z = 0, 1. \tag{9.47}$$

System (9.46), (9.47) may be solved to give the critical Rayleigh number of linear theory, R_L^2, where

$$R_L^2 = \min_{a^2} R^2.$$

Again we have not reproduced linear results here. System (9.46), (9.47) would appear to be ideal for solution via the compound matrix method. But at large Taylor number ($\simeq 10^6$) it becomes very difficult to obtain accurate predictions for critical R^2. However, despite the lack of numerical results for systems (9.44) and (9.46), we must point out that it is the analysis leading up to the conditional stability bound (9.43) which is important in this chapter; it is this analysis which establishes the stabilization effect of rotation even in the presence of a heat source. We intend to analyse systems (9.44) and (9.46) numerically at some future date.

References

Akopyan, R. S. & Zel'dovich, B. Ya. 1985 Natural convection in liquids caused by absorption of laser radiation. *Prikl. Matem. Mekhan.* **49**, 685–688.

Andersland, O. B. & Anderson, D. M. 1978 *Geotechnical Engineering for Cold Regions.* New York: McGraw Hill.

Azouni, M. A. 1981a Oscillatory behaviour in convecting water. *Int. J. Heat Mass Transfer* **24**, 1983–1986.

Azouni, M. A. 1981b A model of rotating convective rolls in water over a freezing front. *J. Crystal Growth* **52**, 450–454.

Azouni, M. A. & Normand, C. 1983a Thermoconvective instabilities in a vertical cylinder of water with maximum density effects. I. Experiments. *Geophys. Astrophys. Fluid Dyn.* **23**, 209–222.

Azouni, M. A. & Normand, C. 1983b Thermoconvective instabilities in a vertical cylinder of water with maximum density effects. II. Theory. *Geophys. Astrophys. Fluid Dyn.* **23**, 223–245.

Barenghi, C. F. & Jones, C. A. 1989 Modulated Taylor–Couette flow. *J. Fluid Mech.* **208**, 127–160.

Beavers, G. S. & Joseph, D. D. 1967 Boundary conditions at a naturally permeable wall. *J. Fluid Mech.* **30**, 197–207.

Caltagirone, J. P. 1980 Stability of a saturated porous layer subject to a sudden rise in surface temperature: comparison between the linear and energy methods. *Q. Jl. Mech. Appl. Math.* **38**, 47–58.

Chandrasekhar, S. 1981 *Hydrodynamic and Hydromagnetic Stability.* Dover: New York.

Chhuon, B. & Caltagirone, J. P. 1979 Stability of a horizontal porous layer with timewise periodic boundary conditions. *J. Heat Transfer* **101**, 244–248.

Coddington, E. A. & Levinson, N. 1955 *Theory of Ordinary Differential Equations.* McGraw Hill. pp.78–81.

Deardorff, J. W., Willis, G. E. & Lilly, D. K. 1969 Laboratory investigation of non–steady penetrative convection. *J. Fluid Mech.* **35**, 7–31.

Drazin, P. G. & Reid, W. H. 1981 *Hydrodynamic Stability.* Cambridge University Press.

Finlayson, B. A. 1972 *Method of Weighted Residuals and Variational Principles.* New York: Academic Press.

Finucane, R. G. & Kelly, R. E. 1976 Onset of instability in a fluid layer heated sinusoidally from below. *Int. J. Heat Mass Transfer* **19**, 71–85.

Freeze, R. A. & Cherry, J. A. 1979 *Groundwater.* N. J. Prentice Hall.

Galdi, G. P. 1985 Nonlinear stability of the magnetic Bénard problem via a generalized energy method. *Arch. Rational Mech. Anal.* **87**, 167–186.

Galdi, G. P. & Padula, M. 1990 A new approach to energy theory in the stability of fluid motion. *Arch. Rational Mech. Anal.* **110**, 187–286.

Galdi, G. P., Payne, L. E., Proctor, M. R. E. & Straughan, B. 1987 Convection in thawing subsea permafrost. *Proc. Roy. Soc. London A* **414**, 83–102.

Galdi, G. P. & Rionero, S. 1983 Local estimates and stability of viscous flows in an exterior domain. *Arch. Rat. Mech. Anal.* **81**, 333–347.

Galdi, G. P. & Straughan, B. 1985 A nonlinear analysis of the stabilizing effect of rotation in the Bénard problem. *Proc. Roy. Soc. London A* **402**, 257–283.

Galdi, G. P. & Straughan, B. 1988 Stability of solutions to the Navier-Stokes equations backward in time. *Arch. Rat. Mech. Anal.* **101**, 107–114.

George, J. H., Gunn, R. D. & Straughan, B. 1989 Patterned ground formation and penetrative convection in porous media. *Geophys. Astrophys. Fluid Dyn.* **46**, 135–158.

Ghosal, S. & Spiegel, E. A. 1991 On thermonuclear convection: I. Shellular instability. *Geophys. Astrophys. Fluid Dyn.* **61**, 161–178.

Gilbarg, D. & Trudinger, N. S. 1977 *Elliptic partial differential equations of second order.* Springer–Verlag, p.148.

Gleason, K. J. 1984 *Nonlinear Boussinesq convection in porous media: application to patterned ground formation.* M.S. Thesis, University of Colorado, Boulder.

Gleason, K. J., Krantz, W. B. & Caine, N. 1988 *Parametric effects in the filtration free convection model for patterned ground.* Proc. Vth International Conf. Permafrost, Trondheim, Norway, pp.349–354.

Goldthwaite, R. P. 1976 Frost sorted patterned ground: A review. *Quarternary Research* **6**, 27–35.

Gresho, P. M. & Sani, R. L. 1970 The effects of gravity modulation on the stability of a heated fluid layer. *J. Fluid Mech.* **40**, 783–806.

Hamabata, H. & Takashima, M. 1983 The effect of rotation on convective instability in a horizontal fluid layer with internal heat generation. *J. Phys. Soc. Japan* **52**, 4145–4151.

Homsy, G. M. 1974 Global stability of time–dependent flows. Part 2. Modulated fluid layers. *J. Fluid Mech.* **62**, 387–403.

Inaba, H. & Fukuda, T. 1984 Natural convection in an inclined square cavity in regions of density inversion of water. *J. Fluid Mech.* **142**, 363–381.

Ince, E. L. 1944 *Ordinary Differential Equations.* Dover.

Ives, J. D. 1973 *Permafrost and its relationship to other enviromental parameters in a mid-latitude, high-altitude setting, Front Range, Colorado Rocky Mountains.* Permafrost. Second International Conference. 13–28 July 1973, Yakutsk, U.S.S.R. North American Contribution, 121–125.

Jones, I. P. 1973 Low Reynolds number flow past a porous spherical shell. *Proc. Camb. Phil. Soc.* **73**, 231–238.

Joseph, D. D. 1976 *Stability of Fluid Motions. Vols I and II.* Berlin–Heidelberg–New York: Springer–Verlag.

Joseph, D. D. & Shir, C. C. 1966 Subcritical convective instability. Part 1. Fluid layers *J. Fluid Mech.* **26**, 753–768.

Knops, R. J. & Payne, L. E. 1968 On the stability of solutions of the Navier-Stokes equations, backward in time. *Arch. Rat. Mech. Anal.* **29**, 331–335.

Krantz, W. B., Gleason, K. J. & Caine, N. 1988 *Patterned ground.* Scientific

American, December 1988, pp.68–76

Lavrentiev, M. N. 1967 *Some improperly posed problems of mathematical physics.* Springer. Tracts in Natural Philosophy, Volume II.

Legros, J. C., Longree, D. & Thomaes, G. 1974 Bénard problem in water near 4°C. *Physica* **72**, 410–414.

Lennie, T. B., McKenzie, D. P., Moore, D. R. & Weiss, N. O. 1988 The breakdown of steady convection. *J. Fluid Mech.* **188**, 47–85.

Lindsay, K. A. & Straughan, B. 1990 Energy methods for nonlinear stability in convection, primarily related to geophysics. *Continuum Mech. Thermodyn.* **2**, 245–277.

McKay, G. 1990 Convection with internal heat generation near the density maximum. *Geophys. Astrophys. Fluid Dyn.* **55**, 183–197.

McKay, G. 1991 Continuous dependence on the heat supply for the Boussinesq equations with a cubic density law. *J. Math. Analysis and Appl.* **161**, 258–273.

McKay, G. 1992 Patterned ground formation and solar radiation heating. *Proc. Roy. Soc. London A* **438**, 249–263.

McKay, G. & Straughan, B. 1991 The influence of a cubic density law on patterned ground formation. *Math. Models and Methods in Appl. Sci.* **1**, 27–39.

McKay, G. & Straughan, B. 1992a Nonlinear energy stability and convection near the density maximum. *Acta Mechanica*, to appear.

McKay, G. & Straughan, B. 1992b Patterned ground formation under water. *Continuum Mech. Thermodyn.*, to appear.

McKenzie, D. P., Roberts, J. M. & Weiss, N. O. 1974 Convection in the Earth's mantle: towards a numerical simulation. *J. Fluid Mech.* **62**, 465–538.

Matthews, P. C. 1988 A model for the onset of penetrative convection. *J. Fluid Mech.* **188**, 571–583.

Matthews, P. C. & Heaney, S. I. 1987 Solar heating and its influence on mixing in ice-covered lakes. *Freshwater Biol.* **18**, 135–149.

Merker, G. P., Waas, P. & Grigull, U. 1979 Onset of convection in a horizontal water layer with maximum density effects. *Int. J. Heat Mass Transfer* **22**,

505–515.

Moore, D. R. & Weiss, N. O. 1973 Nonlinear penetrative convection *J. Fluid Mech.* **61**, 553–581.

Namikawa, T., Takashima, M. & Matsushita, S. 1970 The effect of rotation on convective instability induced by surface tension and buoyancy. *J. Phys. Soc. Japan* **28**, 1340–1349.

Nield, D. A. 1977 Onset of convection in a fluid layer overlying a layer of porous medium. *J. Fluid Mech.* **81**, 513–522.

Nield, D. A. 1983 The boundary correction for the Rayleigh-Darcy problem: limitations of the Brinkman equation. *J. Fluid Mech.* **128**, 37–46.

Niedrauer, T. M. & Martin, S. 1979 An experimental study of brine drainage and convection in young sea ice. *J. Geophys. Res. (C)* **84**, 1176–1186.

Palm, E. 1960 On the tendancy towards hexagonal cells. *J. Fluid Mech.* **8**, 183–192.

Payne, L. E. 1971 Uniqueness and continuous dependence criteria for the Navier-Stokes equations. *Rocky Mtn. J. Math.* **2**, 641–660.

Payne, L. E., Song, J. C. & Straughan, B. 1988 Double diffusive porous penetrative convection; thawing subsea permafrost. *Int. J. Engng. Sci.* **26**, 797–809.

Payne, L. E. & Straughan, B. 1987 Unconditional nonlinear stability in penetrative convection. *Geophys. Astrophys. Fluid Dyn.* **39**, 57–63. (Also, Corrected and extended numerical results. *Geophys. Astrophys. Fluid Dyn.* **43**, (1988) 307–309.)

Ray, R. J., Krantz, W. B., Caine, T. N. & Gunn, R. D. 1983 A model for sorted patterned ground regularity. *J. Glaciology* **29**, 317–337.

Riley, P. J. & Laurence, R. L. 1976 Linear stability of modulated circular Couette flow. *J. Fluid Mech.* **75**, 625–646.

Rionero, S. & Mulone, G. 1988 A nonlinear stability analysis of the magnetic Bénard problem through the Lyapunov direct method. *Arch. Rat. Mech. Anal.* **103**, 347–368.

Roberts, P. H. 1967 Convection in horizontal layers with internal heat generation.

Theory. *J. Fluid Mech.* **30**, 33–49.

Robillard, L. & Vasseur, P. 1982 Convective response of a mass of water near 4°C to a constant cooling rate applied on its boundaries. *J. Fluid Mech.* **118**, 123–141.

Rosenblat, S. & Tanaka, G. A. 1971 Modulation of thermal convection instability. *Phys. Fluids* **14**, 1319–1322.

Rossby, H. T. 1969 A study of Bénard convection with and without rotation. *J. Fluid Mech.* **36**, 309–335.

Ruddick, B. R. & Shirtcliffe, T. G. L. 1979 Data for double diffusers: physical properties of aqueous salt-sugar solutions. *Deep Sea Research* **26**, 775–787.

Schubert, G., Turcotte, D. L. & Oxburgh, E. R. 1969 Stability of planet interiors. *Geophys. J. R. Astron. Soc.* **18**, 441–460.

Song, J. C. 1988 *Some stability criteria in fluid and solid mechanics.* Ph.D. thesis, Cornell University.

Straughan, B. 1985 Finite amplitude instability thresholds in penetrative convection. *Geophys. Astrophys. Fluid Dyn.* **34**, 227–242.

Straughan, B. 1990 Continuous dependence on the heat source and nonlinear stability for convection with internal heat generation. *Math. Meth. Appl. Sci.* **13**, 373–383.

Straughan, B. 1991 Convection caused by radiation through the layer. *IMA J. Appl. Math.* **46**, 211–216.

Straughan, B. 1992a *The energy method, stability, and nonlinear convection.* Springer-Verlag: Ser. in Appl. Math. Sci., vol. **91**.

Straughan, B. 1992b *Mathematical aspects of penetrative convection.* Longman, Harlow, to appear.

Sun, Z. S., Tien, C. & Yen, Y. C. 1969 Thermal instability of a horizontal layer of liquid with maximum density. *Amer. Inst. Chem. Engs. J.* **15**, 910–915.

Thirlby, R. 1970 Convection in an internally heated layer. *J. Fluid Mech.* **44**, 673–693.

Travis, B. J., Anderson, C., Baumgardner, J., Gable, C. W., Hager, B. H.,

O'Connell, R. J., Olson, P., Raefsky, A. & Schubert, G. 1990 A benchmark comparison of numerical methods for infinite Prandtl number thermal convection in two-dimensional Cartesian geometry. *Geophys. Astrophys. Fluid Dyn.* **55**, 137–160.

Tritton, D. T. & Zarraga, M. N. 1967 Convection in horizontal layers with internal heat generation. Experiments. *J. Fluid Mech.* **30**, 21–31.

Vasseur, P., Robillard, L. & Chandra Shekar, B. 1983 Natural convection with heat transfer of water within a horizontal cylindrical annulus with density inversion effects. *J. Heat Transfer* **105**, 117–123.

Veronis, G. 1963 Penetrative convection. *Astrophys. J.* **137**, 641–663.

Walden, R. W. & Ahlers, G. 1981 Non-Boussinesq and penetrative convection in a cylindrical cell. *J. Fluid Mech.* **109**, 89–114.

Washburn, A. L. 1973 *Periglacial Processes and Enviroments.* St. Martins' Press, New York.

Watson, A. 1972 The effect of the inversion temperature on the convection of water in an enclosed rectangular cavity. *Q. Jl. Mech. Appl. Math.* **25**, 423–446.

Weast, R. C. 1988 *Handbook of Chemistry and Physics. Vol 69.* Boca Raton: C.R.C. Press.

Whitehead, J. A. 1971 Upon boundary conditions imposed by a stratified fluid. *Geophys. Fluid Dyn.* **2**, 289–298.

Whitehead, J. A. & Chen M. M. 1970 Thermal instability and convection of a thin layer bounded by a stably stratified region. *J. Fluid Mech.* **40**, 549–576.

Wooding, R. A. 1959 The stability of a viscous liquid in a vertical tube containing porous material. *Proc. Roy. Soc. London A* **252**, 120–134.

Wu, R. S. & Cheng, K. C. 1976 Maximum density effects on thermal instability induced by combined buoyancy and surface tension. *Int. J. Heat Mass Transfer* **19**, 559–565.

Yih, C.-S. & Li, C.-H. 1972 Instability of unsteady flows or configurations. Part 2. Convective instability. *J. Fluid Mech.* **54**, 143–152.